

**Pacific Northwest
National Laboratory**

Operated by Battelle for the
U.S. Department of Energy

**Sensitivity Tests of the
Waste-Form-Alone Design for the
Low-Activity-Waste Disposal System**

M. J. Fayer
M. D. White
C. T. Kincaid

RECEIVED
OCT 27 1997
OSTI

September 1997

MASTER

Prepared for the U.S. Department of Energy
under Contract DE-AC06-76RLO 1830

PNNL-11717

DISCLAIMER

This report was prepared as an account of work sponsored by an agency of the United States Government. Neither the United States Government nor any agency thereof, nor Battelle Memorial Institute, nor any of their employees, makes any warranty, express or implied, or assumes any legal liability or responsibility for the accuracy, completeness, or usefulness of any information, apparatus, product, or process disclosed, or represents that its use would not infringe privately owned rights. Reference herein to any specific commercial product, process, or service by trade name, trademark, manufacturer, or otherwise does not necessarily constitute or imply its endorsement, recommendation, or favoring by the United States Government or any agency thereof, or Battelle Memorial Institute. The views and opinions of authors expressed herein do not necessarily state or reflect those of the United States Government or any agency thereof.

PACIFIC NORTHWEST NATIONAL LABORATORY

operated by

BATTELLE

for the

UNITED STATES DEPARTMENT OF ENERGY

under Contract DE-AC06-76RLO 1830

Printed in the United States of America

Available to DOE and DOE contractors from the
Office of Scientific and Technical Information, P.O. Box 62, Oak Ridge, TN 37831;
prices available from (615) 576-8401.

Available to the public from the National Technical Information Service,
U.S. Department of Commerce, 5285 Port Royal Rd., Springfield, VA 22161



This document was printed on recycled paper.

(9/97)

Sensitivity Tests of the Waste-Form-Alone Design for the Low-Activity-Waste Disposal System

M. J. Fayer
M. D. White
C. T. Kincaid

DISTRIBUTION OF THIS DOCUMENT IS UNLIMITED *ph*

September 1997

MASTER

Prepared for
the U.S. Department of Energy
under Contract DE-AC06-76RLO 1830

Pacific Northwest National Laboratory
Richland, Washington 99352

DISCLAIMER

**Portions of this document may be illegible
in electronic image products. Images are
produced from the best available original
document.**

Acknowledgments

We want to thank Gary Streile of PNNL for his technical review comments. We want to thank Fred Mann of Fluor Daniel Hanford Inc. for his technical review comments and his programmatic support. This work was supported by the U.S. Department of Energy-Richland Operations Office.

Contents

Summary	iii
Acknowledgements	v
1.0 Introduction	1.1
2.0 Brief Problem Description	2.1
3.0 Summary of 1995 Simulations	3.1
3.1 Representation of Glass Waste	3.3
3.2 Diffusion	3.5
3.3 Dispersion	3.5
3.4 Well Intercept	3.5
3.5 Recharge and Dissolution Rates	3.6
4.0 Simulation Results in 1997	4.1
4.1 Grid Resolution	4.1
4.2 Diffusion	4.1
4.3 Glass Fractures	4.6
4.4 Water Consumption	4.12
5.0 Conclusions and Recommendations	5.1
6.0 References	6.1
Appendix - Sensitivity Analysis of Transport Parameters on the Performance of the Waste-Form Alone Design for the Low-Activity-Waste Disposal System	A.1

Figures

2.1	Conceptual model used for 2-D simulations of waste-form-alone disposal in the vadose zone 14	2.2
3.1	Water retention and hydraulic conductivity functions for simulation materials	3.4
4.1	Drinking water dose (repeat of Fig. A.3)	4.2
4.2	Drinking water dose (repeat of Fig. A.3 using the moderate grid)	4.3
4.3	Drinking water dose (repeat of Fig. A.5)	4.4
4.4	Drinking water dose (repeat of Fig. A.5 using the moderate grid)	4.5
4.5	Drinking water dose (repeat of Fig. A.5 with diffusion coefficient increased 10x)	4.7
4.6	Drinking water dose (repeat of Fig. A.5 using Kemper diffusion model)	4.8
4.7	Drinking water dose (repeat of Fig. A.26)	4.9
4.8	Drinking water dose (repeat of Fig. A.26 with a fracture volume of 2%)	4.10
4.9	Drinking water dose (repeat of Fig. A.26 with a fracture volume of 4%)	4.11
4.10	Drinking water dose (repeat of Fig. A.26 with water consumption and solutes excluded)	4.13
4.11	Drinking water dose (repeat of Fig. A.26 with water consumption and solutes included)	4.14

Tables

3.1	Summary of simulation parameters used in the Appendix to support the product specifications	3.2
3.2	Half lives and Derived Concentration Guides (DCGs)	3.3
3.3	Maximum total dose for 100,000 years (corrosion rate is 1×10^{-5} cm/yr; recharge is 0.1 cm/yr; retardation is saturation-independent; no dispersion; well intercept of 0.006)	3.5
3.4	Impact of recharge and dissolution rates on maximum total dose (glass sphere model, radius = 0.25 cm; $D = 10^{-8}$ cm ² /s; minimum $K_r = 0$; $\alpha_L = 6.5$ m; $\alpha_T = 0.65$ m; narrow grid)	3.6

1.0 Introduction

This report summarizes the results of computer simulations executed by the Pacific Northwest National Laboratory (PNNL) to assess the performance of the waste-form-alone (WFA) design for the low-activity-waste (LAW) disposal system. Most of the work was conducted in 1995 and described in a letter report (Kincaid and White 1995^a). The letter report was prepared to support the development of the LAW product acceptance specification. To make it more generally available, the letter report was attached as an appendix to this report. Some editorial changes were made in the appendix, but the technical content remains as it was in 1995.

In FY 1997, PNNL performed additional simulations for Lockheed Martin Hanford Company (LMHC) to address specific questions about the disposal. FDNW manages the Glass Performance Assessment Project for the U.S. Department of Energy (DOE). The objectives of the work in FY 1997 were to demonstrate the impact of grid resolution, diffusion, fracture flow within the waste form, and consumption of water by the waste form. It was assumed that the waste form would be the only part of the engineered disposal system that inhibits radionuclide release, referred to as WFA assumption. All calculations were performed with the latest version of the STOMP (Subsurface Transport Over Multiple Phases) simulator.

(a) Kincaid CT and MD White, 1995. "Sensitivity Analysis of Transport Parameters on the Performance of the Waste-Form-Alone Design for the Low-Activity-Waste Disposal System," Letter report submitted to JL Straalsund on 12 July 1995 to satisfy Milestone # 1.07.02.02.02.03A

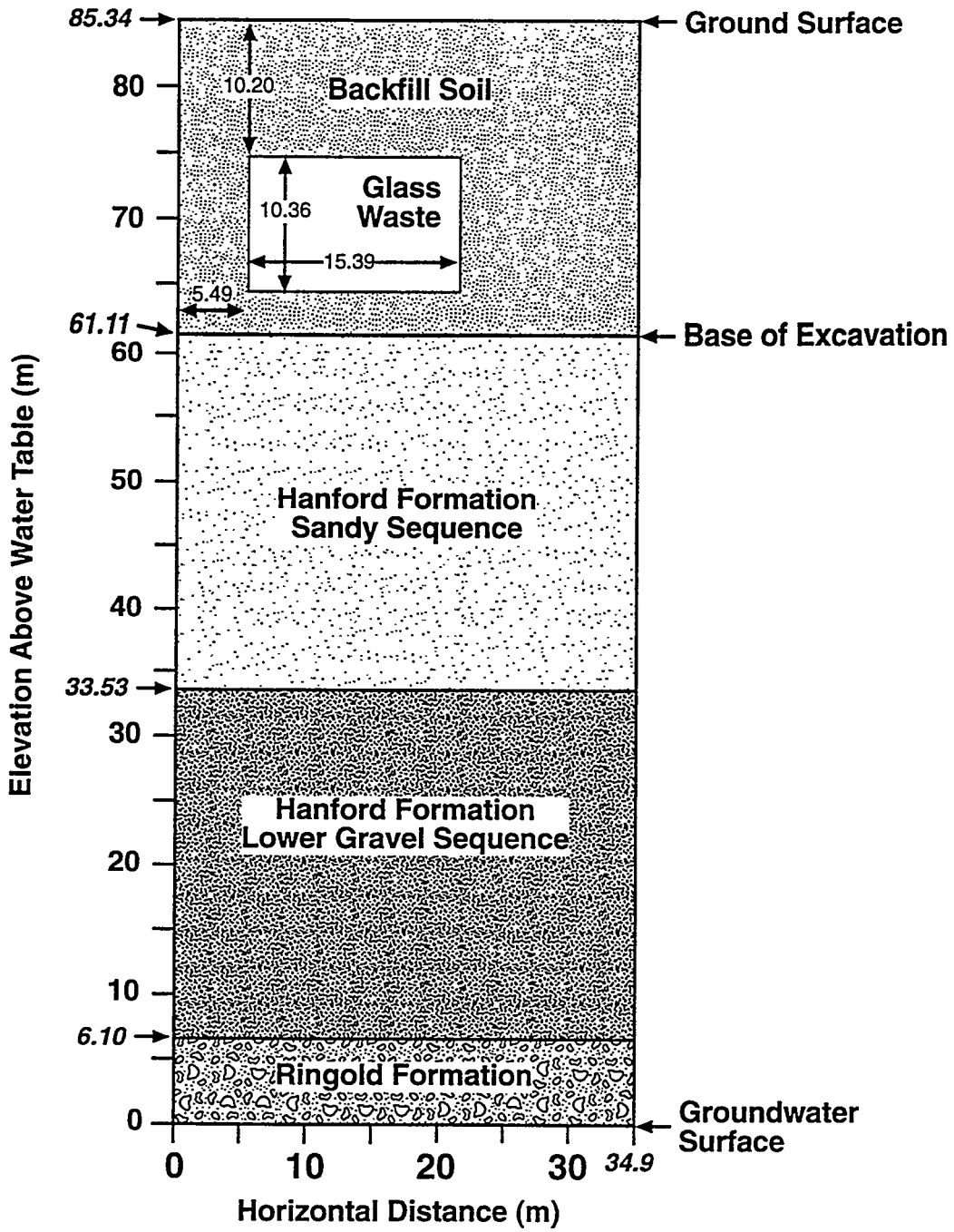
2.0 Brief Problem Description

In 1995, a means was needed to quickly evaluate the WFA disposal performance to support the development of the product acceptance specifications for the privatization proposal. The problem was kept simple by using homogenous and isotropic materials, and by excluding any facility features such as concrete walls and capillary diversion barriers (the WFA assumption). In a further move to keep it simple, the evaluation focused on the sensitivity of only a few parameters and very little multiple parameter sensitivity.

The evaluation was accomplished by setting up a steady-state flow problem and solving the transport equation with the latest version of the STOMP (Subsurface Transport Over Multiple Phases) simulator. The STOMP simulator is a general purpose tool for simulating subsurface flow and transport. The development of STOMP's capabilities was guided by proposed and applied remediation activities at sites contaminated with volatile organic compounds and/or radioactive material. Developed with the support of DOE, the simulator's modeling capabilities address a variety of subsurface environments, including variably saturated, multiple-phased, nonisothermal, and variably frozen soils. The conceptual model used for the present investigations resulted in the use of an equation set option that solved for water and solute transport through a variably saturated porous media system at constant temperature, assuming a passive gas phase at constant pressure. Solute transport was solved sequentially per solute, following the calculation of the aqueous flow field. The full suite of capabilities is described by White and Oostrom (1996).

The Appendix provides the details of the problem description. Basically, a 2-D simulation of a vertical slice through a disposal vault is used to calculate transport to the water table as shown in Figure 2.1. Vadose zone materials include Hanford sands, Hanford gravels, Ringold formation, and backfill. The lateral boundary conditions are no flow conditions. The top boundary is a uniform recharge flux of either 0.01, 0.1, or 1.0 cm/yr. The bottom boundary condition is a static water table that allows for the free movement of water and solutes in and out of the domain.

Specified corrosion rates are used to define the contaminant source terms. To do this, the inventory is assumed to be uniformly distributed throughout the waste. The release of contaminants is then proportional to the corrosion rate. In the post-processing to calculate doses, the full inventory is used to scale the simulation results for a vault slice and calculate the facility doses. Because of multiple dose standards, the drinking water dose results are reported using normalized values in which each result is divided by the appropriate dose standard. The Appendix describes the normalization procedure using the DOE and EPA dose standards.



SG97090035.1

Figure 2.1. Conceptual model used for 2-D simulations of waste-form-alone disposal in the vadose zone

3.0 Summary of 1995 Simulations

The objectives of the 1995 study were to 1) independently check the validity of earlier performance estimates, 2) perform a sensitivity analysis on performance relative to critical transport parameters, and 3) provide a technical basis for estimating the allowed source terms for the LAW disposal system. The Appendix provides the details of the simulations that were performed in 1995. Table 3.1 lists the parameters that were varied to generate each figure in the Appendix. Table 3.2 lists the important radionuclides and their half lives and dose factors (they were not listed in the original report). Mann et al. (1995) indicated that several additional radionuclides, including ^{79}Se , may be present in sufficient quantities to produce significant changes to the predicted drinking water dose. These radionuclides were not in the original 1995 study. They were not included in this study to maintain consistency with the original study and because the focus of this study was the physical processes (e.g., grid resolution; diffusion) rather than the dose.

Kincaid and White (1995) reported that the dominant mode of transport (advective versus diffusion) through the glass-waste disposal zone strongly affects the drinking water dose rates; advective transport generally yields higher dose rates. In a WFA disposal, the dominant mode of transport within the glass-waste engineered system depends strongly on the unsaturated hydraulic properties of the glass-waste zone media. Hence, confidence in the performance of the disposal system will increase when the waste form is known and its hydraulic properties are fully characterized and modeled.

Kincaid and White (1995) extended WFA earlier analyses by expanding the calculation of health effects to include the radiological health effect groups proposed by the Environmental Protection Agency (EPA): beta/photon emitters, total uranium, and gross alpha emitters.

Calculations were performed to show the potential impact of using a sorption model that accounts for the unsaturated state of the vadose zone in calculations of the retardation of sorbed contaminants. Such a model has been found to greatly separate the non-retarded technetium and iodine isotopes from retarded isotopes of uranium, neptunium and plutonium. Kincaid and White (1995) recommended that the retardation model be researched to determine its appropriate form for application to the Hanford vadose zone transport calculations.

Under higher recharge (i.e., 1 cm/yr), the ^{239}Pu isotope reaches the water table and becomes a dominant contributor to dose. Secondary minerals formed as the glass corrodes could increase the retardation of ^{239}Pu in the waste form and thus decrease ^{239}Pu mobility. Consequently, the true release of ^{239}Pu would be delayed and decay would greatly diminish its contribution to dose. Thus, our results showing release and migration of ^{239}Pu are a direct result of simply using a distribution coefficient that does not consider the influence of secondary mineral formation.

The results show the general applicability of the dose versus glass release time curves presented in the Appendix by simulating cases using the corrosion rate and surface-area-to volume ratio of the preliminary product acceptance specification. Results obtained fall on these generic curves of dose versus glass release time. The case of 80% ^{99}Tc removal was also studied; in this case, the beta/photon emitter drinking water standard of 4 mrem/yr could be met.

Table 3.1. Summary of simulation parameters used in the Appendix to support the product specifications (in all cases, the diffusion parameters were $a = 1.0$ and $b = 0.0$; “*” superscript on the figure number indicates 20% ^{99}Tc inventory)

Figure	Corrosion cm/yr	Radius cm	Recharge cm/yr	Diffusion cm ² /s	Glass Hyd. Prop.	Min K_r	Retardation Model	Dispersion m	Well Intercept	Grid
A.1	1.0E-5	0.25	0.1	1E-10	Gravel	1E-10	Sat Indep	0, 0	0.006	narrow
A.2	1.0E-5	0.25	0.1	1E-10	Gravel	1E-10	Sat Indep	0, 0	0.006	moderate
A.3	1.0E-5	0.25	0.1	1E-10	Gravel	0	Sat Indep	0, 0	0.006	narrow
A.4	1.0E-5	0.25	0.1	1E-9	Gravel	0	Sat Indep	0, 0	0.006	narrow
A.5	1.0E-5	0.25	0.1	1E-8	Gravel	0	Sat Indep	0, 0	0.006	narrow
A.6	1.0E-5	0.25	0.1	1E-10	Glass Sphere	0	Sat Indep	0, 0	0.006	narrow
A.7	1.0E-5	0.25	0.1	1E-8	Glass Sphere	0	Sat Indep	0, 0	0.006	narrow
A.8	1.0E-5	0.25	0.1	1E-8	Glass Sphere	0	Sat Indep	6.5, 0.65	0.006	narrow
A.9	1.0E-5	0.25	0.1	1E-8	Glass Sphere	0	Sat Indep	6.5, 0.65	0.01	narrow
A.10	1.0E-5	0.25	0.1	1E-8	Glass Sphere	0	Sat Dep	6.5, 0.65	0.01	narrow
A.11	1.0E-3	0.25	0.1	1E-8	Glass Sphere	0	Sat Indep	6.5, 0.65	0.01	narrow
A.11a	1.0E-3	0.25	0.1	1E-8	Glass Sphere	0	Sat Dep	6.5, 0.65	0.01	narrow
A.12	1.0E-4	0.25	0.1	1E-8	Glass Sphere	0	Sat Indep	6.5, 0.65	0.01	narrow
A.12a	1.0E-4	0.25	0.1	1E-8	Glass Sphere	0	Sat Dep	6.5, 0.65	0.01	narrow
A.13	1.0E-6	0.25	0.1	1E-8	Glass Sphere	0	Sat Indep	6.5, 0.65	0.01	narrow
A.13a	1.0E-6	0.25	0.1	1E-8	Glass Sphere	0	Sat Dep	6.5, 0.65	0.01	narrow
A.14	1.0E-7	0.25	0.1	1E-8	Glass Sphere	0	Sat Indep	6.5, 0.65	0.01	narrow
A.14a	1.0E-7	0.25	0.1	1E-8	Glass Sphere	0	Sat Dep	6.5, 0.65	0.01	narrow
A.15	1.0E-8	0.25	0.1	1E-8	Glass Sphere	0	Sat Indep	6.5, 0.65	0.01	narrow
A.15a	1.0E-8	0.25	0.1	1E-8	Glass Sphere	0	Sat Dep	6.5, 0.65	0.01	narrow
A.16	1.0E-3	0.25	0.01	1E-8	Glass Sphere	0	Sat Indep	6.5, 0.65	0.001	narrow
A.16a	1.0E-3	0.25	0.01	1E-8	Glass Sphere	0	Sat Dep	6.5, 0.65	0.001	narrow
A.17	1.0E-4	0.25	0.01	1E-8	Glass Sphere	0	Sat Indep	6.5, 0.65	0.001	narrow
A.17a	1.0E-4	0.25	0.01	1E-8	Glass Sphere	0	Sat Dep	6.5, 0.65	0.001	narrow
A.18	1.0E-5	0.25	0.01	1E-8	Glass Sphere	0	Sat Indep	6.5, 0.65	0.001	narrow
A.18a	1.0E-5	0.25	0.01	1E-8	Glass Sphere	0	Sat Dep	6.5, 0.65	0.001	narrow
A.19	1.0E-6	0.25	0.01	1E-8	Glass Sphere	0	Sat Indep	6.5, 0.65	0.001	narrow
A.19a	1.0E-6	0.25	0.01	1E-8	Glass Sphere	0	Sat Dep	6.5, 0.65	0.001	narrow
A.20	1.0E-7	0.25	0.01	1E-8	Glass Sphere	0	Sat Indep	6.5, 0.65	0.001	narrow
A.20a	1.0E-7	0.25	0.01	1E-8	Glass Sphere	0	Sat Dep	6.5, 0.65	0.001	narrow
A.21	1.0E-8	0.25	0.01	1E-8	Glass Sphere	0	Sat Indep	6.5, 0.65	0.001	narrow
A.21a	1.0E-8	0.25	0.01	1E-8	Glass Sphere	0	Sat Dep	6.5, 0.65	0.001	narrow
A.22	1.0E-5	0.25	1.0	1E-8	Glass Sphere	0	Sat Indep	6.5, 0.65	0.1	narrow
A.22a	1.0E-5	0.25	1.0	1E-8	Glass Sphere	0	Sat Dep	6.5, 0.65	0.1	narrow
A.23	1.0E-6	0.25	1.0	1E-8	Glass Sphere	0	Sat Indep	6.5, 0.65	0.1	narrow
A.23a	1.0E-6	0.25	1.0	1E-8	Glass Sphere	0	Sat Dep	6.5, 0.65	0.1	narrow
A.24	1.0E-7	0.25	1.0	1E-8	Glass Sphere	0	Sat Indep	6.5, 0.65	0.1	narrow
A.24a	1.0E-7	0.25	1.0	1E-8	Glass Sphere	0	Sat Dep	6.5, 0.65	0.1	narrow
A.25	1.0E-8	0.25	1.0	1E-8	Glass Sphere	0	Sat Indep	6.5, 0.65	0.1	narrow
A.25a	1.0E-8	0.25	1.0	1E-8	Glass Sphere	0	Sat Dep	6.5, 0.65	0.1	narrow
A.26	1.405E-5	10.0	0.1	1E-8	Glass Sphere	0	Sat Indep	6.5, 0.65	0.01	narrow
A.26a	1.405E-5	10.0	0.1	1E-8	Glass Sphere	0	Sat Dep	6.5, 0.65	0.01	narrow
A.26b*	1.405E-5	10.0	0.1	1E-8	Glass Sphere	0	Sat Indep	6.5, 0.65	0.01	narrow
A.26c*	1.405E-5	10.0	0.1	1E-8	Glass Sphere	0	Sat Dep	6.5, 0.65	0.01	narrow

Table 3.2. Half lives and Derived Concentration Guides (DCGs), the inverse of the dose conversion factors used in the Appendix calculations

Radionuclide	Half Life	Derived Concentration Guides $\mu\text{Ci/mL}$ per drem/yr (drem = 0.1 rem)
^{14}C	5730	7.00E-05
^{90}Sr	29	1.00E-06
^{99}Tc	21300	1.00E-04
^{129}I	1.59E+07	5.00E-07
^{137}Cs	30.1	3.00E-06
^{234}U	2.44E+05	5.00E-07
^{235}U	7.04E+08	5.00E-07
^{238}U	4.47E+09	6.00E-07
^{237}Np	2.14E+06	3.00E-08
^{239}Pu	2.44E+04	4.00E-08
^{240}Pu	6.54E+03	4.00E-08
^{241}Am	433	4.00E-08

3.1 Representation of Glass Waste

Two porous media types were used to represent the hydraulic and chemical properties of the glass waste: gravel and glass spheres. Figure 3.1 shows the water retention and hydraulic conductivity functions used to represent these two media as well as the vadose zone porous media. The gravel properties are distinctly different from all of the other media, in contrast to the glass sphere properties, which are similar to the properties of the other geologic media.

Table 3.3 shows that the gravel properties result in a lower maximum 100,000-yr total dose relative to the glass sphere properties. This behavior can be explained by the hydraulic properties. The gravel has a very low in situ water content and hydraulic conductivity, which allows it to act like a capillary break and limit advective flow through the glass zone. Thus, diffusion is the primary means of solute transport.

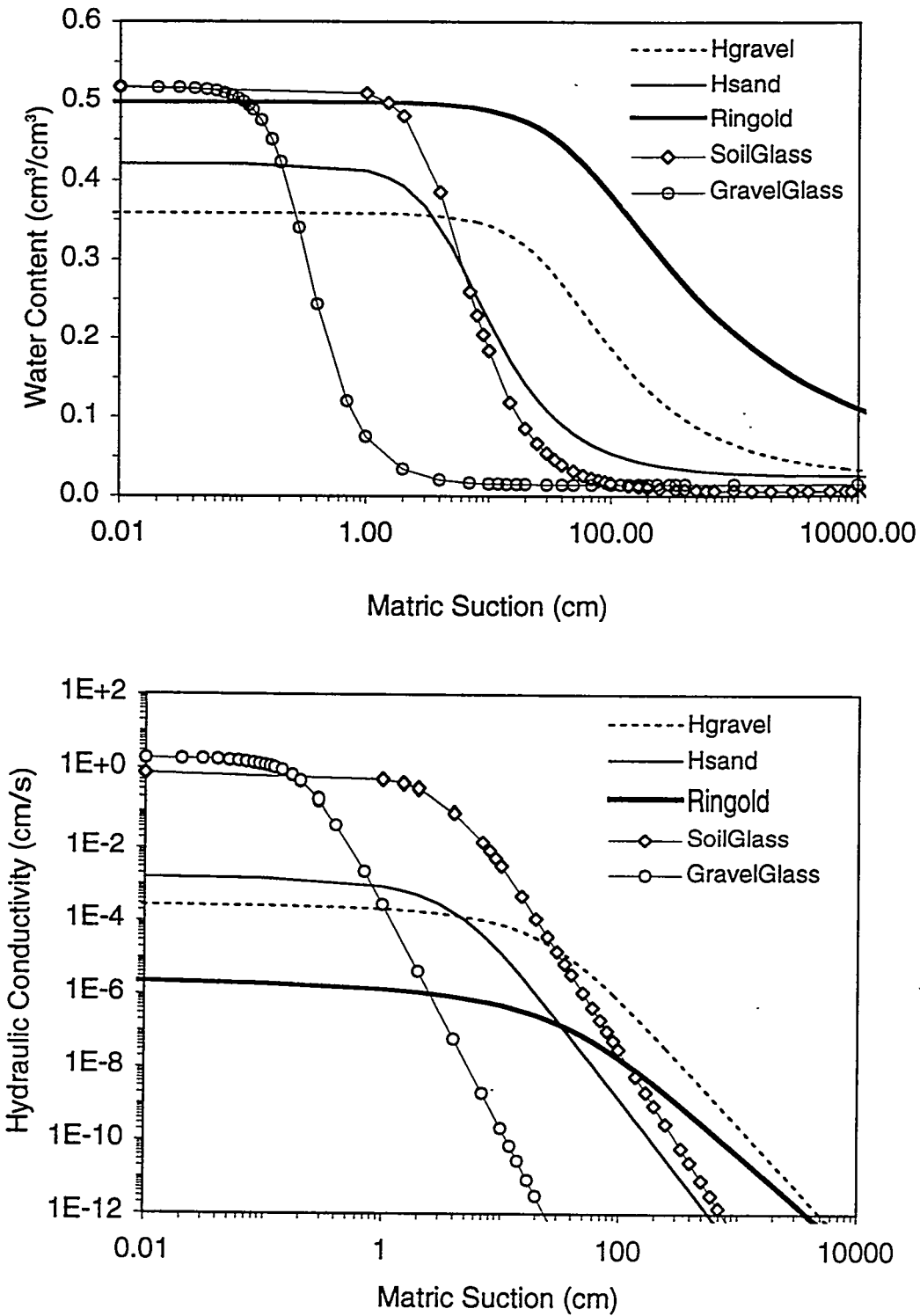


Figure 3.1. Water retention and hydraulic conductivity functions for simulation materials

Table 3.3. Maximum total dose for 100,000 years (corrosion rate is 1×10^{-5} cm/yr; recharge is 0.1 cm/yr; retardation is saturation-independent; no dispersion; well intercept of 0.006)

Glass Hydraulic Property Model	Maximum Total Dose in 100,000 Years (mrem/yr)		
	Constant Glass Diffusion Coefficient (cm ² /s)		
	10 ⁻⁸	10 ⁻⁹	10 ⁻¹⁰
gravel	140.5 [Fig. A.5]	61.3 [Fig. A.4]	17.6 [Fig. A.3]
glass sphere	172.3 [Fig. A.7]	--	172.3 [Fig. A.6]

3.2 Diffusion

Diffusion is the proportionality factor in Fick's law that relates the diffusive transport flux to the gradient in solute concentration. The difference in flow behavior between the gravel and glass spheres can be inferred from the sensitivity to the diffusion parameter. Table 3.3 shows that the maximum total dose increases significantly in the gravel as diffusion is increased, whereas for the glass spheres the total dose hardly changes at all.

3.3 Dispersion

Dispersivity, when multiplied by the pore water velocity, yields the mechanical dispersion coefficient, which in turn relates the dispersive solute flux to the concentration gradient. Two simulations (Figures A.7 and A.8) demonstrated that the inclusion of dispersion caused a decrease in the maximum total dose of 8.5%. Additional simulations would be needed with other sets of parameters to demonstrate the general sensitivity to dispersion.

3.4 Well Intercept

The well intercept factor is the ratio of the volume of contaminated water entering the aquifer to the total volume of water withdrawn from the well. In effect, the well intercept factor is a measure of the dilution that occurs when clean aquifer water mixes with the contaminated water entering the aquifer from the vadose zone. The calculated dose values scale directly with this parameter, as shown in Figures A.8 and A.9. In the 1995 report, the well intercept value was varied along with the recharge rate. Because the well intercept value is in the numerator and the recharge value is in the denominator of the dose calculation, the result of this joint variation is that their ratio remains constant. Thus, as the recharge rate was reduced from 0.1 to 0.01 cm/yr, the well intercept was reduced from 0.01 to 0.001 without discussion. Although it has a significant impact on dose, the well intercept is not a particularly well-defined parameter and perhaps deserves more attention.

3.5 Recharge and Dissolution Rates

White and Kincaid (1995) evaluated the impacts of three recharge rates and six dissolution rates on dose. Table 3.4 shows that doses increased substantially as the recharge and dissolution rates were increased. As discussed in the previous section, the well intercept factor was varied directly with the recharge rate. Were it not, the dose differences caused by changes in recharge rate would be even more substantial.

Table 3.4. Impact of recharge and dissolution rates on maximum total dose (glass sphere model, radius = 0.25 cm; $D = 10^{-8}$ cm²/s; minimum $K_r = 0$; $\alpha_L = 6.5$ m; $\alpha_T = 0.65$ m; narrow grid)

Corrosion and Dissolution Rates (cm/yr, yr-1)	Total Maximum Dose (mrem/yr) in 10 ⁵ years					
	Recharge = 0.01 cm/yr Well Intercept = 0.001		Recharge = 0.1 cm/yr Well Intercept = 0.01		Recharge = 1.0 cm/yr Well Intercept = 0.1	
	Saturation- Independent	Saturation- Dependent	Saturation- Independent	Saturation- Dependent	Saturation- Independent	Saturation- Dependent
10 ⁻³ , 1.2 x 10 ⁻²	53.3 [Fig. A.16]	52.8 [Fig A.16a]	528 [Fig. A.11]	527 [Fig. A.11a]	nc	nc
10 ⁻⁴ , 1.2 x 10 ⁻³	53.2 [Fig. A.17]	52.7 [Fig A.17a]	520 [Fig. A.12]	518 [Fig. A.12a]	nc	nc
10 ⁻⁵ , 1.2 x 10 ⁻⁴	52.4 [Fig. A.18]	51.7 [Fig A.18a]	263 [Fig. A.9]	255 [Fig. A.10]	1834 [Fig. A.22]	403.6 [Fig A.22a]
10 ⁻⁶ , 1.2 x 10 ⁻⁵	21.8 [Fig. A.19]	20.3 [Fig A.19a]	49.1 [Fig. A.13]	38.9 [Fig. A.13a]	522.9 [Fig. A.3]	62.3 [Fig A.23a]
10 ⁻⁷ , 1.2 x 10 ⁻⁶	3.1 [Fig. A.20]	2.8 [Fig A.20a]	7.3 [Fig. A.14]	4.4 [Fig. A.14a]	61.8 [Fig. A.24]	9.4 [Fig A.24a]
10 ⁻⁸ , 1.2 x 10 ⁻⁷	0.3 [Fig. A.21]	0.3 [Fig A.21a]	0.8 [Fig. A.15]	0.5 [Fig. A.15a]	6.3 [Fig. A.25]	1.0 [Fig A.25a]

4.0 Simulation Results in 1997

In the two years since the Kincaid and White (1995) report, several conceptual model issues have been identified: grid resolution, diffusion versus advection as the dominant transport mechanism, fracture flow, water consumption as the glass corrodes, thermal effects, and osmotic potential inducements of vapor flow. Temperature changes resulting from the disposal facility were conservatively estimated to be no more than 7°C after 15 years, decreasing progressively thereafter to less than 1°C (McGrail and Mahoney 1995). Such a small temperature change is expected to have a negligible effect on flow and transport rates in the vadose zone; thus, no analyses were performed.

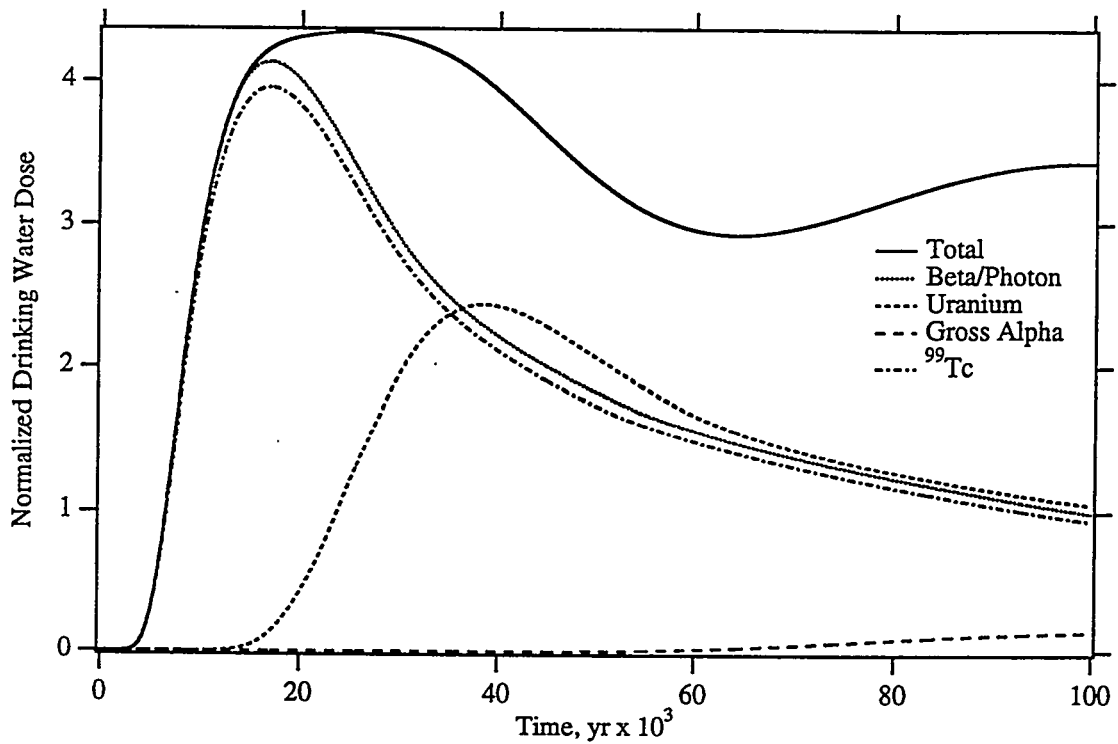
Osmotic lowering of vapor pressure was calculated for a 2 molal NaCl solution (a possible upper bound concentration) and found to be only 3.5%, indicating that osmotic effects on system performance may be minor. Simulations performed by Bacon and McGrail (1997) using a reactive transport computer code support the assumption that osmotic effects are minor. Furthermore, the WFA analyses allow significant amounts of water to move through the waste zone, keeping matric potential values above 0.1 Mpa and in the range where vapor flow is an insignificant component of the overall water flux. For these reasons, no analyses of osmotic effects were performed.

4.1 Grid Resolution

The only 1995 simulation that examined grid resolution used a minimum K_r value of 10^{-10} . Use of this minimum value may have influenced the results. Therefore, two of the 1995 simulations, A.3 and A.5, were repeated for both the narrow grid (10 nodes in the x-direction) and the moderate grid (20 nodes in the x-direction). Figures 4.1 (which duplicates A.3) and 4.2 (which duplicates A.3 but with a moderate grid) show that the moderate grid resulted in an increase in the maximum total dose of 14.6%. For these two simulations, the glass diffusion coefficient was 10^{-10} cm²/s. In contrast, Figures 4.3 (which duplicates A.5) and 4.4 (which duplicates A.5 but with a moderate grid) show that the moderate grid produced only a 0.3% increase. The diffusion coefficient for these two simulations was 10^{-8} cm²/s. These results suggest that, as the diffusion coefficient is decreased, a smaller grid resolution becomes more necessary. This result could be important if the eventual disposal facility is designed to create a diffusion environment within the waste zone.

4.2 Diffusion

In the 1995 simulations, the diffusion parameter was far more important for the gravel model than the sphere model. In those simulations, the diffusion coefficient used for the glass waste was constant at 10^{-8} cm²/s or lower, whereas the value used for the other media was 2.5×10^{-5} cm²/s multiplied by a factor that depended on the water content. For example, at a water content of 0.05 m³/m³, the effective diffusion coefficient in the vadose zone would be 2.06×10^{-7} cm²/s. This approach to calculating effective diffusion by making it a function of the water content was used for the vadose zone transport calculations in the Grout Performance Assessment (Kincaid et al. 1995). It is similar to the constant value of 2.5×10^{-7} cm²/s used for all materials in the unit cell simulations in the Interim Performance Assessment, or IPA (Mann et al. 1996).

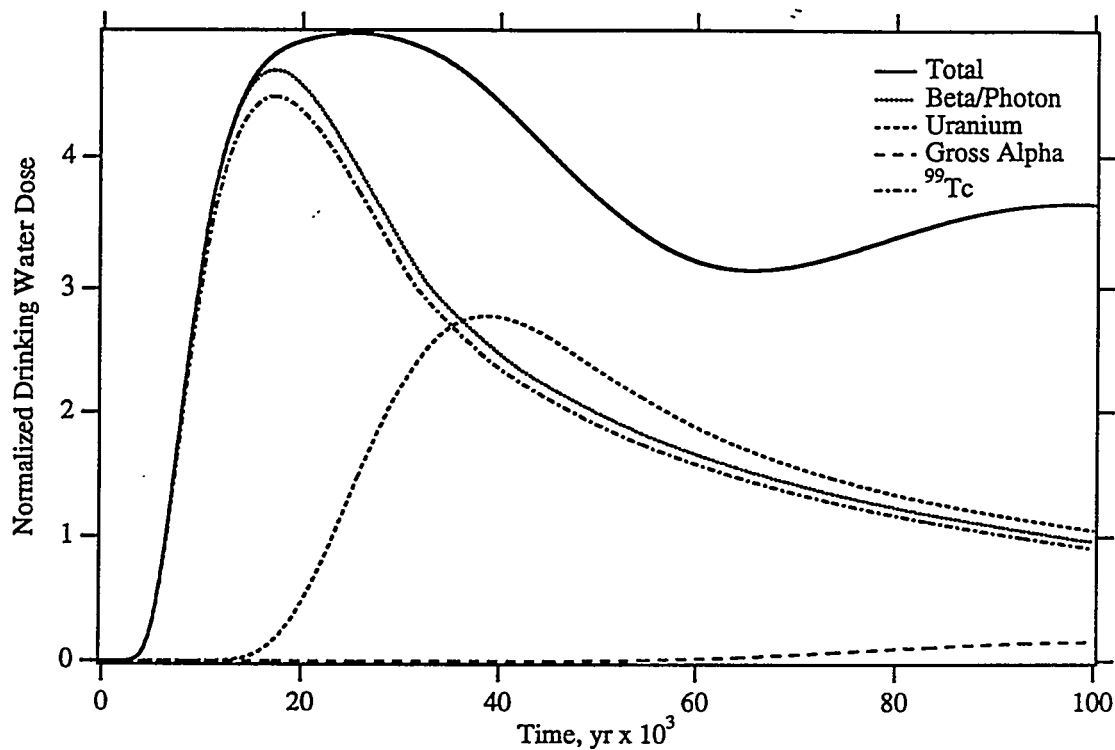


Corrosion: 10^{-5} cm/yr
 Glass Radius: 0.25 cm
 Recharge: 0.1 cm/yr
 Solute Diffusion Coefficient: $D_{ab} = 10^{-10}$ cm²/s, $a = 1$, $b = 0$
 Glass Hydraulic Properties: Gravel
 Minimum Relative Permeability: 0.
 Retardation Model: Saturation-Independent
 Hydraulic Dispersion: $\alpha_L = 0.0$ m, $\alpha_T = 0.0$ m
 Well Interception Factor: 0.006
 Grid: Narrow (10 x 162)

Maximum Dose Records 100,000 yr [10,000 yr]

Total	17.37 [11.67] mrem/yr
Beta/Photon	16.53 [11.67] mrem/yr
⁹⁹ Tc	15.81 [11.17] mrem/yr
¹²⁹ I	0.7099 [0.4903] mrem/yr
Uranium	48.64 [0.004204] μg/L
Gross Alpha	2.104 [3.005e-22] pCi/L

Figure 4.1. Drinking Water Dose (repeat of Fig. A.3)

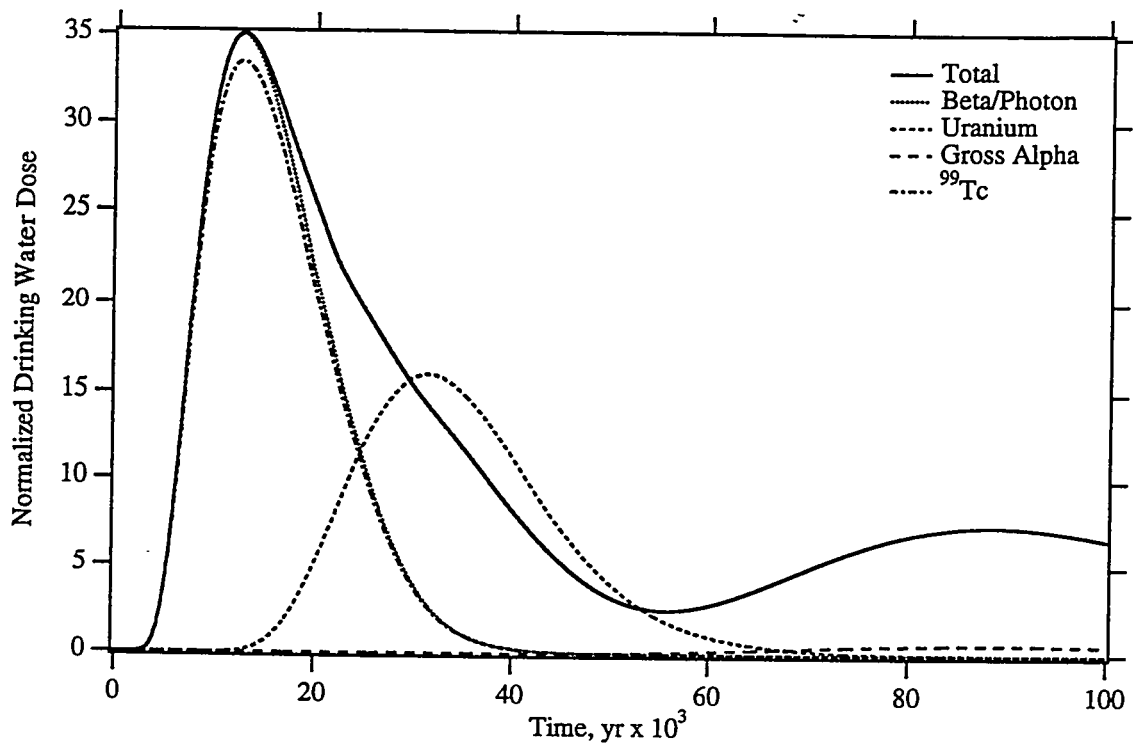


Corrosion: 10^{-5} cm/yr
 Glass Radius: 0.25 cm
 Recharge: 0.1 cm/yr
 Solute Diffusion Coefficient: $D_{ab} = 10^{-10}$ cm²/s, a = 1, b = 0
 Glass Hydraulic Properties: Gravel
 Minimum Relative Permeability: 0.
 Retardation Model: Saturation-Independent
 Hydraulic Dispersion: $\alpha_L = 0.0$ m, $\alpha_T = 0.0$ m
 Well Interception Factor: 0.006
 Grid: Moderate (20 x 162)

Maximum Dose Records 100,000 yr [10,000 yr]

Total	19.90 [12.84] mrem/yr
Beta/Photon	18.75 [12.84] mrem/yr
⁹⁹ Tc	17.94 [12.29] mrem/yr
¹²⁹ I	0.8064 [0.5394] mrem/yr
Uranium	55.45 [0.005029] μg/L
Gross Alpha	2.372 [3.173e-22] pCi/L

Figure 4.2. Drinking Water Dose (repeat of Fig. A.3 using the moderate grid)

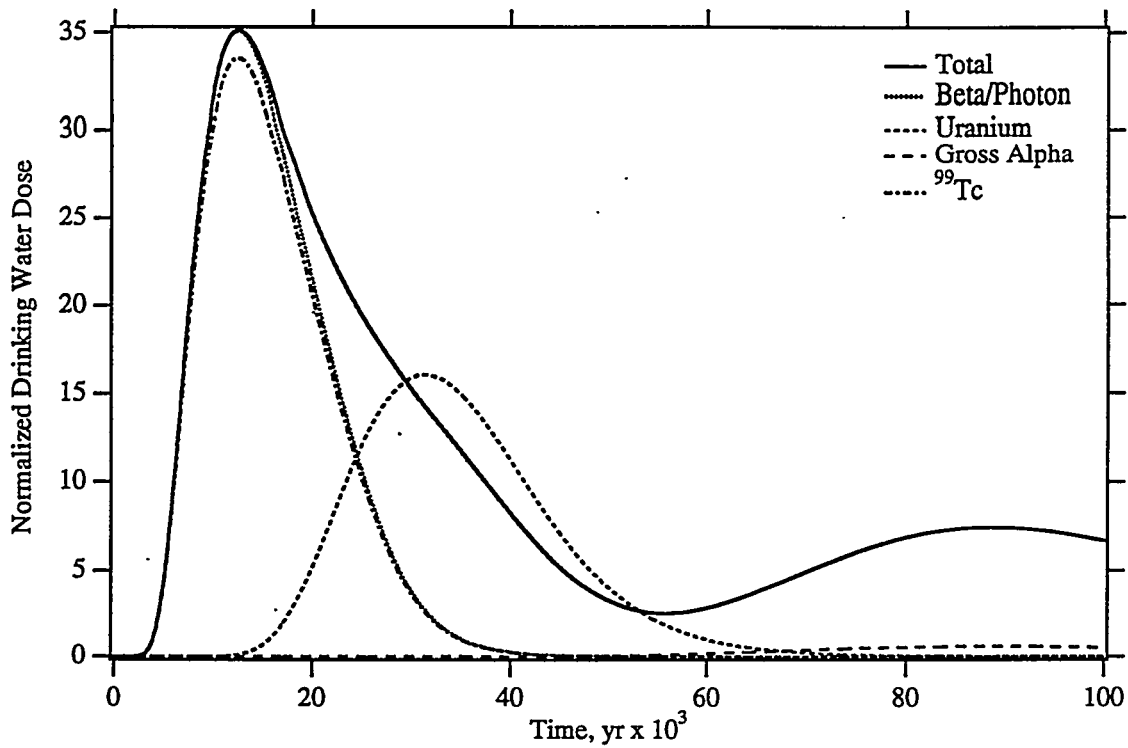


Corrosion: 10^{-5} cm/yr
 Glass Radius: 0.25 cm
 Recharge: 0.1 cm/yr
 Solute Diffusion Coefficient: $D_{ab} = 10^{-8}$ cm²/s, a = 1, b = 0
 Glass Hydraulic Properties: Gravel
 Minimum Relative Permeability: 0.
 Retardation Model: Saturation-Independent
 Hydraulic Dispersion: $\alpha_L = 0.0$ m, $\alpha_T = 0.0$ m
 Well Interception Factor: 0.006
 Grid: Narrow (10 x 162)

Maximum Dose Records 100,000 yr [10,000 yr]

Total	140.1 [125.5] mrem/yr
Beta/Photon	139.8 [125.5] mrem/yr
⁹⁹ Tc	133.8 [120.1] mrem/yr
¹²⁹ I	5.923 [5.271] mrem/yr
Uranium	320.0 [0.08142] μg/L
Gross Alpha	8.880 [1.213e-20] pCi/L

Figure 4.3. Drinking Water Dose (repeat of Fig. A.5)



Corrosion: 10^{-5} cm/yr
 Glass Radius: 0.25 cm
 Recharge: 0.1 cm/yr
 Solute Diffusion Coefficient: $D_{ab} = 10^{-8}$ cm²/s, a = 1, b = 0
 Glass Hydraulic Properties: Gravel
 Minimum Relative Permeability: 0.
 Retardation Model: Saturation-Independent
 Hydraulic Dispersion: $\alpha_L = 0.0$ m, $\alpha_T = 0.0$ m
 Well Interception Factor: 0.006
 Grid: Moderate (20 x 162)

Maximum Dose Records 100,000 yr [10,000 yr]

Total	140.5 [127.1] mrem/yr
Beta/Photon	140.2 [127.1] mrem/yr
⁹⁹ Tc	134.2 [121.7] mrem/yr
¹²⁹ I	5.938 [5.342] mrem/yr
Uranium	320.3 [0.09297] μg/L

Figure 4.4. Drinking Water Dose (repeat of Fig. A.5 using the moderate grid)

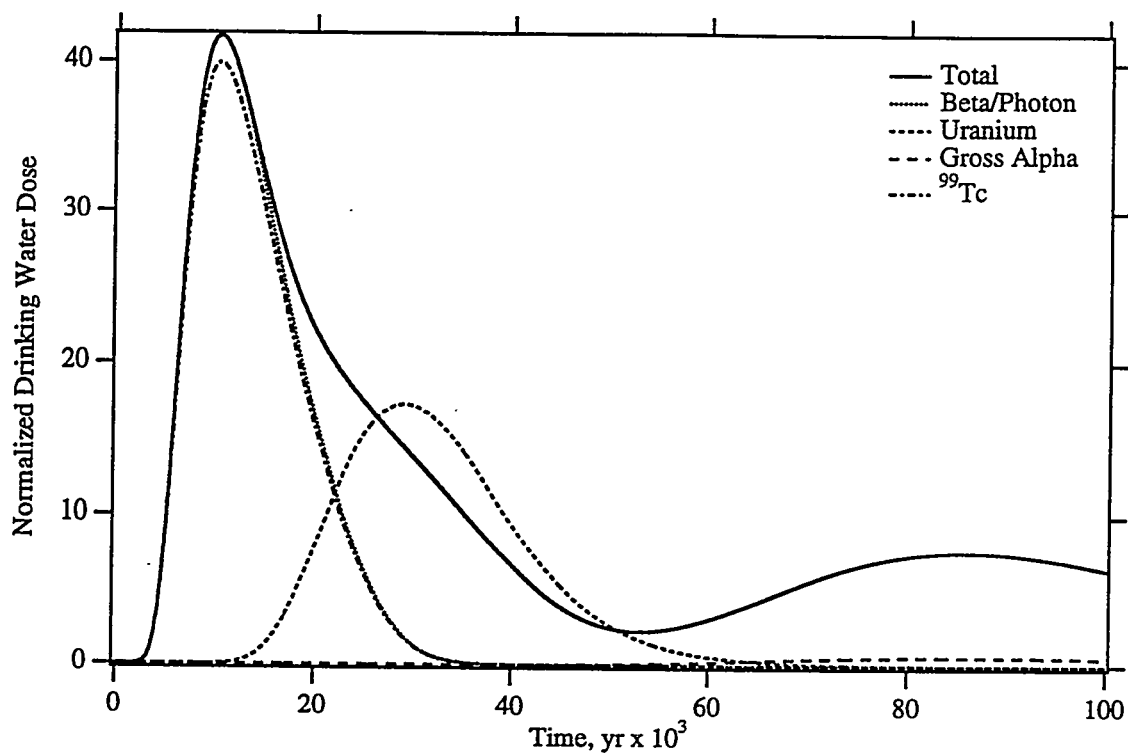
The gravel model of glass was simulated using a diffusion coefficient of 10^{-7} cm²/s. Figure 4.5 shows that the maximum total dose increased 19% relative to the results in Figure 4.3 (for which the diffusion coefficient was 10^{-8} cm²/s). Based on the results in Figure 4.5 and Table 3.3, further increases in the diffusion coefficient will have progressively smaller impacts. A second simulation with the gravel model was performed in which effective diffusion within the glass waste was calculated in the same manner as the surrounding soil, i.e., using the Kemper effective diffusion model. Figure 4.6 shows that the maximum total dose is about equal to that in Figure 4.5, where diffusion was fixed at 10^{-7} cm²/s.

For some simulations of the facility model in the IPA, diffusion was held constant at a value as high as 5×10^{-6} cm²/s. To see the impact of higher diffusion within the sphere model of glass, two additional simulations were conducted in 1997 with diffusion coefficients of 10^{-6} and 10^{-7} cm²/s (all other parameters were as specified in Figure A.26). Although not plotted for this report, the calculated doses for both simulations were nearly identical to the results in Figure A.26, which is further proof that diffusion is not important to the soil model of glass under the WFA assumption.

4.3 Glass Fractures

The actual glass waste form is likely to have significant fracturing. One way of representing the hydraulics of this type of waste is to use the dual porosity model that is available in STOMP. In that model, the fractures and the matrix are assigned separate hydraulic properties. The hydraulic properties of each computational cell are calculated by summing the contributions from the fractures and the matrix and weighting the contributions by the fractional volume. Thus, a fracture volume of 2% would result in the fractures contributing 2% and the matrix contributing 98% to the computational cell hydraulic properties. An important assumption of the dual porosity model is that the fracture and matrix are in hydraulic equilibrium at all times.

To demonstrate the impact of fractures, three simulations were run, one as a repeat of A.26 in the Appendix and two using hypothetical fracture volumes of 2 and 4% (actual volumes are not yet known). The fracture properties were represented with the parameters used for the gravel model of glass and the matrix properties were represented with the parameters for the glass sphere model. Figures 4.7 to 4.9 show that the presence of fractures had little if any effect on maximum dose rates. This result is understandable. In the waste zone, matric potential values ranged from -140 to -290 cm. For significant water movement to occur within the fractures, the matric potentials would have to increase to at least -6 to -11 cm. At these and higher potentials, most porous mediums are typically saturated, or nearly so. For the WFA analyses presented in this report, conditions do not approach saturation because the flux is constant and there is no mechanism for the water flow to concentrate to a significant degree in any location such that water could enter the fractures. In contrast, the inclusion of disposal facility features, transient flow, and vadose zone heterogeneity could contribute to flow concentration that could eventually lead to fracture filling and flow. To more effectively determine the sensitivity to fracture volumes, a more realistic representation of the final disposal facility will be needed.

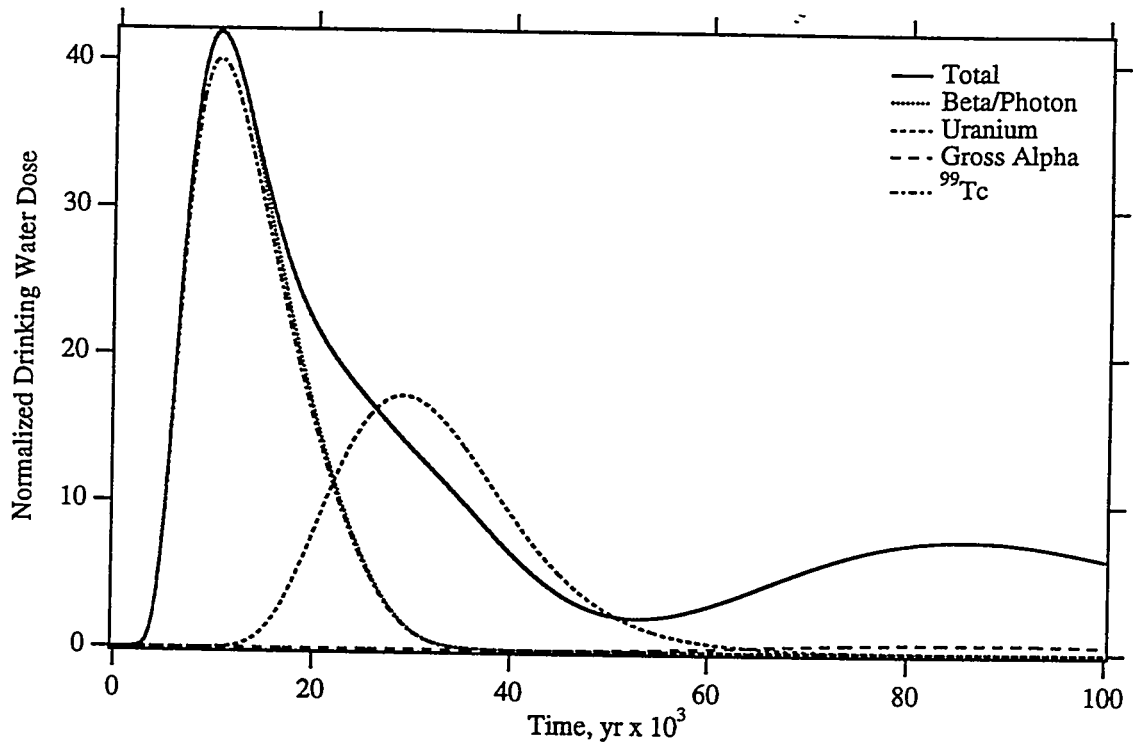


Corrosion: 10^{-5} cm/yr
 Glass Radius: 0.25 cm
 Recharge: 0.1 cm/yr
 Solute Diffusion Coefficient: $D_{ab} = 10^{-7}$ cm²/s, a = 1, b = 0
 Glass Hydraulic Properties: Gravel
 Minimum Relative Permeability: 0.
 Retardation Model: Saturation-Independent
 Hydraulic Dispersion: $\alpha_L = 0.0$ m, $\alpha_T = 0.0$ m
 Well Interception Factor: 0.006
 Grid: Narrow (10 x 162)

Maximum Dose Records 100,000 yr [10,000 yr]

Total	166.8 [166.6] mrem/yr
Beta/Photon	166.8 [166.6] mrem/yr
⁹⁹ Tc	159.6 [159.4] mrem/yr
¹²⁹ I	7.013 [6.998] mrem/yr
Uranium	343.9 [0.2014] μg/L
Gross Alpha	9.120 [4.201e-20] pCi/L

Figure 4.5. Drinking Water Dose (repeat of Fig. A.5 with diffusion coefficient increased 10x)

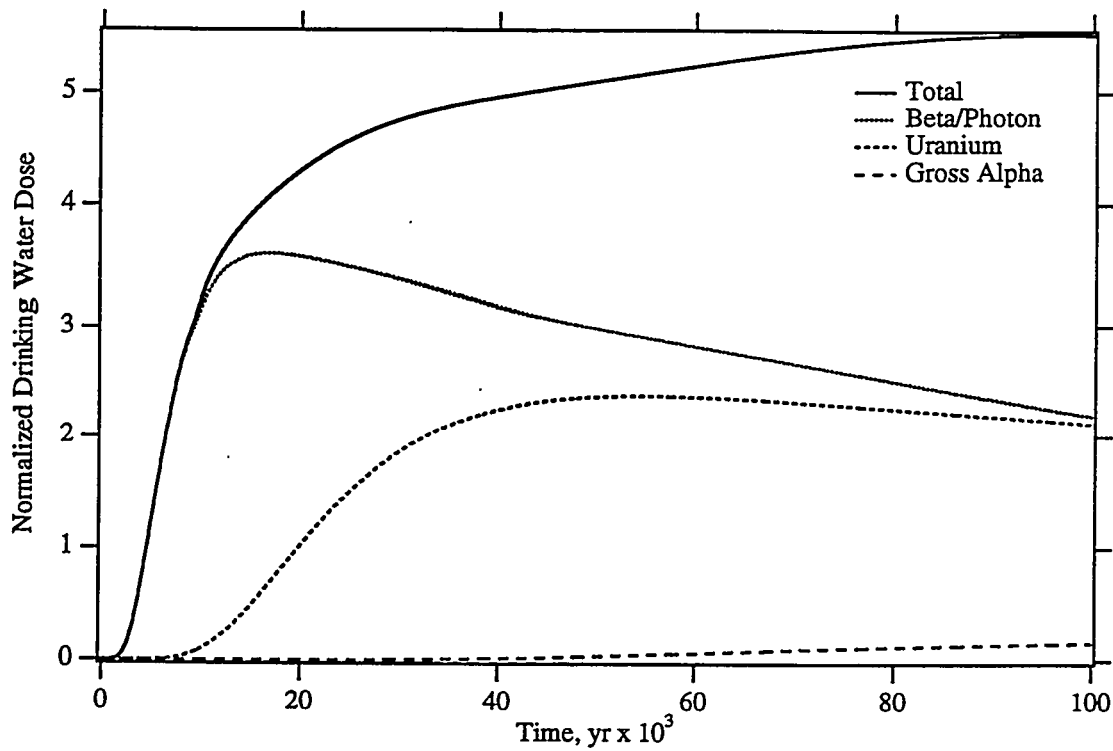


Corrosion: 10^{-5} cm/yr
 Glass Radius: 0.25 cm
 Recharge: 0.1 cm/yr
 Solute Diffusion Coefficient: $D_{ab} = 2.5 \times 10^{-5}$ cm²/s, $a = 0.005$, $b = 10$
 Glass Hydraulic Properties: Gravel
 Minimum Relative Permeability: 0.
 Retardation Model: Saturation-Independent
 Hydraulic Dispersion: $\alpha_L = 0.0$ m, $\alpha_T = 0.0$ m
 Well Interception Factor: 0.006
 Grid: Narrow (10 x 162)

Maximum Dose Records 100,000 yr [10,000 yr]

Total	167.4 [167.4] mrem/yr
Beta/Photon	167.4 [167.3] mrem/yr
⁹⁹ Tc	160.2 [160.2] mrem/yr
¹²⁹ I	7.037 [7.031] mrem/yr
Uranium	345.1 [0.2149] µg/L
Gross Alpha	9.163 [4.684e-20] pCi/L

Figure 4.6. Drinking Water Dose (repeat of Fig. A.5 using Kemper diffusion model)

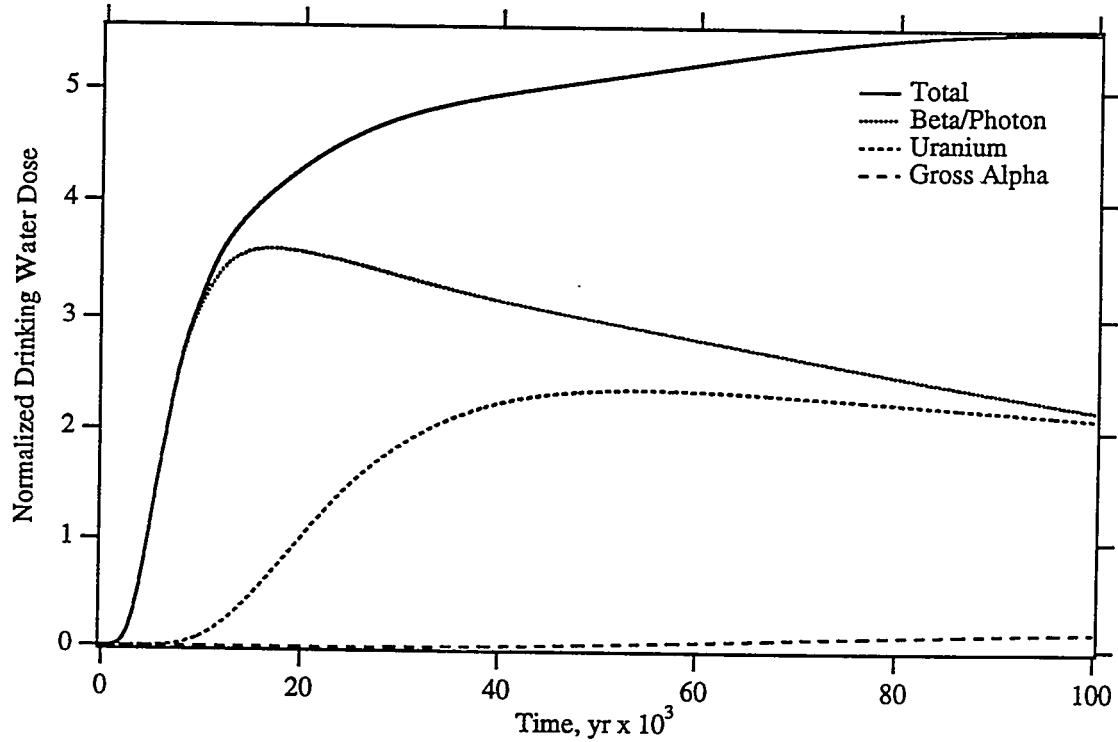


Corrosion: 1.405×10^{-5} cm/yr
 Glass Radius: 10. cm
 Recharge: 0.1 cm/yr
 Solute Diffusion Coefficient: $D_{ab} = 10^{-8}$ cm²/s, a = 1, b = 0
 Glass Hydraulic Properties: Glass Spheres (SOILPROP)
 Minimum Relative Permeability: 0.
 Retardation Model: Saturation-Independent
 Hydraulic Dispersion: $\alpha_L = 6.5$ m, $\alpha_T = 0.65$ m
 Well Interception Factor: 0.01
 Grid: Narrow (10 x 162)

Maximum Dose Records 100,000 yr [10,000 yr]

Total	22.12 [12.94] mrem/yr
Beta/Photon	14.31 [12.64] mrem/yr
⁹⁹ Tc	13.69 [12.10] mrem/yr
¹²⁹ I	0.6162 [0.5310] mrem/yr
Uranium	47.17 [2.044] µg/L
Gross Alpha	2.370 [1.768e-06] pCi/L

Figure 4.7. Drinking Water Dose (repeat of Fig. A.26)

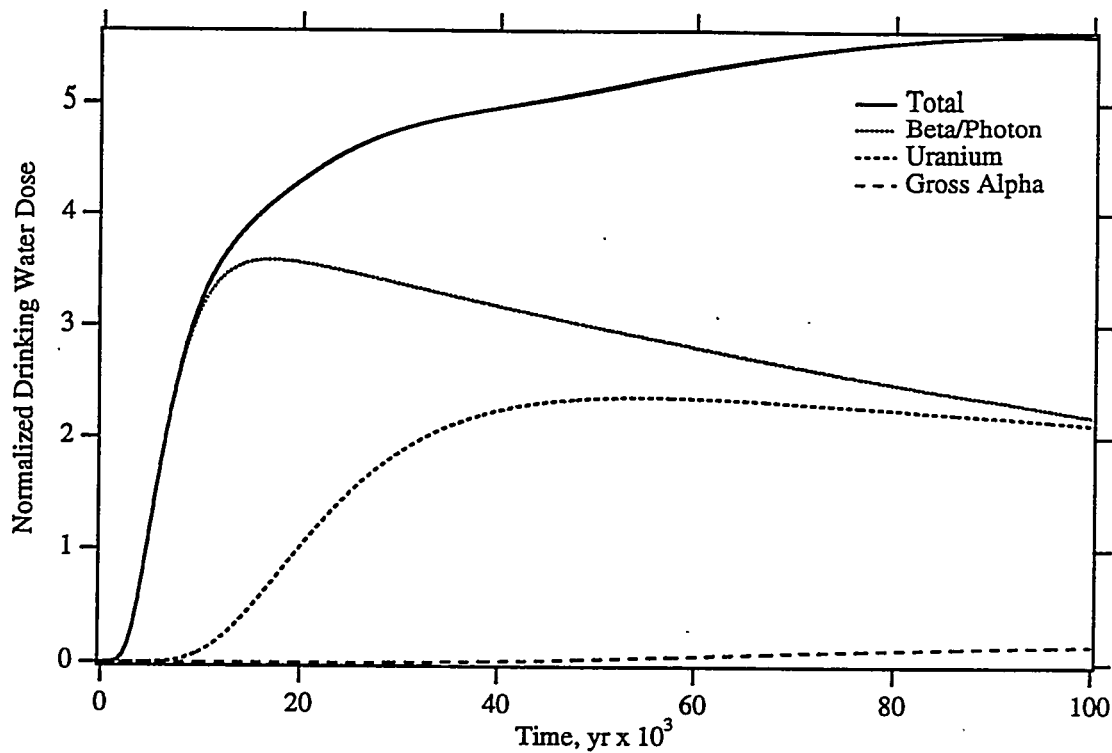


Corrosion: 1.405×10^{-5} cm/yr
 Glass Radius: 10. cm
 Recharge: 0.1 cm/yr
 Solute Diffusion Coefficient: $D_{ab} = 10^{-8}$ cm²/s, a = 1, b = 0
 Glass Hydraulic Properties: Fracture volume 2%; fracture material is gravel;
 soil matrix is Glass Spheres
 Minimum Relative Permeability: 0.
 Retardation Model: Saturation-Independent
 Hydraulic Dispersion: $\alpha_L = 6.5$ m, $\alpha_T = 0.65$ m
 Well Interception Factor: 0.01
 Grid: Narrow (10 x 162)

Maximum Dose Records 100,000 yr [10,000 yr]

Total	22.13 [12.95] mrem/yr
Beta/Photon	14.32 [12.64] mrem/yr
⁹⁹ Tc	13.70 [12.10] mrem/yr
¹²⁹ I	0.6165 [0.5312] mrem/yr
Uranium	47.19 [2.043] µg/L
Gross Alpha	2.371 [1.768e-06] pCi/L

Figure 4.8. Drinking Water Dose (repeat of Fig. A.26 with a fracture volume of 2%)



Corrosion: 1.405×10^{-5} cm/yr
 Glass Radius: 10. cm
 Recharge: 0.1 cm/yr
 Solute Diffusion Coefficient: $D_{ab} = 10^{-8}$ cm²/s, a = 1, b = 0
 Glass Hydraulic Properties: Fracture vol. 4%; fracture material is gravel;
 soil matrix is glass spheres
 Minimum Relative Permeability: 0.
 Retardation Model: Saturation-Independent
 Hydraulic Dispersion: $\alpha_L = 6.5$ m, $\alpha_T = 0.65$ m
 Well Interception Factor: 0.01
 Grid: Narrow (10 x 162)

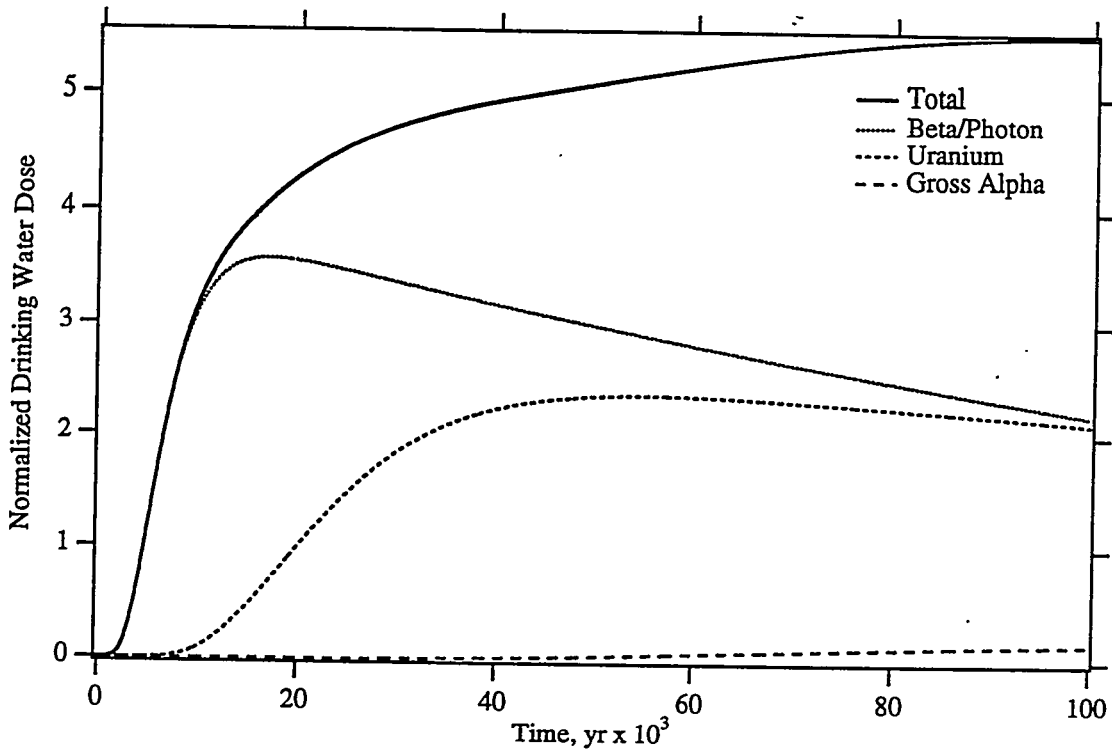
Maximum Dose Records 100,000 yr [10,000 yr]

Total	22.13 [12.94] mrem/yr
Beta/Photon	14.32 [12.64] mrem/yr
⁹⁹ Tc	13.70 [12.10] mrem/yr
¹²⁹ I	0.6168 [0.5311] mrem/yr
Uranium	47.21 [2.037] µg/L
Gross Alpha	2.371 [1.759e-06] pCi/L

Figure 4.9. Drinking Water Dose (repeat of Fig. A.26 with a fracture volume of 4%)

4.4 Water Consumption

As the glass corrodes, water will be consumed in the reactions. According to a PNNL staff member (BP McGrail), the maximum water consumption rate is 0.34 g water / g glass corroded. To judge the impact of water consumption during the corrosion process, a simulation was performed in which the glass waste was specified as a sink for water. This simulation required that STOMP be modified to exclude solute from the water sink. A second simulation was run with the standard version of STOMP, which allowed solute to be removed with the consumption of the water. In this case, the analogy is that the solute removed is incorporated in the corrosion precipitates. Figures 4.10 and 4.11 show that, relative to the results in Figure 4.7, the impact of water consumption is negligible. The total volume of water consumed represents only about 2.8% of the volume of recharge water moving through the simulation domain during the 100,000-year period. Because the impact is so small, even when using the maximum possible consumption rate, water consumption is not thought to be a significant factor in assessing the performance of WFA disposal. However, it should be emphasized that this evaluation did not consider changes in hydraulic and chemical properties as the secondary minerals are formed (and consuming water). Bacon and McGrail (1997) considered such changes using a 1-D reactive transport model and arrived at a similar conclusion. The Glass PA program plans to measure such changes and verify these simulation results.

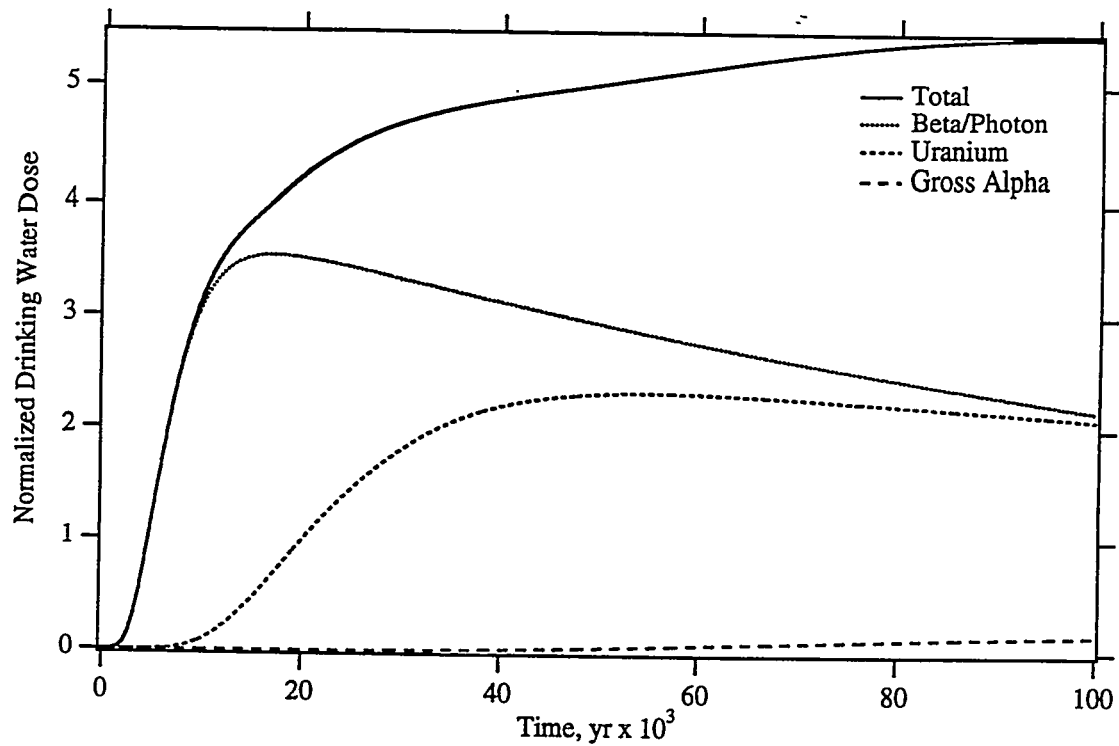


Corrosion: 1.405×10^{-5} cm/yr
 Glass Radius: 10. cm
 Recharge: 0.1 cm/yr
 Solute Diffusion Coefficient: $D_{ab} = 10^{-8}$ cm²/s, a = 1, b = 0
 Glass Hydraulic Properties: Glass Spheres (SOILPROP)
 Minimum Relative Permeability: 0.
 Retardation Model: Saturation-Independent
 Hydraulic Dispersion: $\alpha_L = 6.5$ m, $\alpha_T = 0.65$ m
 Well Interception Factor: 0.01
 Grid: Narrow (10 x 162)

Maximum Dose Records 100,000 yr [10,000 yr]

Total	22.08 [12.87] mrem/yr
Beta/Photon	14.31 [12.58] mrem/yr
⁹⁹ Tc	13.69 [12.04] mrem/yr
¹²⁹ I	0.6166 [0.5286] mrem/yr
Uranium	47.20 [1.959] µg/L
Gross Alpha	2.356 [1.564e-06] pCi/L

Figure 4.10. Drinking Water Dose (repeat of Fig. A.26 with water consumption and solutes excluded)



Corrosion: 1.405×10^{-5} cm/yr
 Glass Radius: 10. cm
 Recharge: 0.1 cm/yr
 Solute Diffusion Coefficient: $D_{ab} = 10^{-8}$ cm²/s, a = 1, b = 0
 Glass Hydraulic Properties: Glass Spheres (SOILPROP)
 Minimum Relative Permeability: 0.
 Retardation Model: Saturation-Independent
 Hydraulic Dispersion: $\alpha_L = 6.5$ m, $\alpha_T = 0.65$ m
 Well Interception Factor: 0.01
 Grid: Narrow (10 x 162)

Maximum Dose Records 100,000 yr [10,000 yr]

Total	21.80 [12.68] mrem/yr
Beta/Photon	14.10 [12.39] mrem/yr
⁹⁹ Tc	13.49 [11.86] mrem/yr
¹²⁹ I	0.6073 [0.5207] mrem/yr
Uranium	46.52 [1.937] µg/L
Gross Alpha	2.325 [1.552e-06] pCi/L

Figure 4.11. Drinking Water Dose (repeat of Fig. A.26 with water consumption and solutes included)

5.0 Conclusions and Recommendations

PNNL conducted computer simulations in FY 1997 to assess of the performance of the WFA design for the LAW disposal system to supplement the analyses conducted in FY 1995. Multiple simulations were used to identify specific parameter and conceptual model sensitivities.

The corrosion rate, recharge rate, hydraulic properties, and hydraulic and retardation models were shown to be important. The Glass PA project is supporting an ongoing effort to collect the data needed to define these parameters for the disposal system materials (LMHC 1997).

The well interception factor was shown to be important to the calculation of dose, but there is little physical basis for a specific value(s). Some effort ought to be expended determining appropriate values for this parameter for the various recharge scenarios.

The grid resolution was shown to be important when the diffusion coefficient in the disposal facility was sufficiently small and advective transport was limited. This occurred for the gravel model of glass and could occur as the glass sphere diameter is increased, particularly when there is no matrix (or filler) material.

Diffusion was shown to be important for the gravel model of glass but not the soil model. This finding is most likely the result of the soil model allowing significant advective flow through the waste zone, whereas the gravel model tended to lessen advective flow, similar to the effect of a capillary barrier. If the glass sphere diameter is increased, particularly in the absence of filler material, advection could be limited to such an extent that diffusion becomes a more important parameter.

Water consumption during corrosion and fracture flow within the glass were evaluated and found to have a minimal effect on the dose calculations. The impacts of temperature changes and osmotically-driven vapor flow were discussed and determined to be negligible.

The steady-state simulations of the WFA disposal have been useful as a guide for understanding the disposal and highlighting some important features and parameters. However, this type of analysis should not be relied on to provide a complete analysis of disposal sensitivities. The concern is that the importance of some parameters and processes depends on the actual facility design, materials, and waste form. To supplement and complement this type of study, additional detailed simulations ought to be conducted using the actual facility design, measured hydraulic and chemical properties, and reasonable estimates of the disposal waste form corrosion rate, formation of secondary minerals, and resulting changes in properties.

6.0 References

Bacon DH and McGrail BP, 1997. "Source Term Analysis for Hanford Low-Activity Tank Waste Using the Storm Code: A Coupled Unsaturated Flow and Reactive Transport Model," PNNL-SA-29252, Pacific Northwest National Laboratory, Richland, Washington.

Kincaid CT, JW Shade, GA Whyatt, MG Piepho, K Rhoads, JA Voogd, JH Westsik, Jr., MD Freshley, KA Blanchard, and BG Lauzon, 1995. "Volume 1: Performance Assessment of Grouted Double-Shell Tank Waste Disposal at Hanford," WHC-SD-WM-EE-004, Rev. 1, Vol. 1, Westinghouse Hanford Company, Richland, Washington.

LMHC, 1997. "Statements of Work for FY 1998 to 2003 for the Hanford Low-Level Tank Waste Performance Assessment Activity," HNF-SD-WM-PAP-062, Rev. 2, Lockheed Martin Hanford Company, Richland, Washington.

Mann FM, CR Eiholzer, NW Kline, BP McGrail and MG Piepho, 1995. "Impacts of Disposal System Design Options on Low-Level Glass Waste Disposal System Performance," WHC-EP-0810, Westinghouse Hanford Company, Richland, Washington.

McGrail BP and LA Mahoney, 1995. "Selection of a Computer Code for Hanford Low-Level Waste Performance Assessment," PNL-10830, Pacific Northwest National Laboratory, Richland, Washington.

White MD and M Oostrom, 1996. "STOMP Subsurface Transport Over Multiple Phases: Theory Guide," PNNL-11217, Pacific Northwest National Laboratory, Richland, Washington.

Appendix

Sensitivity Analysis of Transport Parameters on the Performance of the Waste-Form-Alone Design for the Low-Activity-Waste Disposal System

C. T. Kincaid
M. D. White

Appendix

Sensitivity Analysis of Transport Parameters on the Performance of the Waste-Form-Alone Design for the Low-Activity-Waste Disposal System

This appendix documents computer simulations executed to assess the performance of the waste-form-alone (WFA) design for the low-activity-waste (LAW) disposal system. Objectives for this work were to 1) independently check the validity of the performance estimates from the report entitled, *Impacts of Disposal System Options on Low-Level Glass Waste Disposal System Performance* (hereinafter referred to as the Rawlins report^(a)), 2) perform a sensitivity analysis on performance relative to critical transport parameters, and 3) provide a technical basis for estimating the allowed source terms for the LAW disposal system. All objectives were to be performed assuming that the waste form would be the only part of the engineered disposal system that inhibits radionuclide release—the waste-form-alone assumption. Unless specifically addressed, parameters for radionuclide transport, glass corrosion, and drinking water dilution were obtained directly from the Rawlins report. Calculations were performed with a modified version of the STOMP (Subsurface Transport over Multiple Phases) simulator (White and Oostrom 1996).^(b,c)

A.1 Simulator Overview

The STOMP simulator was designed to be a general purpose tool for simulating subsurface flow and transport and to complement other analytical capabilities developed by Pacific Northwest National Laboratory's Environmental Technologies Division. The simulator was specifically designed to provide scientists and engineers from varied disciplines with multidimensional capabilities for modeling subsurface flow and transport phenomena. STOMP's target capabilities were guided by proposed and applied remediation activities at sites contaminated with volatile organic compounds and/or radioactive material. Developed with the support of the U.S. Department of Energy, Office of Environmental Restoration and Waste Management, the simulator's modeling capabilities address a variety of subsurface environments, including variably saturated, multiple-phased, nonisothermal, and variably frozen soils. The STOMP simulator has a configurable structure that allows the code to efficiently model a variety of physical systems and phase conditions. The configuration used for our investigations solved for water and solute transport through a variably saturated porous media system, assuming a passive gas phase at constant pressure. Transport was solved sequentially per solute, following the calculation of the aqueous flow field.

(a) Rawlins JA, RA Karnesky, R Khaleel, AH Lu, FM Mann, BP McGrail, WJ McMahon, MG Piepho, PD Rittmann, and F Schmittroth, 1995. "Impacts of Disposal System Options on Low-Level Glass Waste Disposal System Performance," Draft report dated March 1995, Westinghouse Hanford Company, Richland, Washington. March 1995. The report was later modified and published (Mann et al. 1995).

(b) White MD and M Oostrom. 1995. *STOMP Subsurface Transport Over Multiple Phases, User's Guide* (draft). Pacific Northwest Laboratory, Richland, Washington.

(c) Nichols WE, NJ Aimo, M Oostrom, and MD White. 1995. *STOMP Subsurface Transport over Multiple Phases, Application Guide* (draft). Pacific Northwest Laboratory, Richland, Washington.

A.2 Simulator Modifications

To verify the simulation results in the Rawlins report for radionuclide transport and drinking water dose, two aspects of the STOMP simulator were modified. The first aspect involved the expression for solute partitioning in partially saturated soils, and the second involved the expression for the effective solute diffusion coefficient in partially saturated soils. The STOMP simulator had originally been formulated with different models for these constitutive relations than those used for the Rawlins report simulations. Verification of the simulation results in the Rawlins report required that the STOMP simulator be modified to include these constitutive relations.

A.2.1 Solute Partitioning Modifications

The original model for solute partitioning in partially saturated soils coded in the STOMP simulator assumes that all solid surfaces remain wetted, regardless of the liquid saturation, as

$$K_{sl} = \frac{C_s}{C_l \rho_s}$$

where K_{sl} is the solid-aqueous distribution coefficient (m^3/kg), C_s is the solute concentration adsorbed on the solid phase (Ci/m^3), C_l is the solute concentration dissolved in the aqueous phase (Ci/m^3), and ρ_s is the solid grain density (kg/m^3). This approach leads to an effective retardation coefficient defined as

$$R_D = 1 + \frac{(1 - n_T) \rho_s K_{sl}}{n_D s_l}$$

where R_D is the dimensionless retardation coefficient, n_T is the dimensionless total porosity, n_D is the dimensionless diffusive porosity, and s_l is the dimensionless aqueous saturation. This formulation for the retardation coefficient will be referred to as saturation-dependent retardation. An alternative model used in the Rawlins report simulations assumes that the solid surfaces available for solute adsorption are proportional to the liquid saturation as

$$K_{sl} = \frac{C_s}{C_l \rho_s s_l}$$

This assumption implies that all solid surfaces are not covered with water until the porous medium is saturated. Although it may be true at very low saturations, this assumption is not valid over the entire range of saturation. Using the alternative model of K_{sl} leads to an alternative definition of the retardation coefficient as

$$R_D = 1 + \frac{(1 - n_T) \rho_s K_{sl}}{n_D}$$

The alternative K_{sl} formulation yields lower retardation coefficients (i.e., faster migration rates) than the original model coded in the STOMP simulator. The STOMP simulator was modified to allow use of either distribution constitutive relation. This formulation for the retardation coefficient will be referred to as saturation-independent retardation.

A.2.2 Solute Diffusion Modifications

The model for solute diffusion in the STOMP simulator uses an effective diffusion coefficient defined as

$$D_{le} = \tau_l s_l^n D_l$$

where D_{le} is the effective diffusion coefficient (m^2/s), τ_l is the dimensionless tortuosity for the aqueous phase, and D_l is the molecular diffusion coefficient (m^2/s). The tortuosity is typically a function of aqueous saturation and porosity according to the theory of Millington and Quirk (1959). The simulator in the Rawlins report uses an alternative approach, known as the Kemper effective diffusion model, to compute the effective diffusion coefficient as

$$D_{le} = D_l a_s \exp(b_s s_l^n)$$

where a_s and b_s are empirical parameters that are functions of the solute and soil pair. The STOMP simulator was modified to allow either definition for the effective diffusion coefficient.

A.3 Dose Calculations

The conversion from solute concentrations at the water table to drinking water dose was neither completely described in the Rawlins report nor recorded in the simulation input files. The descriptions in the following paragraphs document conversions used in these assessment and verification studies. Solute concentrations and sources in the STOMP simulations were expressed as volume (m^3) of dissolved glass per unit aqueous-phase volume (m^3). Transport of radionuclides from the proposed disposal vaults to the groundwater was simulated by organizing the inventory of radionuclides into four groups according to soil sorption characteristics. Results from STOMP simulations were expressed in volumetric fluxes (dissolved glass) at the water table. The results were then converted to inventory flux rates or inventory concentrations at the water table.

Doses for each radionuclide were then computed by considering the radionuclide's inventory, radioactive decay rate, and dose conversion factors. The following equations document the conversion of simulation results for volumetric glass flux at the water table into drinking water dose. Two standards were followed in computing drinking water doses. In the first approach drinking water conversion factors proposed by the U.S. DOE (draft 10 CFR 834) were used to convert well water concentrations from curies to dose. "Total" dose under this approach was computed by summing the individual doses computed for each radionuclide. This standard will be referred to as the DOE Dose Standard. In the second approach, radionuclides were divided into three categories, beta particles and photon emitters (referred to as beta/photon emitters), uranium isotopes, and gross alpha emitters, based on the U.S. Environmental Protection Agency proposed national primary drinking water regulations for radionuclides (40 CFR 141-142). Under this standard, "total" dose is computed for each category of radionuclide by summing the individual doses computed for each radionuclide within the category. This standard will be referred to as the EPA Dose Standard.

A.3.1 DOE Dose Standard

Radionuclide flux rates at the water table were computed from volumetric fluxes (dissolved glass) as

$$\dot{C}_{wt}^{\gamma} = \frac{\dot{q}_{wt}^g C_i^{\gamma}}{V^v V_f^g} \exp\left(\frac{-t \ln(2)}{\lambda^{\gamma}}\right)$$

where \dot{C}_{wt}^{γ} is the radionuclide flux at the water table (Ci/yr), \dot{q}_{wt}^g is the equivalent dissolved glass volumetric flux at the water table ($\text{m}^3_{\text{glass}}/\text{yr m}_{\text{vault}}$), C_i^{γ} is the radionuclide inventory (Ci), V^v is the vault volume ($\text{m}^3_{\text{vault}}/\text{m}_{\text{vault}}$), V_f^g is the glass volume fraction ($\text{m}^3_{\text{glass}}/\text{m}^3_{\text{vault}}$), t is the time (yr),

λ^{γ} is the radionuclide half-life (yr), and the superscript γ represents the radionuclide. Radionuclide concentrations at the water table were computed from the radionuclide flux rates and the infiltration rate as

$$c_{wt}^{\gamma} = \frac{\dot{C}_{wt}^{\gamma}}{\dot{q}_{wt}^w A^d}$$

where c_{wt}^{γ} is the radionuclide concentration at the water table ($\text{Ci}/\text{m}^3_{\text{water}}$), \dot{q}_{wt}^w is the infiltration rate at the water table ($\text{m}^3_{\text{water}}/\text{yr m}^2_{\text{domain}}$), and A^d is the domain area ($\text{m}^2_{\text{domain}}$). Doses were computed from radionuclide concentrations at the water table through a well intercept factor and dose conversion factor as

$$D^{\gamma} = c_{wt}^{\gamma} F_{wi} F_{dc}^{\gamma}$$

where D^{γ} is the radionuclide dose (mrem/yr), F_{wi} is the well intercept factor ($\text{m}^3_{\text{water}}/\text{m}^3_{\text{drinking water}}$), and F_{dc}^{γ} is the dose conversion factor ($(\text{mrem/yr})/(\mu\text{Ci}/\text{mL}_{\text{drinking water}})$). The well intercept factor converted concentrations of the radionuclides at the water table to those in pumped drinking water. The dose conversion factor converted concentrations of the radionuclides in drinking water to human doses to a "reference man" who consumes 740 liters of drinking water per year (draft 10 CFR 834). The dose conversion factors are equivalent to the DOE Dose Standard conversions. Combining the above dose conversion equations produces the conversion for equivalent glass volumetric flux rate at the water table to radionuclide dose as

$$D^{\gamma} = \frac{\dot{q}_{wt}^g C_i^{\gamma} F_{wi} F_{dc}^{\gamma} \exp\left(\frac{-t \ln(2)}{\lambda^{\gamma}}\right)}{\dot{q}_{wt}^w A^d V^v V_f^g}$$

"Total" doses were computed by summing the dose contributions for each radionuclide over the inventory of radionuclides as

$$D = \sum_{\gamma=^{14}\text{C}, ^{90}\text{Sr}, \dots} D^{\gamma}$$

The total dose was then referenced to the DOE dose standard of 4 mrem/yr. This dose calculation approach follows the techniques specified in the Rawlins report and will be used to compute dose rates for the discussions on the simulation results. An alternative dose calculation approach, which divides the dose calculations into three water quality standards, will be described below. This

alternative dose calculation technique is used to assess low-level waste inventory limits for the candidate radionuclides. For reference, the radionuclide inventories studied in the Rawlins report are shown in Table A.1. Included in the table is an inventory level for ^{99}Tc that has been reduced to 20% of the preliminary inventory, referred to as 20% ^{99}Tc .

Table A.1. Preliminary Inventories for Low-Level Waste (LLW) Disposal

<u>Radionuclide</u>	<u>Before Separation</u>	<u>Before Melter</u>	<u>LLW Glass</u>
^{14}C	$5.3 \times 10^3 \text{ Ci}$	$5.0 \times 10^3 \text{ Ci}$	$5.0 \times 10^1 \text{ Ci}$
$^{90}\text{Sr}, \text{Y}$	$1.4 \times 10^8 \text{ Ci}$	$6.0 \times 10^6 \text{ Ci}$	$6.0 \times 10^6 \text{ Ci}$
^{99}Tc	$4.0 \times 10^4 \text{ Ci}$	$2.4 \times 10^4 \text{ Ci}$	$2.4 \times 10^4 \text{ Ci}$
20% ^{99}Tc	$4.0 \times 10^4 \text{ Ci}$	---	$4.8 \times 10^3 \text{ Ci}$
^{129}I	$5.1 \times 10^1 \text{ Ci}$	$5.1 \times 10^1 \text{ Ci}$	$5.1 \times 10^0 \text{ Ci}$
$^{137}\text{Cs}, \text{Ba}$	$1.0 \times 10^8 \text{ Ci}$	$1.0 \times 10^6 \text{ Ci}$	$1.0 \times 10^6 \text{ Ci}$
^{234}U	$6.6 \times 10^2 \text{ Ci}$	$3.9 \times 10^1 \text{ Ci}$	$3.9 \times 10^1 \text{ Ci}$
^{235}U	$2.0 \times 10^1 \text{ Ci}$	$1.2 \times 10^0 \text{ Ci}$	$1.2 \times 10^0 \text{ Ci}$
^{238}U	$4.7 \times 10^2 \text{ Ci}$	$2.8 \times 10^1 \text{ Ci}$	$2.8 \times 10^1 \text{ Ci}$
^{237}Np	$6.2 \times 10^1 \text{ Ci}$	$6.2 \times 10^0 \text{ Ci}$	$6.2 \times 10^0 \text{ Ci}$
^{239}Pu	$3.1 \times 10^4 \text{ Ci}$	$1.6 \times 10^3 \text{ Ci}$	$1.6 \times 10^3 \text{ Ci}$
^{240}Pu	$8.0 \times 10^3 \text{ Ci}$	$4.0 \times 10^2 \text{ Ci}$	$4.0 \times 10^2 \text{ Ci}$
^{241}Am	$1.5 \times 10^5 \text{ Ci}$	$8.0 \times 10^3 \text{ Ci}$	$8.0 \times 10^3 \text{ Ci}$

A.3.2 EPA Dose Standard

An alternative approach to computing drinking water dose divides the nuclides into three radionuclide categories, 1) beta/photon emitters, 2) uranium isotopes, and 3) gross alpha emitters. Using this approach, the drinking water standard for beta/photon emitters is 4 mrem/yr and is computed according to the technique already described. The drinking water standard for uranium isotopes, which includes ^{234}U , ^{235}U , and ^{238}U , is 20 $\mu\text{g/L}$. Computation of the uranium isotope dose requires the conversion of the drinking water concentration from $\mu\text{Ci/mL}$ to $\mu\text{g/L}$ through a specific activity conversion factor. A list of specific activities for the uranium isotopes is shown in Table A.2. The drinking water standard for alpha emitters, which for the current proposed inventory includes ^{237}Np , ^{239}Pu , ^{240}Pu , and ^{241}Am , is 15 pCi/L. Doses for alpha emitters are computed following the techniques already described, with the exception of the dose-conversion factor, which is replaced with a standard conversion factor of 10^9 to convert concentrations from $\mu\text{Ci/mL}$ into pCi/L.

Table A.2. Specific Activity for Uranium Isotopes

<u>Radionuclide</u>	<u>Half-Life</u>	<u>Specific Activity</u>
^{234}U	$2.445 \times 10^5 \text{ yr}$	$6.254 \times 10^{-3} \text{ Ci/g}$
^{235}U	$7.038 \times 10^8 \text{ yr}$	$2.163 \times 10^{-6} \text{ Ci/g}$
^{238}U	$4.468 \times 10^9 \text{ yr}$	$3.365 \times 10^{-7} \text{ Ci/g}$

A.4 Simulation Results and Discussions

This investigation primarily involved four activities. The first set of simulations performed was used to validate the results reported in the Rawlins report. These simulations were designed to replicate to a reasonable accuracy the "central analysis case" (CAC) in the Rawlins report. The second set of simulations was used to define a "preliminary estimate case" (PEC) for performance

of the WFA design for the LAW disposal system. The conceptual model for the PEC simulation differed from that of the CAC simulation and represented an independent approach. The third set of simulations investigated the sensitivity of system performance on the critical hydrologic, meteoric/surface, and transport parameters. These simulations do not represent a complete treatment of processes that potentially affect the performance of the disposal system, but they do consider critical transport processes. The fourth set of simulations makes a preliminary examination of the draft product acceptance specifications for the glass waste. Viewed as a whole, these simulations demonstrate a critical need to 1) specify the waste form and associated matrix media and 2) develop hydraulic and transport properties for that waste form.

Because of the multiple dose standards, many drinking water dose results are reported using normalized values. Drinking water dose results labeled "total" refer to the DOE Dose Standard and are referenced to a 4 mrem/yr standard. Drinking water dose results labeled "Beta / Photon" refer to the beta/photon emitters of the EPA Dose Standard and are referenced to the same standard. Drinking water dose results labeled "Uranium" refer to the dose from all uranium isotopes according to the EPA Dose Standard and are referenced to a 20 µg/L standard. Drinking water dose results labeled "Gross Alpha" refer to the alpha emitters of the EPA Dose Standard and are referenced to a 15 pCi/L standard. Drinking water dose standards for the reported results are summarized in Table A.3. The Rawlins report showed that the radionuclides ⁹⁹Tc and ¹²⁹I contributed a significant fraction of the total dose. Therefore, Table A.3 lists the dose standard for each of these radionuclides.

Table A.3. Drinking Water Dose Standards

<u>Label</u>	<u>Radionuclides</u>	<u>Standard</u>
Total	¹⁴ C, ⁹⁰ Sr, ⁹⁹ Tc, ¹²⁹ I, ¹³⁷ Cs, ²³⁴ U, ²³⁵ U, ²³⁸ U, ²³⁷ Np, ²³⁹ Pu, ²⁴⁰ Pu, ²⁴¹ Am	4 mrem/yr
⁹⁹ Tc	⁹⁹ Tc	4 mrem/yr
¹²⁹ I	¹²⁹ I	4 mrem/yr
Beta/Photon	¹⁴ C, ⁹⁰ Sr, ⁹⁹ Tc, ¹²⁹ I, ¹³⁷ Cs	4 mrem/yr
Uranium	²³⁴ U, ²³⁵ U, ²³⁸ U	20 µg/L
Gross Alpha	²³⁷ Np, ²³⁹ Pu, ²⁴⁰ Pu, ²⁴¹ Am	15 pCi/L

A.4.1 Validation Exercise

A validation simulation was performed with STOMP based on the simulation described as the CAC in the Rawlins report. This simulation involves the packaging of the LAW in 0.25-cm-radius glass spheres with a corrosion rate of 10⁻⁵ cm/yr. Surface recharge is fixed at 0.1 cm/yr. An attempt was made to duplicate the CAC simulation with two notable changes to the initial conditions and grid domain. Both changes were motivated by the need to shorten execution times to meet the time and work scope requirements of this study. The CAC simulation used nonsteady flow initial conditions and allowed the flow field to equilibrate over a 3000-year period, after which steady-flow conditions were applied; the present simulations used steady flow initial conditions. Because both approaches start with an essentially dry domain, neither is believed to significantly alter release in the first 3000-year period. By using a steady flow field and eliminating the need for computing a transient flow, the transport simulations were executed in less time. The CAC simulation used a computational domain that contained 77 nonboundary nodes arranged horizontally across the simulated domain; and the present simulations used 10 nonboundary nodes in the horizontal direction. The number of nodes in the vertical direction was identical in both simulations. This approach significantly reduced the bandwidth of the equation set and allowed more efficient simulations.

In addition to the modifications to the STOMP code for the Kemper effective diffusion model and the saturation-independent retardation factor, simulating the CAC required that a relative permeability minimum of 10^{-10} be applied. The PORFLOW code allows the user to specify a minimum value for the relative permeability where the default value is 10^{-10} (Runchal and Sagar 1992). Because no value was specified in the conceptual model for the CAC, as executed with PORFLOW, a minimum relative permeability of 10^{-10} was applied. Combined with the relatively high saturated hydraulic conductivity of 5.83×10^5 m/yr, a minimum unsaturated hydraulic conductivity of 5.83×10^{-5} m/yr resulted for the glass waste material. This artificial relative permeability limit will be shown to have a marked impact on predicting system performance both in terms of drinking water doses and transport processes. With a relative permeability minimum of 10^{-10} applied in the STOMP simulator, drinking water dose results for the CAC simulation for the present analysis are shown in Figure A.1. The results reported as "total" dose are comparable to those reported in Figure A.3 of the Rawlins report.

Comparing the two figures reveals moderate differences (~10%) between the results in terms of drinking water dose peaks and distributions for each radionuclide (e.g., STOMP peak ~165 mrem/yr, CAC peak ~140 mrem/yr). Integrated values of drinking water doses show close agreement between the two figures, which suggests that the dose calculations follow the same theory. Three possibilities have been identified that could explain the moderate differences between the results. As described previously, the STOMP simulations used a conceptual model with a coarser grid in the horizontal direction than that reported in the Rawlins report. The STOMP simulations were also initiated from a steady flow field, whereas the simulations of the Rawlins report were initiated with a pseudo steady flow field that required 3000 years of simulation time to equilibrate. The third possibility is that unknown differences remain in the flow and transport algorithms between the PORFLOW and STOMP simulators. To test the impact of grid coarseness on the drinking water dose results, a simulation was executed with double the number of nodes along the horizontal direction. Results from this simulation are shown in Figure A.2. Because the results in the figure differ only slightly from those in Figure A.1, we conclude that the conceptual model with the narrow grid in the horizontal direction provides ample noding resolution.

To investigate the impact of the relative permeability limit, imposed for the simulations reported in the Rawlins report, the CAC simulation was executed without a minimum relative permeability limit. The results of this simulation are shown in Figure A.3. With the relative permeability limit lifted, transport of the radionuclides through the glass waste changes from being advection-dominated to being diffusion-dominated. This result can be seen by the contrast in the ^{99}Tc dose profiles between Figures A.1 and A.3. Not only is the peak ^{99}Tc dose, of Figure A.3, lower but the low effective diffusion coefficient specified for the glass waste serves to retain a portion of the ^{99}Tc inventory in the glass waste beyond 100,000 years. This hypothesis is further supported by the results in Figures A.4 and A.5, where the effective diffusion coefficients for the glass waste are increased to 10^{-9} cm²/s and 10^{-8} cm²/s, respectively. Each increase in the effective diffusion coefficient for the glass waste yields significantly higher peak doses and more narrow "breakthrough" profiles.

A.4.2 Preliminary Estimate Case

Without the relative permeability limit, the glass-waste material performs as a nearly ideal hydraulic barrier with the transport rate for radionuclides being controlled by diffusion through the medium to the surrounding flow field. Images of the flow field under these conditions show all of the infiltrating water being shunted around the waste disposal zone. However, confidence is low that the glass waste will act as an ideal hydraulic barrier over a 100,000-year period. To model manufacturing variations and degradation of the glass beads, hydraulic properties were generated based on a distribution of glass bead radii of about 0.25 cm. The SOILPROP computer code

generates estimates of saturated hydraulic conductivity, irreducible saturation, and soil moisture retention parameters from particle size distribution data (Mishra and Parker 1991). The glass waste hydraulic properties were estimated from a particle size distribution of 20% medium sand, 60% coarse sand, and 20% very coarse sand with a porosity of 0.518. The resulting hydraulic properties are shown in Table A.4. These parameters were then substituted for the glass waste hydraulic parameters, and the transport simulation was reexecuted. The effective diffusion coefficient for this simulation was reset to the 10^{-10} cm²/s value established for the Rawlins report. The results in terms of drinking water dose, shown in Figure A.6, demonstrate the sensitivity of the transport solution to the hydraulic properties of the glass waste. Transport within the glass waste has switched again from diffusion-dominated to advection-dominated, where the new glass waste hydraulic properties yield higher saturations and aqueous flow rates vertically through the glass waste. These results are similar to those in the Rawlins report, in that the artificial minimum relative permeability created an advectively dominated transport domain within the glass waste.

Table A.4. Glass Waste Hydraulic Property Parameters

Parameter	Value
Hydraulic conductivity	6.38×10^4 m/yr
Irreducible saturation	0.01
van Genuchten α	21.5 1/m
van Genuchten n	2.26

To test the hypothesis that transport within the glass waste was advection-dominated, the effective diffusion coefficient was increased from 10^{-10} to 10^{-8} cm²/s. Results from this simulation are shown in Figure A.7. As expected, for an advection-dominated region the local diffusion coefficient had practically no effect on the overall transport of radionuclides. Because the radionuclide transport appears to be generally advectively dominated, hydraulic dispersion should be considered. In the simulations performed for the Rawlins report hydraulic dispersion was ignored, therefore, to account for hydraulic dispersion, longitudinal and transverse dispersivities of 6.5 m and 0.65 m were applied. These dispersivities represent 1/10 and 1/100 of the vertical distance from the glass waste disposal system to the water table. Transport simulations were executed using these hydraulic dispersivities, and their results are shown in Figure A.8. As expected, increasing hydraulic dispersion lowers the peak doses and spreads the dose profile. Although the input parameters differ significantly, the resulting dose curves coincidentally resemble those from the Rawlins report for the CAC conditions.

The well intercept factor of 0.006 used in the Rawlins report was modified from the Hanford grout performance assessment value of 0.01 with the justification that the larger area of the glass vaults could be an advantage. The reduction in the well intercept factor was founded on the assumption that the disposal facility could be oriented to take advantage of the groundwater flow direction. However, confidence that the groundwater flow will maintain in a constant direction over the next 10,000 years is low; therefore, a well interception factor of 0.01 was reapplied. Because the well intercept factor is applied in a linear fashion to the transport results, increasing it directly yields greater dose rates, as shown in Figure A.9, which can be compared with the results shown in Figure A.8.

The dose results shown in Figure A.9 will be used for comparison purposes in the sensitivity analysis and represent the combination of simulation parameters referred to as the PEC (preliminary estimate case). The PEC differs from the CAC of the Rawlins report in five respects: 1) the effective diffusion coefficient for the glass waste was increased from 10^{-10} to 10^{-8} cm²/s,

2) the hydraulic properties for the glass waste were changed from those for gravel to those for a distribution of particle sizes of about 0.25 cm radii, 3) the minimum relative permeability was lowered from 10^{-10} to zero, 4) hydraulic dispersion was included, and 5) the well interception factor was increased from 0.006 to 0.01. This investigation has demonstrated the importance of characterizing the hydraulic and transport properties of the glass waste. The parameters selected for the PEC do not necessarily represent the best estimate of a conceptual model for the glass waste disposal system, but do represent the current understanding for the WFA design. Prior to investigating the sensitivity of the PEC to infiltration rate and corrosion rate, one simulation was executed to examine the sensitivity of the PEC to the retardation model. The PEC used the retardation factor that was independent of saturation, whereas this simulation used the saturation-dependent retardation factor. Results from this simulation are shown in Figure A.10. The unretarded radionuclides (e.g., ^{99}Tc and ^{129}I) show identical dose profiles; however, the retarded radionuclides (e.g., ^{234}U , ^{235}U , ^{238}U , and ^{237}Np) show delayed peak arrival times and more diffuse profiles. These results indicate that the saturation-independent retardation coefficient yield significantly higher peak doses for retarded radionuclides over the saturation-dependent coefficients. If the pore walls are continuously wetted from the water table to the glass waste (which is indicated by the steady-flow saturation profiles), the saturation-dependent model more accurately describes the phase distribution physics.

A.4.3 Sensitivity Analysis

Using the narrow computation grid, a sensitivity analysis was performed to determine the response of the disposal system (in terms of drinking water dose) to variations in critical parameters. Two critical parameters were chosen for this analysis: infiltration rate and glass waste corrosion rate. These parameters compose only a limited set of candidate model parameters and were selected because they represent design options for the WFA disposal system and yield a nonlinear variation in the dose rate. Parameters such as the loading density and radionuclide source terms scale linearly and therefore were not selected for this sensitivity analysis. Simulations were executed which varied from the PEC values of 0.1 cm/yr and 10^{-5} cm/yr for infiltration and corrosion rates, respectively. Simulated infiltration rates included those at 0.01 cm/yr, 0.1 cm/yr, and 1.0 cm/yr, and simulated glass waste corrosion rates included those at 10^{-8} , 10^{-7} , 10^{-6} , 10^{-5} , 10^{-4} , and 10^{-3} cm/yr. Each sensitivity case was executed with both retardation coefficient models, the saturation-dependent and saturation-independent formulations.

Simulation results for the PEC with variations in corrosion rates from 10^{-3} to 10^{-8} cm/yr are shown in Figures A.9 and A.11 through A.15 using saturation-independent retardation. Results for the same simulations using saturation-dependent retardation are shown in Figures A.10 and A.11a through A.15a. These simulations used a common infiltration rate fixed at 0.1 cm/yr. For those simulations with high corrosion rates, transport through the hydrologic system controls the peak doses and dose profiles. This is evidenced by comparing the simulations for corrosion rates of 10^{-3} and 10^{-4} cm/yr (Figures A.11 and A.12), where the peak doses and dose profiles are nearly identical. Corrosion rates faster than 10^{-3} cm/yr would show similar results. At the corrosion rates of 10^{-5} and 10^{-6} cm/yr (Figures A.9 and A.13), both the glass corrosion and hydraulic system influence the dose profiles. For corrosion rates at or below 10^{-7} cm/yr (Figures A.14 and A.15), the corrosion rate primarily controls the dose profiles. These results indicate that the dose profiles for the PEC are influenced by both transport through the hydrologic system and release of radionuclides through glass corrosion. At higher infiltration rates one would expect the corrosion rate to dominate the dose profiles. Conversely, at lower infiltration rates, transport and retardation in the hydrologic system would be expected to dominate the dose rates. Maximum dose rates for the combined inventory of radionuclides require a glass release time of approximately 5×10^6 years to meet drinking water standards over the 100,000-year period.

Compared with saturation-independent retardation, the saturation-dependent retardation formulation yields longer travel times through the vadose zone for the retarded radionuclides. Travel times for the unretarded radionuclides (e.g., ^{99}Tc , ^{129}I) are independent of the retardation formulation. Generally, the saturation-dependent retardation simulations yield lower drinking water doses because the retarded radionuclides are held longer within the vadose zone. The most significant differences in total drinking water dose between saturation-dependent and -independent retardation occur when the retarded radionuclides have relatively short travel times and contribute significantly to the dose, as shown by comparing Figures A.15 and A.15a.

The effects of glass corrosion rates from 10^{-3} to 10^{-8} cm/yr for an infiltration rate of 0.01 cm/yr are shown in Figures A.16 through A.21 using saturation-independent retardation. Results for the same simulations using saturation-dependent retardation are shown in Figures A.16a through A.21a. As anticipated, the lower infiltration rate favors the hydrologic system as the controlling component. At this infiltration rate, the dose peaks and profiles are nearly identical for the glass corrosion values of 10^{-3} , 10^{-4} , and 10^{-5} cm/yr (Figures A.16 through A.18). Results for the corrosion rate of 10^{-6} (Figure A.19) show the influence of both the corrosion rate and hydrologic system. Glass waste with corrosion rates below 10^{-7} (Figures A.20 and A.21) yield dose profiles characterized as corrosion-controlled. Maximum dose rates for the combined inventory of radionuclides require a glass release time of approximately 2×10^6 years to meet the drinking water standards over the 100,000-year period.

The effects of glass corrosion rates from 10^{-5} to 10^{-8} cm/yr for an infiltration rate of 1.0 cm/yr are shown in Figures A.22 through A.25, using saturation-independent retardation. Results for the same simulations using saturation-dependent retardation are shown in Figures A.22a through A.25a. As anticipated, the higher infiltration rate favors the glass corrosion rate as the controlling component. More importantly, the infiltration rate is sufficient to transport ^{239}Pu to the water table within the 100,000-year period studied. Because of the higher drinking-water dose factor for ^{239}Pu , this radionuclide dominates the drinking water dose peaks at later times. Moreover, the doses from ^{239}Pu are high enough to prevent the system from meeting the drinking water standards over the 100,000-year period for all of the simulated corrosion rates. To demonstrate the importance of the retardation factor model, the simulation with a corrosion rate of 10^{-5} cm/yr and an infiltration rate of 1.0 cm/yr was reexecuted using the saturation-dependent retardation factor model. Dose results from this simulation are shown in Figure A.22a. Assuming the pore surfaces remain water-wet for partially saturated systems changes the dynamics of the ^{239}Pu retardation and resulting dose profiles. This assumption retards the ^{239}Pu movement within the vadose zone, allows decay to occur, and delays ^{239}Pu release to the water table to the 100,000-year time frame, making ^{99}Tc the dominant dose source.

A.4.4 Draft Product Acceptance Specifications

The draft product acceptance specifications call for a waste form with a long-term glass mass loss rate, C_{gm} , of 1×10^{-3} g/m²d and a surface area to volume ratio of 30 m⁻¹. The volumetric corrosion rate of the glass, C_{gv} , in cm/yr is given by dividing the mass loss rate by the mass density of glass, ρ_g , as

$$C_{gv} = \frac{C_{gm}}{\rho_g}$$

For this study the mass density is assumed to be 2.6 g/cm³. The corresponding corrosion rate is 1.405 x 10⁻⁵ cm/yr. For this analysis we have assumed the waste form has a spherical shape. For a sphere, the surface-to-volume ratio is 3/r, where *r* is the sphere radius. For a sphere with a surface to volume ratio of 30 m⁻¹ (i.e., 10 cm radius), the time required for complete release of the glass, *t_r*, is given by dividing the radius by the volumetric corrosion rate as

$$t_r = \frac{r}{C_{gv}} = \frac{r \rho_g}{C_{gm}}$$

which yields 7.12 x 10⁵ years for complete release of the radionuclide inventory. Four simulations were executed using these draft product acceptance specifications for the glass radius and corrosion rate. The first simulation, shown in Figure A.26, used the preliminary estimate case parameters except for the glass radius and corrosion rate. In this simulation, the beta/photon emitter peak dose is predicted to be 14.33 mrem/yr and results from the superposition of the peaks of ⁹⁹Tc and ¹²⁹I. The second simulation, shown in Figure A.26a, repeated the first but used saturation-dependent retardation. The results for this simulation show the effect of the more realistic and hence less conservative saturation-dependent retardation. The retarded radionuclides of the uranium and gross alpha emitter groups are further delayed in the vadose zone profile that overlies the ground-water aquifer. Because of this retention the dose curves for these groups are shifted farther out in time. Accordingly, the drinking water doses decrease. The third simulation, shown in Figure A.26b, repeated the first simulation with the ⁹⁹Tc inventory reduced to 20% of the preliminary design inventory. The results from this simulation show that 80% removal of the ⁹⁹Tc inventory yields beta/photon emitter dose levels slightly below the 4 mrem/yr standard. Doses from the uranium group, however, exceed the 20 µg/L standard. The fourth simulation, shown in Figure A.26c, repeated the second simulation with the ⁹⁹Tc inventory reduced to 20% of the preliminary design inventory. The saturation-dependent retardation formulation generally slows the travel time for the uranium group of radionuclides, but the 20 µg/L is exceeded nevertheless. Dose standards for all radionuclide groups are met over the shorter dose record period of 10,000 years.

A.4.5 Maximum Dose Results

Results in terms of maximum doses from the sensitivity analysis and draft product acceptance simulations were combined as shown in Figures A.27 through A.30. All plots show results for a dose record length of 100,000 years. Maximum drinking water doses in terms of the DOE standard are shown in Figure A.27 for both the saturation-dependent and -independent retardation simulations. This plot shows maximum drinking water doses, normalized to the 4-mrem/yr standard, for the "total" group of radionuclides versus the glass release time, where glass release time is defined as the glass radius divided by the linear corrosion rate. Drinking water standards are met for normalized values below 1.0. The simulation results for the draft product acceptance analysis (10.0-cm-radius glass spheres) follow the trends established with the sensitivity analysis (0.25-cm-radius glass spheres). This result was expected because the hydraulic properties were the same as for the 0.25-cm-radius glass spheres. Use of the hydraulic properties of 0.25-cm-radius spheres allowed water to enter and transmit through the 10.0-cm-radius spheres more readily than if properties for 10-cm-radius spheres were used. Differences in "total" drinking water dose between the saturation-dependent and -independent retardation increase with recharge. At high recharge rates the "total" maximum drinking water dose is dominated by the appearance of ²³⁹Pu using saturation-independent retardation. For saturation-dependent retardation the appearance of ²³⁹Pu is delayed beyond the 100,000-year dose record length. At low recharge rates the "total" maximum drinking water dose is dominated by contributions from the unretarded radionuclides (e.g., ⁹⁹Tc and ¹²⁹I). The saturation-independent retardation simulations show minor contributions from the uranium isotopes late in the 100,000-year record. For the saturation-dependent retardation simulations, arrival of the uranium isotopes is delayed beyond 100,000 years.

Using the proposed EPA drinking water standards, the maximum doses for beta/photon emitters, the uranium isotopes, and gross alpha emitters are shown in Figures A.28 through A.30, respectively. Because the "beta/photon" dose category includes the primary unretarded radionuclides (i.e., ^{99}Tc and ^{129}I), the maximum dose result levels and trends, shown in Figure A.28, match those reported for the DOE standard, according to Figure A.27. Maximum drinking water doses for the uranium isotopes display opposite trends from the "total" dose with respect to comparisons of saturation-dependent and -independent retardation. The sensitivity of maximum dose to the retardation formulation decreases with increasing recharge rates. At higher recharge rates the peaks in the uranium isotopes dose occur within the 100,000-year dose record period. In contrast, at lower recharge rates appearance of uranium at the water table using saturation-dependent retardation is delayed beyond 100,000 years. Maximum drinking water doses for the gross alpha emitters, shown in Figure A.30, display similar trends to those for the uranium isotopes with differences in the retardation formulation decreasing with increasing recharge rates. Except for the cases involving high recharge and corrosion rates maximum drinking water doses for the gross alpha emitters are generally below the proposed EPA standards.

A.5 Inventory Analysis

The maximum fractional release rate, f_r , is a function of the surface area to volume ratio. The rate is given by the product of mass loss rate and surface area to volume ratio divided by the mass density of the glass. For a spherical shape this is given by

$$f_r = \frac{3 C_{gm}}{r \rho_g} = \frac{3}{t_r}$$

For the simulations shown in Figures A.26 through A.26c with a release time of 7.12×10^5 years, the maximum fractional release rate is $4.2 \times 10^{-6} \text{ yr}^{-1}$. The maximum fractional release rate occurs when the sphere has its maximum radius. As radius decreases, the annular volume of the spherical shell described by the reduction in radius decreases, causing the fractional release rate to decrease also. Clearly, the maximum fractional release rate is a function of the shape of the waste form. Before the maximum fractional release rate can be known with confidence, the waste form shape must be known.

Other than the product acceptance simulations, the sensitivity analyses we report were all completed for a sphere with a radius of 0.25 cm. Assuming they represent the response of any combination of mass loss rate and sphere radius, the sensitivity analyses were used to calculate total release times (t_r), maximum fractional releases (f_r), and maximum inventories. The total release times for each specific standard were interpolated from the results in Figures A.27 to A.30. Table A.5 shows the total release times required for each radionuclide group to meet the appropriate standards. Table A.6 shows the corresponding maximum fractional release rates.

The draft product acceptance specification for a mass loss rate of $10^{-3} \text{ g/m}^2 \text{ d}$ and a sphere radius of 10 cm translates to a volumetric corrosion rate of $1.405 \times 10^{-5} \text{ cm/yr}$ and a total release time of 7.12×10^5 years. Total release times shown in Table A.5 that are greater than that for the draft product acceptance specification indicate that the disposal system will fail to meet the drinking water standards for the preliminary inventories shown in Table A.1. Because dose scales linearly with inventory, maximum inventories for the different radionuclide groups can be computed from a ratio of the draft product acceptance release time of 7.12×10^5 years to the total release times in Table A.5. Maximum inventories expressed as a fraction of the preliminary inventory are shown in Table A.7 for each radionuclide group.

Table A.5. Total Release Time (yr) for Meeting Drinking Water Standards, Saturation-Independent-Retardation [saturation-dependent retardation]

<u>Radionuclide Group</u>	<u>0.01 cm/yr</u>	<u>Recharge Rate</u>	
		<u>0.1 cm/yr</u>	<u>1.0 cm/yr</u>
Total	1.84 x 10 ⁶ [1.63 x 10 ⁶]	4.65 x 10 ⁶ [2.73 x 10 ⁶]	3.94 x 10 ⁷ [5.99 x 10 ⁶]
⁹⁹ Tc	1.53 x 10 ⁶ [1.53 x 10 ⁶]	2.49 x 10 ⁶ [2.49 x 10 ⁶]	2.72 x 10 ⁶ [2.72 x 10 ⁶]
¹²⁹ I	<2.5 x 10 ² [<2.5 x 10 ²]	8.44 x 10 ⁴ [8.44 x 10 ⁴]	1.11 x 10 ⁵ [1.11 x 10 ⁵]
Beta/Photon Emitters	1.63 x 10 ⁶ [1.63 x 10 ⁶]	2.61 x 10 ⁶ [2.61 x 10 ⁶]	2.84 x 10 ⁶ [2.84 x 10 ⁶]
Gross Alpha Emitters	<2.5 x 10 ² [<2.5 x 10 ²]	<2.5 x 10 ² [<2.5 x 10 ²]	3.70 x 10 ⁶ [9.10 x 10 ⁴]
Uranium Isotopes	2.64 x 10 ⁵ [<2.5 x 10 ²]	1.77 x 10 ⁶ [1.24 x 10 ⁶]	1.90 x 10 ⁶ [1.87 x 10 ⁶]

Table A.6. Maximum Fractional Release Rates (yr⁻¹) for Meeting Drinking Water Standards, Saturation-Independent Retardation [saturation-dependent retardation]

<u>Radionuclide Group</u>	<u>0.01 cm/yr</u>	<u>Recharge Rate</u>	
		<u>0.1 cm/yr</u>	<u>1.0 cm/yr</u>
Total	1.63 x 10 ⁻⁶ [1.84 x 10 ⁻⁶]	6.45 x 10 ⁻⁷ [1.10 x 10 ⁻⁶]	7.61 x 10 ⁻⁸ [5.01 x 10 ⁻⁷]
⁹⁹ Tc	1.96 x 10 ⁻⁶ [1.96 x 10 ⁻⁶]	1.20 x 10 ⁻⁶ [1.20 x 10 ⁻⁶]	1.10 x 10 ⁻⁶ [1.10 x 10 ⁻⁶]
¹²⁹ I	>1.2 x 10 ⁻² [>1.2 x 10 ⁻²]	3.55 x 10 ⁻⁵ [3.55 x 10 ⁻⁵]	2.71 x 10 ⁻⁵ [2.71 x 10 ⁻⁵]
Beta/Photon Emitters	1.84 x 10 ⁻⁶ [1.84 x 10 ⁻⁶]	1.15 x 10 ⁻⁶ [1.15 x 10 ⁻⁶]	1.06 x 10 ⁻⁶ [1.06 x 10 ⁻⁶]
Gross Alpha Emitters	>1.2 x 10 ⁻² [>1.2 x 10 ⁻²]	>1.2 x 10 ⁻² [>1.2 x 10 ⁻²]	8.11 x 10 ⁻⁷ [3.30 x 10 ⁻⁵]
Uranium Isotopes	1.13 x 10 ⁻⁵ [>1.2 x 10 ⁻²]	1.69 x 10 ⁻⁶ [2.42 x 10 ⁻⁶]	1.58 x 10 ⁻⁶ [1.60 x 10 ⁻⁶]

Table A.7. Maximum Inventories (fraction of the preliminary inventory) for Drinking Water Standards, Saturation-Independent Retardation [saturation-dependent retardation]

<u>Radionuclide Group</u>	<u>Recharge Rate</u>		
	<u>0.01 cm/yr</u>	<u>0.1 cm/yr</u>	<u>1.0 cm/yr</u>
Total	0.387 [0.437]	0.153 [0.261]	0.018 [0.119]
⁹⁹ Tc	0.466 [0.466]	0.286 [0.286]	0.262 [0.262]
¹²⁹ I	1.00 [1.00]	1.00 [1.00]	1.00 [1.00]
Beta/Photon Emitters	0.437 [0.437]	0.273 [0.273]	0.251 [0.251]
Gross Alpha Emitters	1.00 [1.00]	1.00 [1.00]	0.192 [1.00]
Uranium Isotopes	1.00 [1.00]	0.407 [0.574]	0.374 [0.381]

A.6 Conclusions

In this investigation of the performance of the WFA design for the LAW disposal system, we reviewed previously published studies and examined the sensitivity of system performance on critical parameters. The review component of this investigation was directed at verifying the dose rate calculations for the central analysis case reported in the Rawlins report. These calculations were verified by regenerating the dose predictions using an independent calculation scheme, which involved numerically modeling the flow and transport of radionuclides through the engineered and hydrologic system and then converting those data to drinking water dose rates. Two conclusions were drawn from this verification work. The first was that the dose results reported in the Rawlins report depended strongly on an imposed relative permeability limit of 10^{-10} . With this limit imposed, the mode of transport for radionuclides through the glass waste engineered system is primarily advective. Without this limit, the mode of transport through the glass waste is primarily diffusive, resulting in significantly lower dose rates. The second conclusion was that the mode of transport (advective or diffusive) through the glass waste disposal zone strongly affects the drinking water dose rates; advective transport generally yielded higher drinking water dose rates.

The sensitivity component of this investigation involved developing a preliminary conceptual model for the hydrologic and engineered systems and a sensitivity assessment of the disposal system performance to variations in the infiltration rate and glass corrosion rate. Using a more realistic saturation-dependent retardation coefficient model was also studied and we found that the dose peaks of retarded radionuclides were shifted to later times, eliminating the superposition of doses. The main conclusion drawn from this component of the investigation was that drinking water dose rates could be achieved within the regulatory standards either through controlling glass corrosion and/or hydrologic processes within the waste disposal zone. It will be imperative to properly characterize the hydrologic processes of the disposal system. Another important conclusion from the sensitivity study is that the ²³⁹Pu radionuclide could dominate the maximum dose rates for high recharge rates. This result would indicate that, unless surface barriers that ensure low recharge rates are implemented or the ²³⁹Pu isotope is shown to be highly retarded in the secondary minerals of the LAW, ²³⁹Pu will be an inappropriate component of the LAW inventory.

The preliminary inventory for the low-level waste disposal system comprises a large variety of radionuclides. The contribution to drinking water dose for a particular radionuclide depends on its half-life, distribution coefficients, and dose conversion factors. Drinking water standards for radionuclides, however, depend on radiologic health factors and vary among the radionuclides. Dose calculations in the Rawlins report examined the impact of the entire radionuclide inventory on drinking water and compared results to the 4-mrem/yr standard. This study used an alternative drinking water standard based on the three radiological health groups (beta/photon emitters, alpha emitters, and uranium isotopes ^{234}U , ^{235}U , and ^{238}U).

A.7 References

10 CFR 834. 1993. U.S. Department of Energy, "Radiation Protection of the Public and the Environment; Proposed Rule." U.S. Code of Federal Regulations.

40 CFR 141-142. 1991. U.S. Environmental Protection Agency, "National Primary Drinking Water Regulations, Radionuclides; Proposed Rule." U.S. Code of Federal Regulations.

Kincaid C, JW Shade, GA Whyatt, MG Piepho, K Rhoads, JA Voogd, JH Westsik Jr., MD Freshley, KA Blanchard, and BG Lauzon. 1995. *Performance Assessment of Grouted Double-Shell Tank Waste Disposal at Hanford*. WHC-SD-WM-EE-004 Rev. 1, Westinghouse Hanford Company, Richland, Washington.

Mann FM, CR Eiholzer, NW Kline, BP McGrail, and MG Piepho. 1995. *Impacts of Disposal System Design Options on Low-Level Glass Waste Disposal System Performance*. WHC-EP-0810, Westinghouse Hanford Company, Richland, Washington.

Millington RJ and P. Quirk. 1959. "Permeability in Porous Media." *Nature*, 183:387-388.

Mishra S and JC Parker. 1991. *SoilProp A Program to Estimate Unsaturated Soil Hydraulic Properties from Particle Size Distribution Data User and Technical Guide Version 2.1*. Environmental Systems and Technologies Inc., Blacksburg, Virginia.

Runchal AK and B Sagar. 1992. *PORFLOW: A Model for Fluid Flow, Heat, and Mass Transport in Multifluid, Multiphase Fractured or Porous Media, Version 2.40*. ACRi/016/Rev. G, ACFi, Bel Air, California.

White MD and M Oostrom. 1996. *STOMP Subsurface Transport Over Multiple Phases, Theory Guide*. Pacific Northwest Laboratory, Richland, Washington.

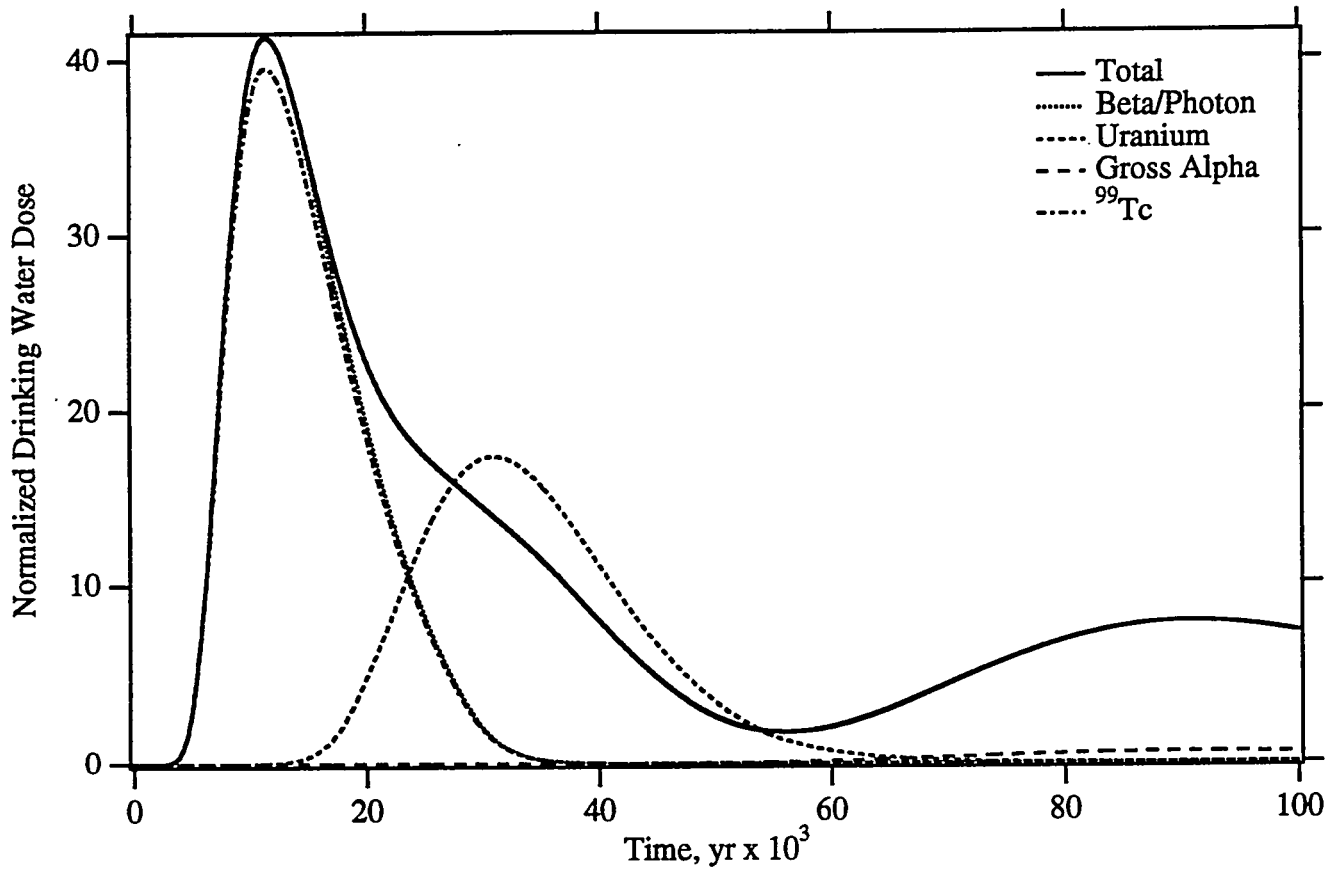


Figure A.1. Drinking Water Dose

Corrosion: 10^{-5} cm/yr
 Glass Radius: 0.25 cm
 Recharge: 0.1 cm/yr
 Solute Diffusion Coefficient: $D_{ab} = 10^{-10}$ cm²/s, a = 1, b = 0
 Glass Hydraulic Properties: Gravel
 Minimum Relative Permeability: 10^{-10}
 Retardation Model: Saturation-Independent
 Hydraulic Dispersion: $\alpha_L = 0.0$ m, $\alpha_T = 0.0$ m
 Well Interception Factor: 0.006
 Grid: Narrow (10 x 162)

Maximum Dose Records 100,000 yr [10,000 yr]

Total	165.3 [156.2] mrem/yr
Beta/Photon	165.3 [156.2] mrem/yr
⁹⁹ Tc	158.2 [149.5] mrem/yr
¹²⁹ I	6.976 [6.563] mrem/yr
Uranium	347.9 [0.03450] µg/L
Gross Alpha	9.306 [4.629e-21] pCi/L

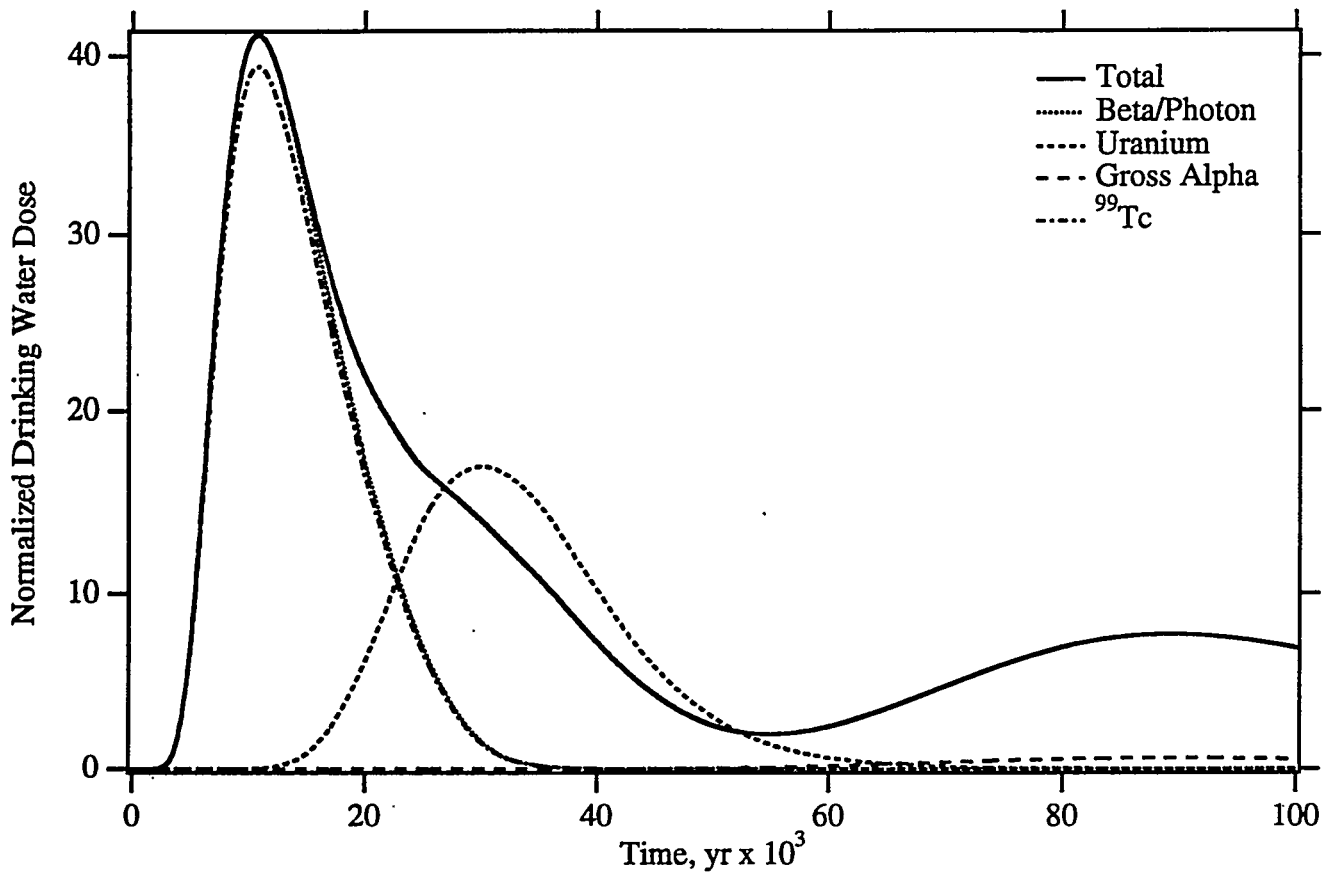


Figure A.2. Drinking Water Dose

Corrosion: 10^{-5} cm/yr
 Glass Radius: 0.25 cm
 Recharge: 0.1 cm/yr
 Solute Diffusion Coefficient: $D_{ab} = 10^{-10}$ cm²/s, a = 1, b = 0
 Glass Hydraulic Properties: Gravel
 Minimum Relative Permeability: 10^{-10}
 Retardation Model: Saturation-Independent
 Hydraulic Dispersion: $\alpha_L = 0.0$ m, $\alpha_T = 0.0$ m
 Well Interception Factor: 0.006
 Grid: Moderate (20 x 162)

Maximum Dose Records 100,000 yr [10,000 yr]

Total	164.7 [162.3] mrem/yr
Beta/Photon	164.6 [162.3] mrem/yr
⁹⁹ Tc	157.5 [155.4] mrem/yr
¹²⁹ I	6.933 [6.820] mrem/yr
Uranium	345.5 [0.1726] µg/L
Gross Alpha	9.252 [5.256e-20] pCi/L

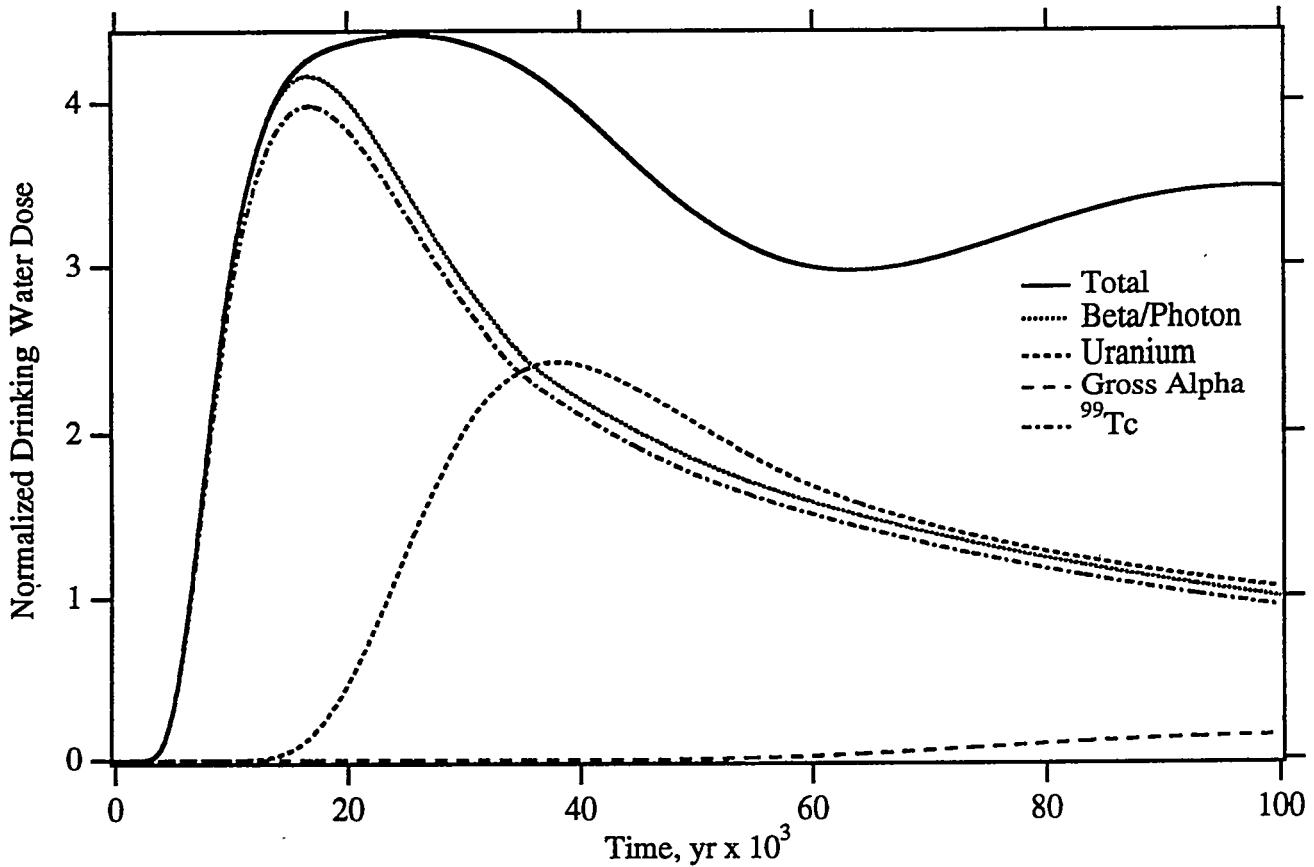


Figure A.3. Drinking Water Dose

Corrosion: 10^{-5} cm/yr
 Glass Radius: 0.25 cm
 Recharge: 0.1 cm/yr
 Solute Diffusion Coefficient: $D_{ab} = 10^{-10}$ cm²/s, a = 1, b = 0
 Glass Hydraulic Properties: Gravel
 Minimum Relative Permeability: 0.
 Retardation Model: Saturation-Independent
 Hydraulic Dispersion: $\alpha_L = 0.0$ m, $\alpha_T = 0.0$ m
 Well Interception Factor: 0.006
 Grid: Narrow (10 x 162)

Maximum Dose Records 100,000 yr [10,000 yr]

Total	17.61 [11.91] mrem/yr
Beta/Photon	16.64 [11.91] mrem/yr
⁹⁹ Tc	15.92 [11.40] mrem/yr
¹²⁹ I	0.7143 [0.5004] mrem/yr
Uranium	49.10 [0.005336] μg/L
Gross Alpha	2.158 [4.303e-22] pCi/L

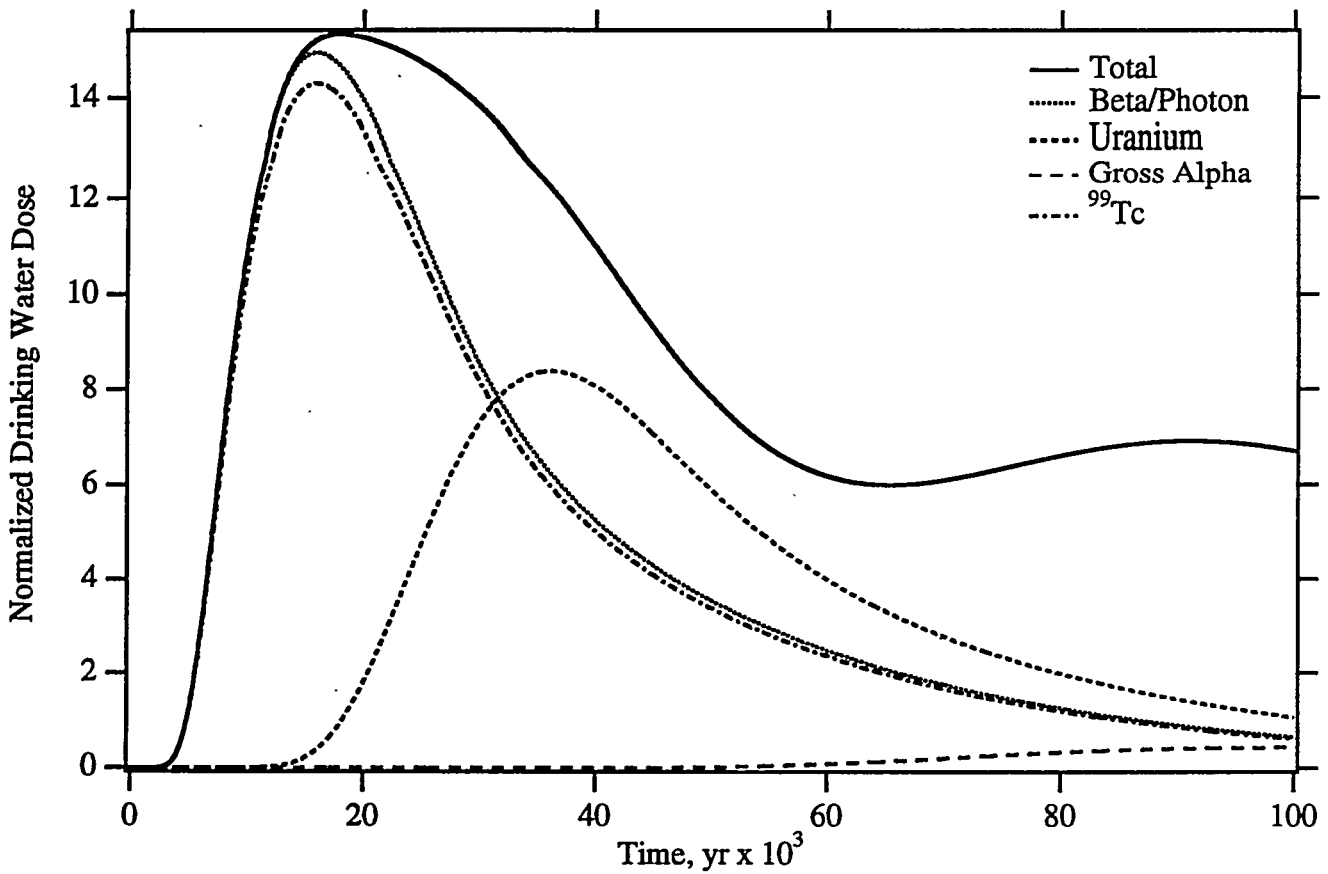


Figure A.4. Drinking Water Dose

Corrosion: 10^{-5} cm/yr

Glass Radius: 0.25 cm

Recharge: 0.1 cm/yr

Solute Diffusion Coefficient: $D_{ab} = 10^{-9}$ cm²/s, a = 1, b = 0

Glass Hydraulic Properties: Gravel

Minimum Relative Permeability: 0.

Retardation Model: Saturation-Independent

Hydraulic Dispersion: $\alpha_L = 0.0$ m, $\alpha_T = 0.0$ m

Well Interception Factor: 0.006

Grid: Narrow (10 x 162)

Maximum Dose Records 100,000 yr [10,000 yr]

Total	61.33 [43.72] mrem/yr
Beta/Photon	59.75 [43.71] mrem/yr
⁹⁹ Tc	57.17 [41.84] mrem/yr
¹²⁹ I	2.559 [1.837] mrem/yr
Uranium	168.0 [0.02337] µg/L
Gross Alpha	6.450 [2.949e-21] pCi/L

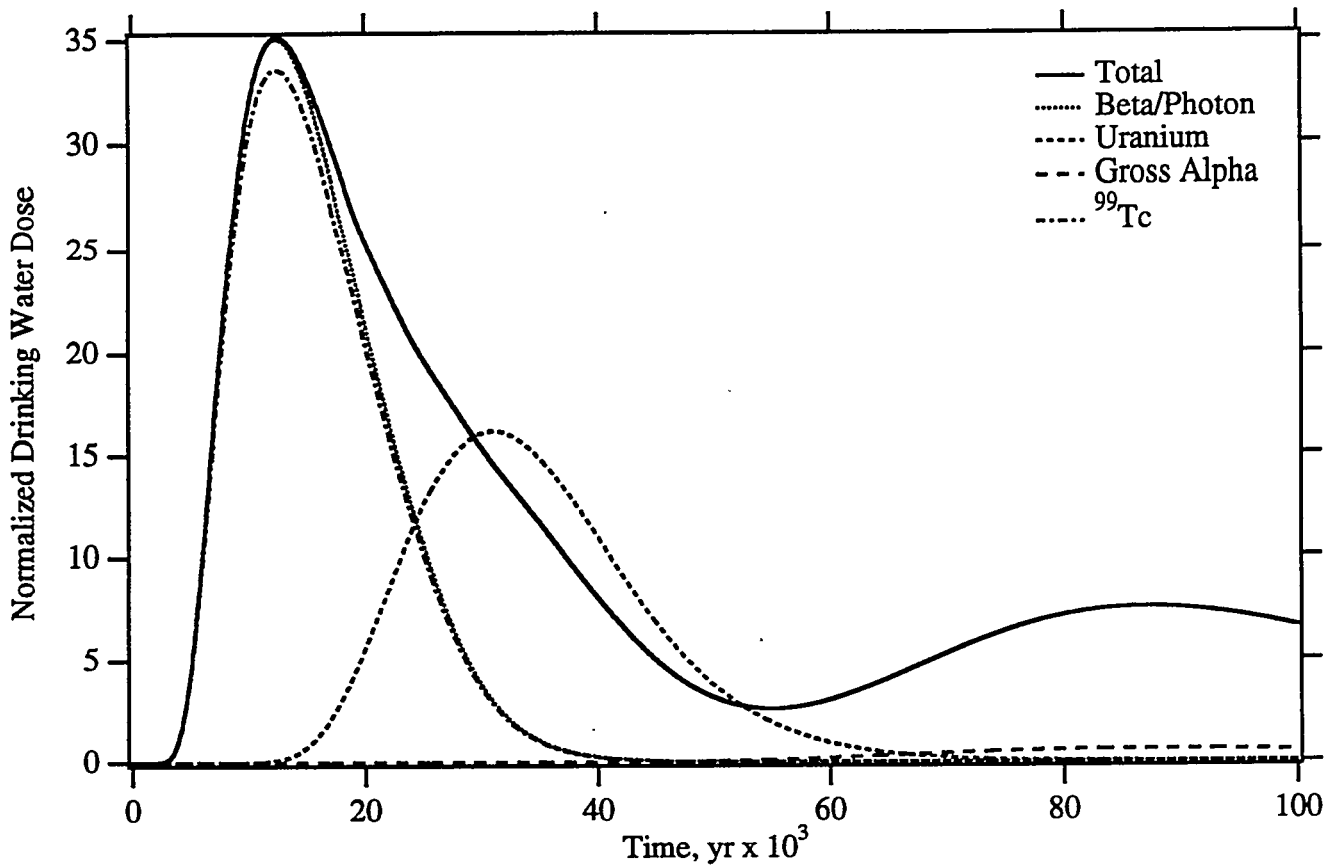


Figure A.5. Drinking Water Dose

Corrosion: 10^{-5} cm/yr
 Glass Radius: 0.25 cm
 Recharge: 0.1 cm/yr
 Solute Diffusion Coefficient: $D_{ab} = 10^{-8}$ cm²/s, a = 1, b = 0
 Glass Hydraulic Properties: Gravel
 Minimum Relative Permeability: 0.
 Retardation Model: Saturation-Independent
 Hydraulic Dispersion: $\alpha_L = 0.0$ m, $\alpha_T = 0.0$ m
 Well Interception Factor: 0.006
 Grid: Narrow (10 x 162)

Maximum Dose Records 100,000 yr [10,000 yr]

Total	140.5 [127.1] mrem/yr
Beta/Photon	140.2 [127.1] mrem/yr
⁹⁹ Tc	134.2 [121.6] mrem/yr
¹²⁹ I	5.938 [5.338] mrem/yr
Uranium	322.8 [0.1011] µg/L
Gross Alpha	9.024 [1.821e-20] pCi/L

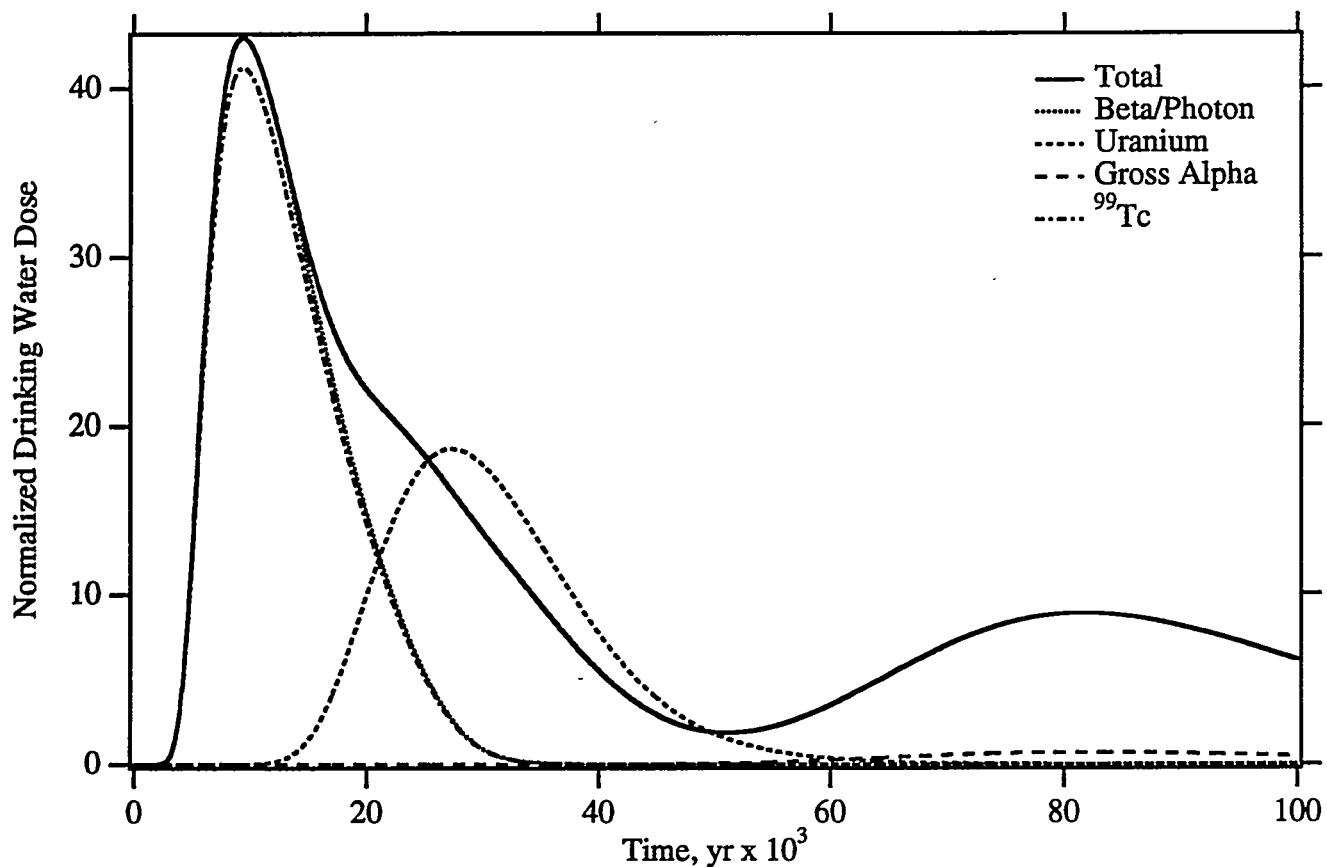


Figure A.6. Drinking Water Dose

Corrosion: 10^{-5} cm/yr
 Glass Radius: 0.25 cm
 Recharge: 0.1 cm/yr
 Solute Diffusion Coefficient: $D_{ab} = 10^{-10}$ cm²/s, a = 1, b = 0
 Glass Hydraulic Properties: Glass Spheres (SOILPROP)
 Minimum Relative Permeability: 0.
 Retardation Model: Saturation-Independent
 Hydraulic Dispersion: $\alpha_L = 0.0$ m, $\alpha_T = 0.0$ m
 Well Interception Factor: 0.006
 Grid: Narrow (10 x 162)

Maximum Dose Records 100,000 yr [10,000 yr]

Total	172.3 [172.3] mrem/yr
Beta/Photon	172.2 [172.2] mrem/yr
⁹⁹ Tc	164.9 [164.9] mrem/yr
¹²⁹ I	7.224 [7.224] mrem/yr
Uranium	373.5 [0.1846] µg/L
Gross Alpha	10.61 [1.405e-20] pCi/L

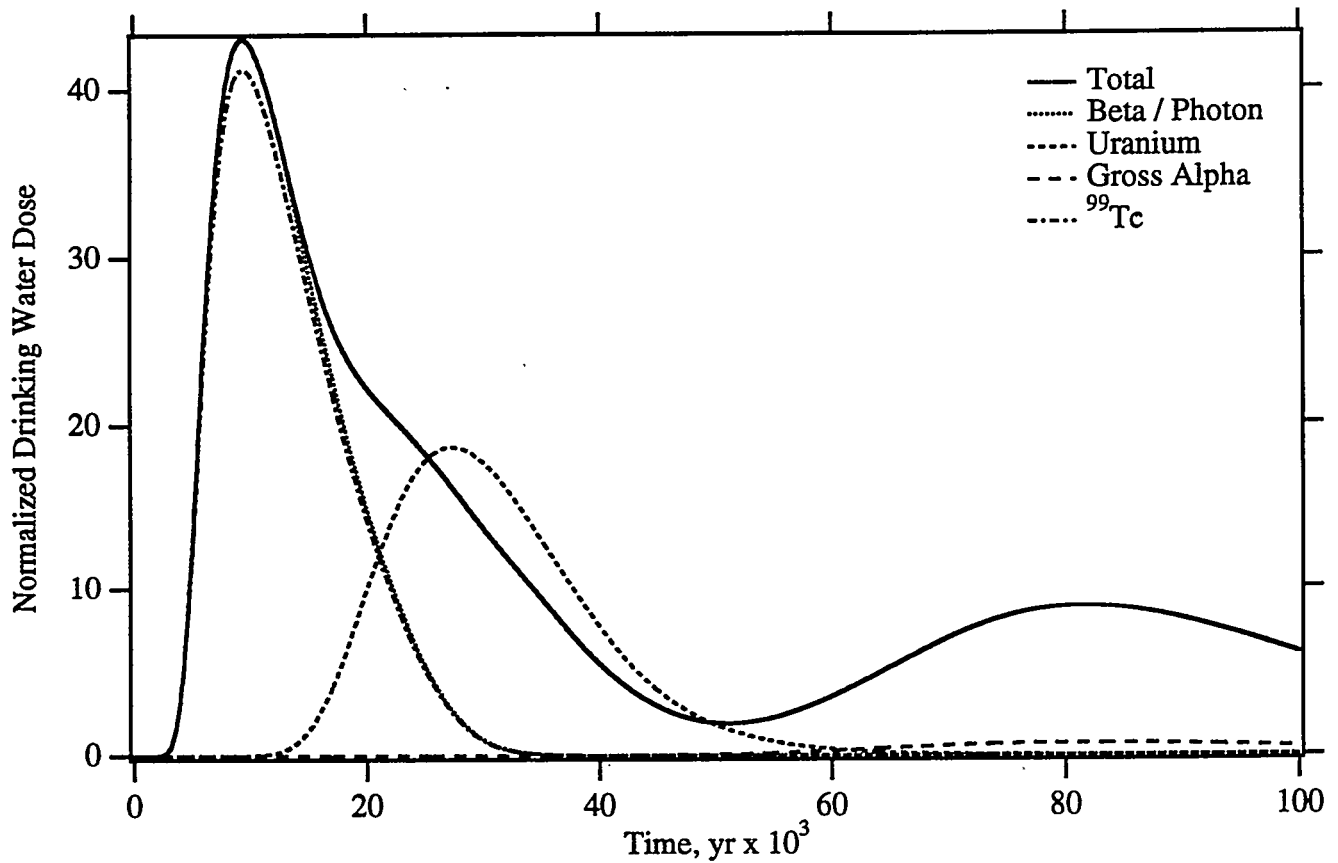


Figure A.7. Drinking Water Dose

Corrosion: 10^{-5} cm/yr
 Glass Radius: 0.25 cm
 Recharge: 0.1 cm/yr
 Solute Diffusion Coefficient: $D_{ab} = 10^{-8}$ cm²/s, $a = 1$, $b = 0$
 Glass Hydraulic Properties: Glass Spheres (SOILPROP)
 Minimum Relative Permeability: 0.
 Retardation Model: Saturation-Independent
 Hydraulic Dispersion: $\alpha_L = 0.0$ m, $\alpha_T = 0.0$ m
 Well Interception Factor: 0.006
 Grid: Narrow (10 x 162)

Maximum Dose Records 100,000 yr [10,000 yr]

Total	172.3 [172.3] mrem/yr
Beta/Photon	172.3 [172.3] mrem/yr
⁹⁹ Tc	164.9 [164.9] mrem/yr
¹²⁹ I	7.224 [7.224] mrem/yr
Uranium	373.5 [0.1888] µg/L
Gross Alpha	10.61 [1.491e-20] pCi/L

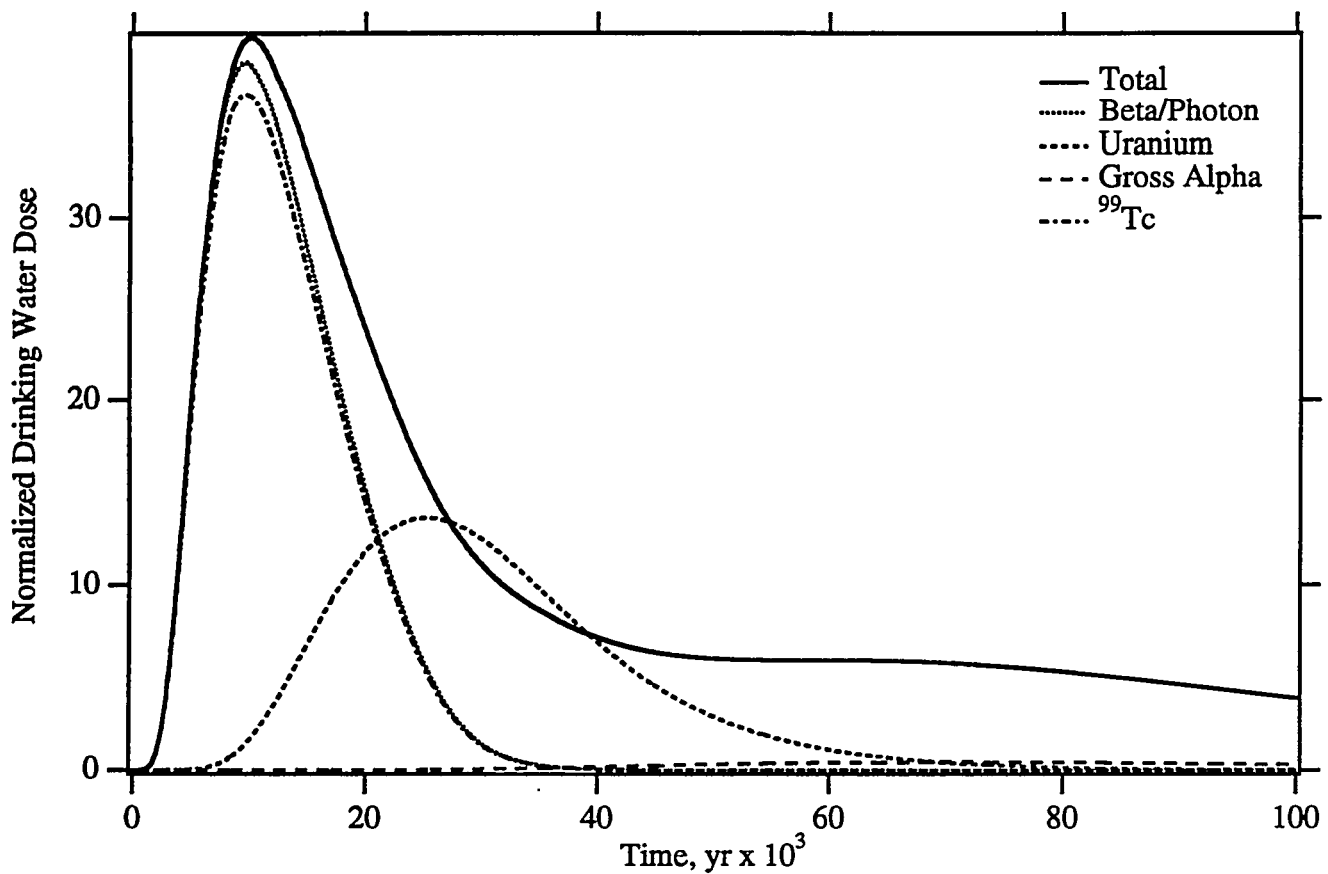


Figure A.8. Drinking Water Dose

Corrosion: 10^{-5} cm/yr
 Glass Radius: 0.25 cm
 Recharge: 0.1 cm/yr
 Solute Diffusion Coefficient: $D_{ab} = 10^{-8}$ cm²/s, a = 1, b = 0
 Glass Hydraulic Properties: Glass Spheres (SOILPROP)
 Minimum Relative Permeability: 0.
 Retardation Model: Saturation-Independent
 Hydraulic Dispersion: $\alpha_L = 6.5$ m, $\alpha_T = 0.65$ m
 Well Interception Factor: 0.006
 Grid: Narrow (10 x 162)

Maximum Dose Records 100,000 yr [10,000 yr]

Total	157.8 [157.7] mrem/yr
Beta/Photon	153.2 [153.2] mrem/yr
^{99}Tc	146.6 [146.6] mrem/yr
^{129}I	6.429 [6.429] mrem/yr
Uranium	273.2 [32.70] $\mu\text{g/L}$
Gross Alpha	6.611 [3.275e-05] pCi/L

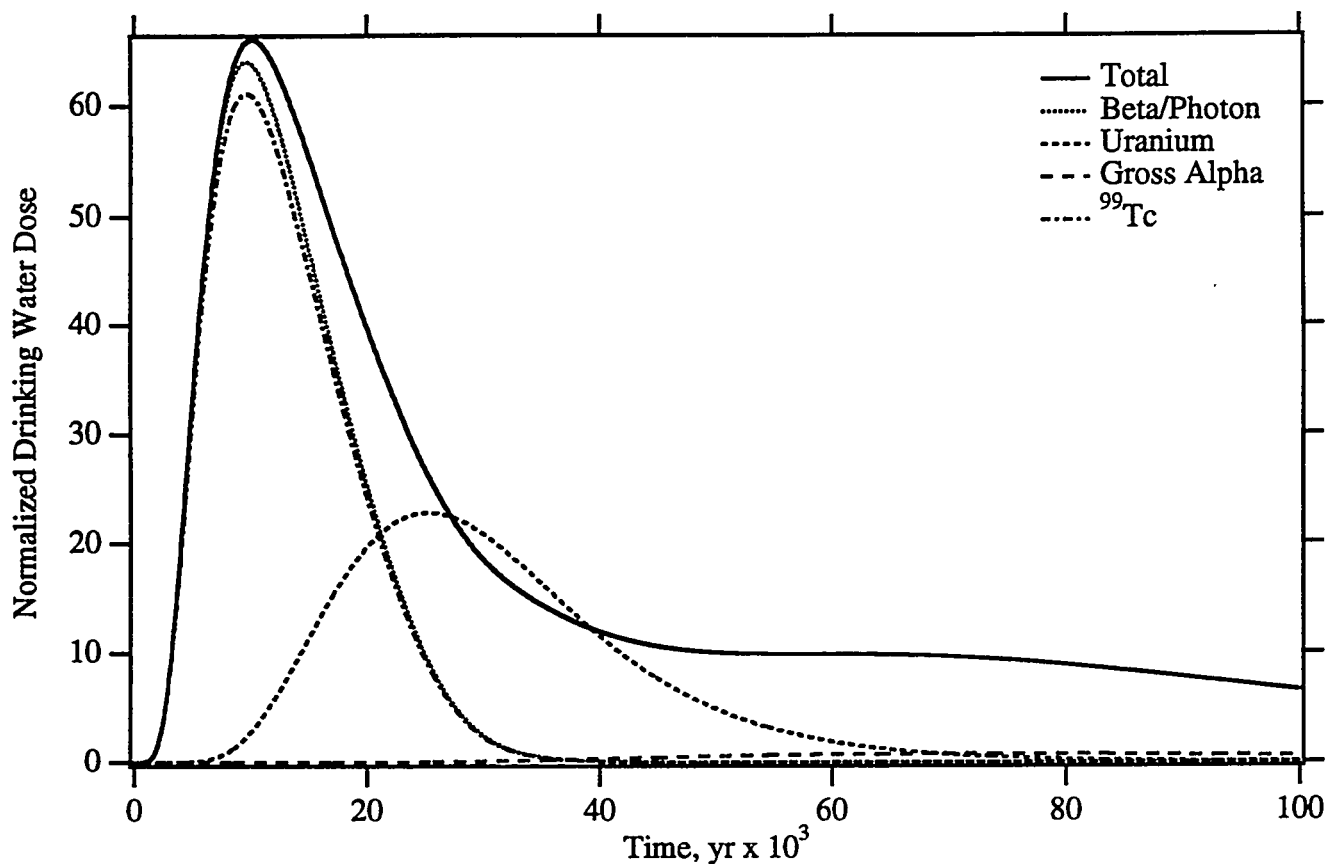


Figure A.9. Drinking Water Dose

Corrosion: 10^{-5} cm/yr
 Glass Radius: 0.25 cm
 Recharge: 0.1 cm/yr
 Solute Diffusion Coefficient: $D_{ab} = 10^{-8}$ cm²/s, a = 1, b = 0
 Glass Hydraulic Properties: Glass Spheres (SOILPROP)
 Minimum Relative Permeability: 0.
 Retardation Model: Saturation-Independent
 Hydraulic Dispersion: $\alpha_L = 6.5$ m, $\alpha_T = 0.65$ m
 Well Interception Factor: 0.01
 Grid: Narrow (10 x 162)

Maximum Dose Records 100,000 yr [10,000 yr]

Total	263.0 [262.9] mrem/yr
Beta/Photon	255.3 [255.3] mrem/yr
⁹⁹ Tc	244.3 [244.3] mrem/yr
¹²⁹ I	10.71 [10.71] mrem/yr
Uranium	455.4 [54.50] μ g/L
Gross Alpha	11.02 [5.459e-05] pCi/L

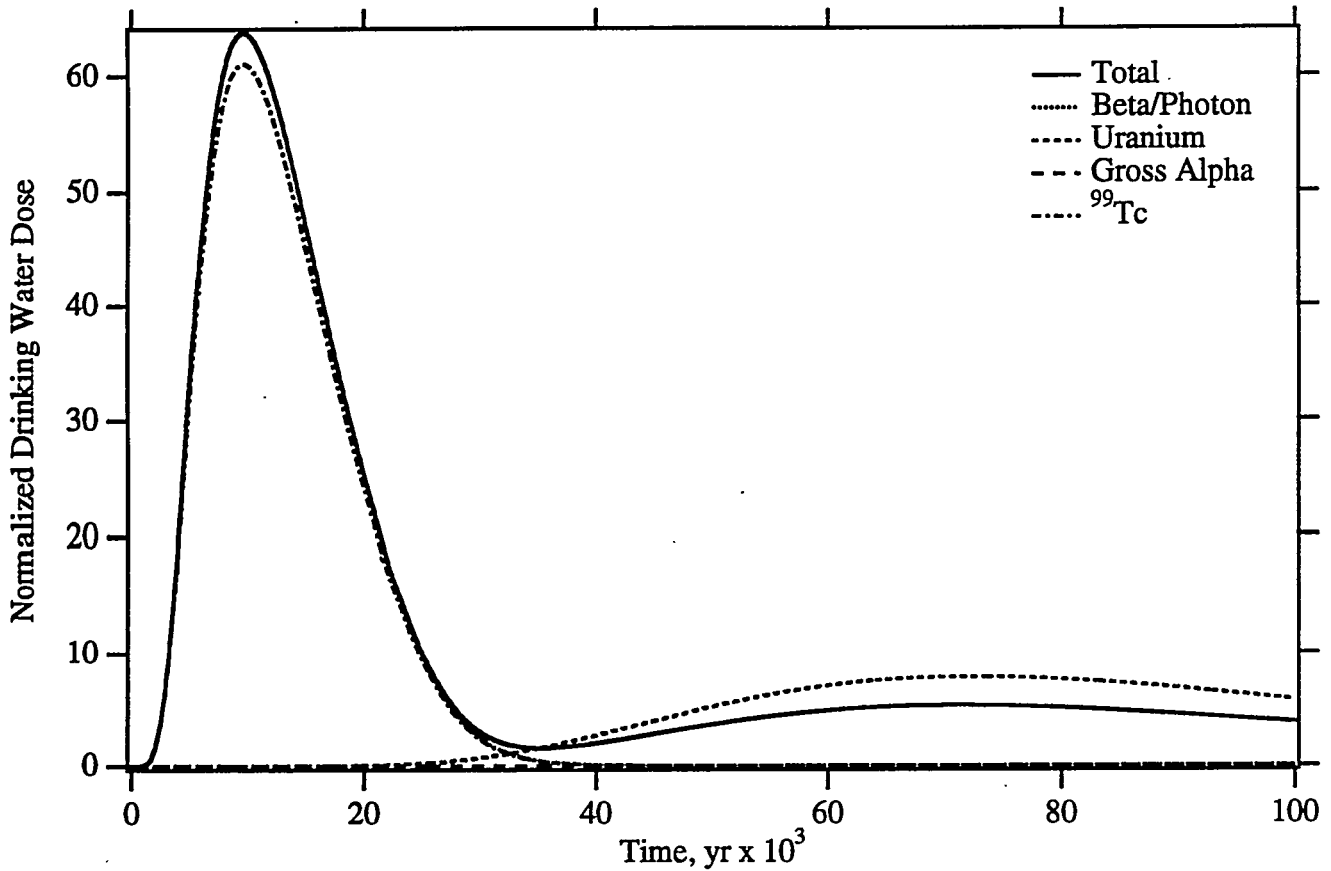


Figure A.10. Drinking Water Dose

Corrosion: 10^{-5} cm/yr
 Glass Radius: 0.25 cm
 Recharge: 0.1 cm/yr
 Solute Diffusion Coefficient: $D_{ab} = 10^{-8}$ cm²/s, a = 1, b = 0
 Glass Hydraulic Properties: Glass Spheres (SOILPROP)
 Minimum Relative Permeability: 0.
 Retardation Model: Saturation-Dependent
 Hydraulic Dispersion: $\alpha_L = 6.5$ m, $\alpha_T = 0.65$ m
 Well Interception Factor: 0.01
 Grid: Narrow (10 x 162)

Maximum Dose Records 100,000 yr [10,000 yr]

Total	255.3 [255.3] mrem/yr
Beta/Photon	255.3 [255.3] mrem/yr
⁹⁹ Tc	244.3 [244.3] mrem/yr
¹²⁹ I	10.71 [10.71] mrem/yr
Uranium	156.0 [0.0003043] µg/L
Gross Alpha	0.1156 [4.146e-22] pCi/L

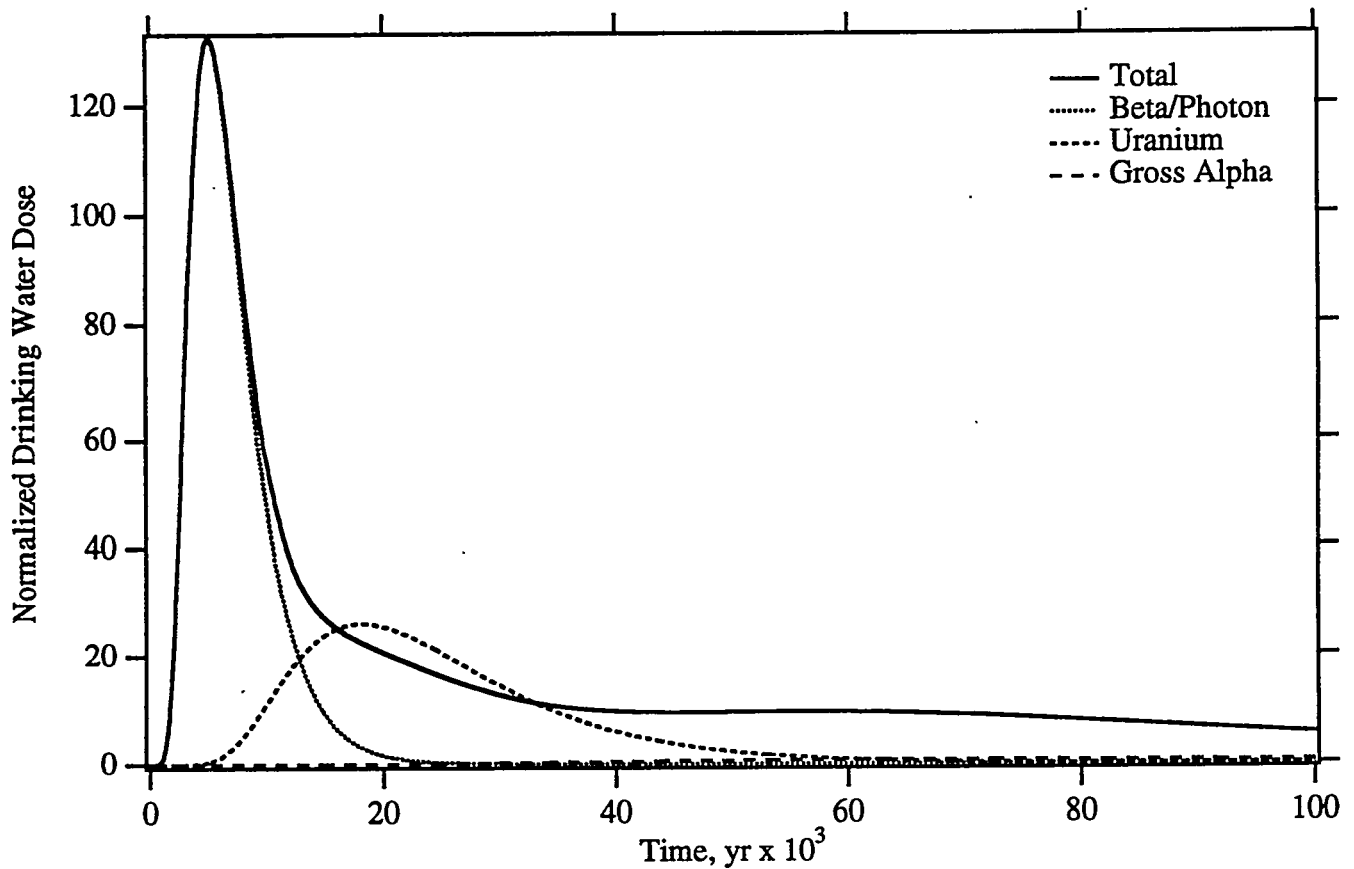


Figure A.11. Drinking Water Dose

Corrosion: 10^{-3} cm/yr
 Glass Radius: 0.25 cm
 Recharge: 0.1 cm/yr
 Solute Diffusion Coefficient: $D_{ab} = 10^{-8}$ cm²/s, a = 1, b = 0
 Glass Hydraulic Properties: Glass Spheres (SOILPROP)
 Minimum Relative Permeability: 0.
 Retardation Model: Saturation-Independent
 Hydraulic Dispersion: $\alpha_L = 6.5$ m, $\alpha_T = 0.65$ m
 Well Interception Factor: 0.01
 Grid: Narrow (10 x 162)

Maximum Dose Records 100,000 yr [10,000 yr]

Total	528.3 [528.3] mrem/yr
Beta/Photon	527.0 [527.0] mrem/yr
⁹⁹ Tc	504.4 [504.4] mrem/yr
¹²⁹ I	21.79 [21.79] mrem/yr
Uranium	519.2 [225.9] µg/L
Gross Alpha	10.85 [0.0005465] pCi/L

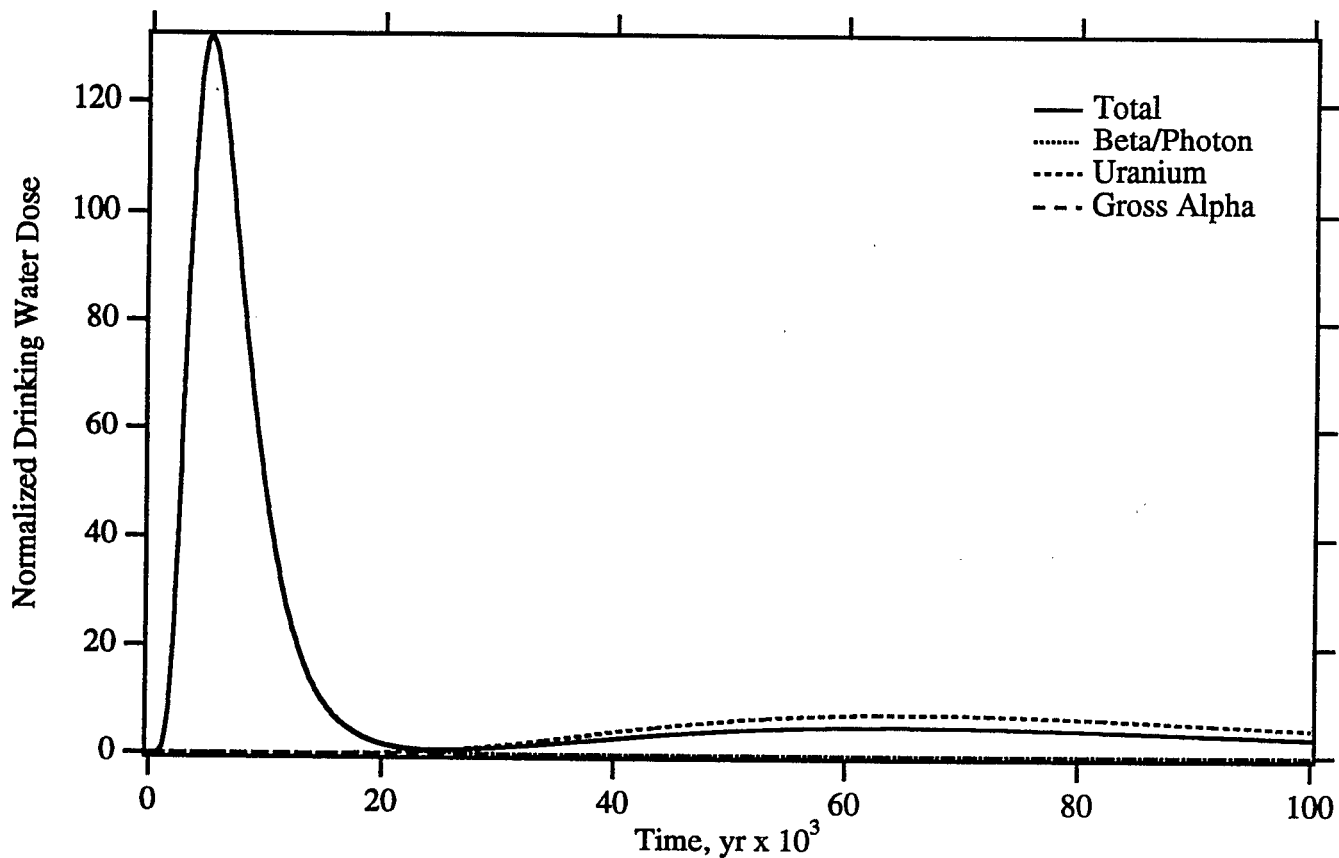


Figure A.11a. Drinking Water Dose

Corrosion: 10^{-3} cm/yr
 Glass Radius: 0.25 cm
 Recharge: 0.1 cm/yr
 Solute Diffusion Coefficient: $D_{ab} = 10^{-8}$ cm²/s, a = 1, b = 0
 Glass Hydraulic Properties: Glass Spheres (SOILPROP)
 Minimum Relative Permeability: 0.
 Retardation Model: Saturation-Dependent
 Hydraulic Dispersion: $\alpha_L = 6.5$ m, $\alpha_T = 0.65$ m
 Well Interception Factor: 0.01
 Grid: Narrow (10 x 162)

Maximum Dose Records 100,000 yr [10,000 yr]

Total	527.0 [527.0] mrem/yr
Beta/Photon	527.0 [527.0] mrem/yr
⁹⁹ Tc	504.4 [504.4] mrem/yr
¹²⁹ I	21.79 [21.79] mrem/yr
Uranium	153.3 [0.003156] μ g/L
Gross Alpha	0.1604 [1.039e-20] pCi/L

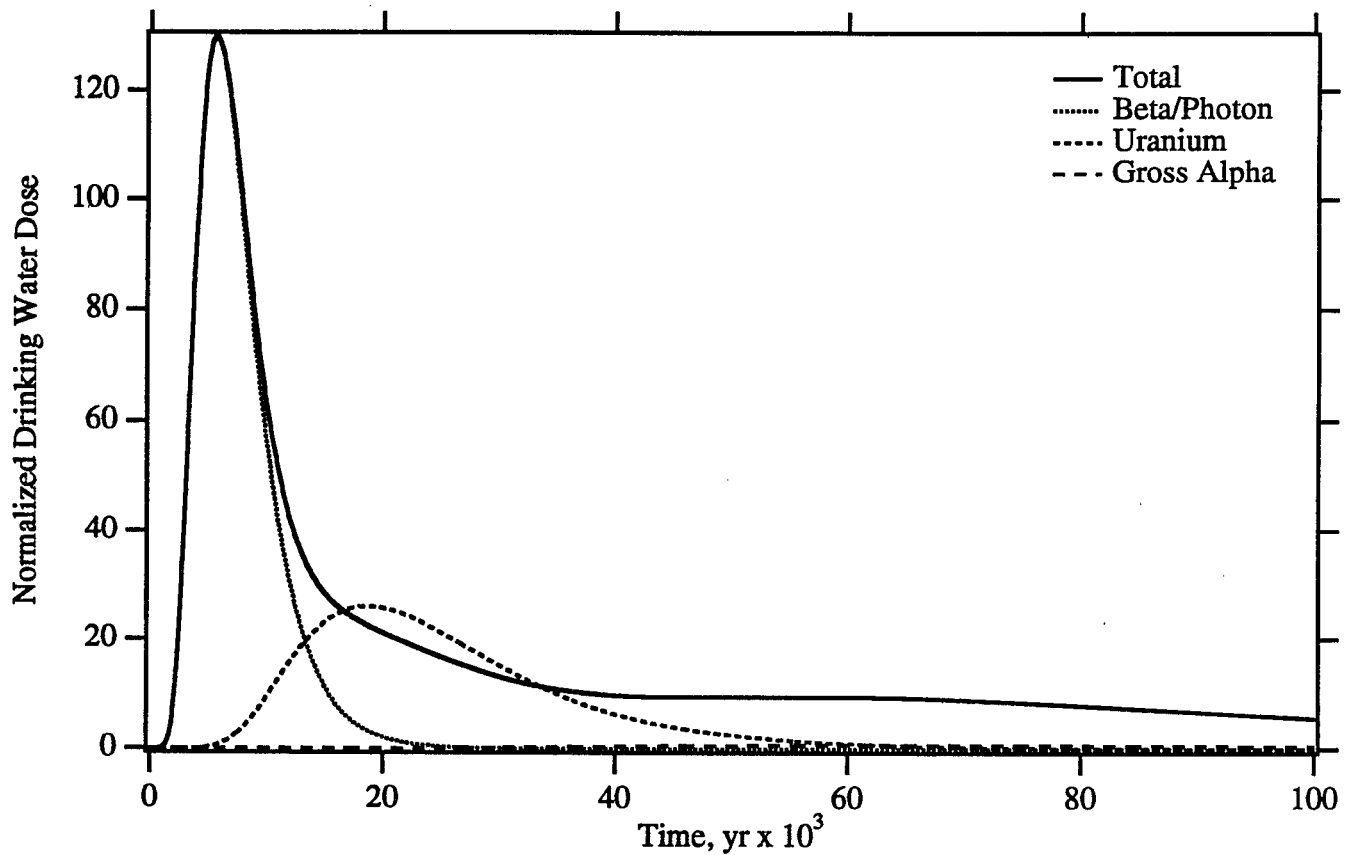


Figure A.12. Drinking Water Dose

Corrosion: 10^{-4} cm/yr
 Glass Radius: 0.25 cm
 Recharge: 0.1 cm/yr
 Solute Diffusion Coefficient: $D_{ab} = 10^{-8}$ cm²/s, a = 1, b = 0
 Glass Hydraulic Properties: Glass Spheres (SOILPROP)
 Minimum Relative Permeability: 0.
 Retardation Model: Saturation-Independent
 Hydraulic Dispersion: $\alpha_L = 6.5$ m, $\alpha_T = 0.65$ m
 Well Interception Factor: 0.01
 Grid: Narrow (10 x 162)

Maximum Dose Records 100,000 yr [10,000 yr]

Total	519.8 [519.8] mrem/yr
Beta/Photon	518.2 [518.2] mrem/yr
⁹⁹ Tc	495.9 [495.9] mrem/yr
¹²⁹ I	21.47 [21.47] mrem/yr
Uranium	518.6 [195.2] µg/L
Gross Alpha	10.85 [0.0003221] pCi/L

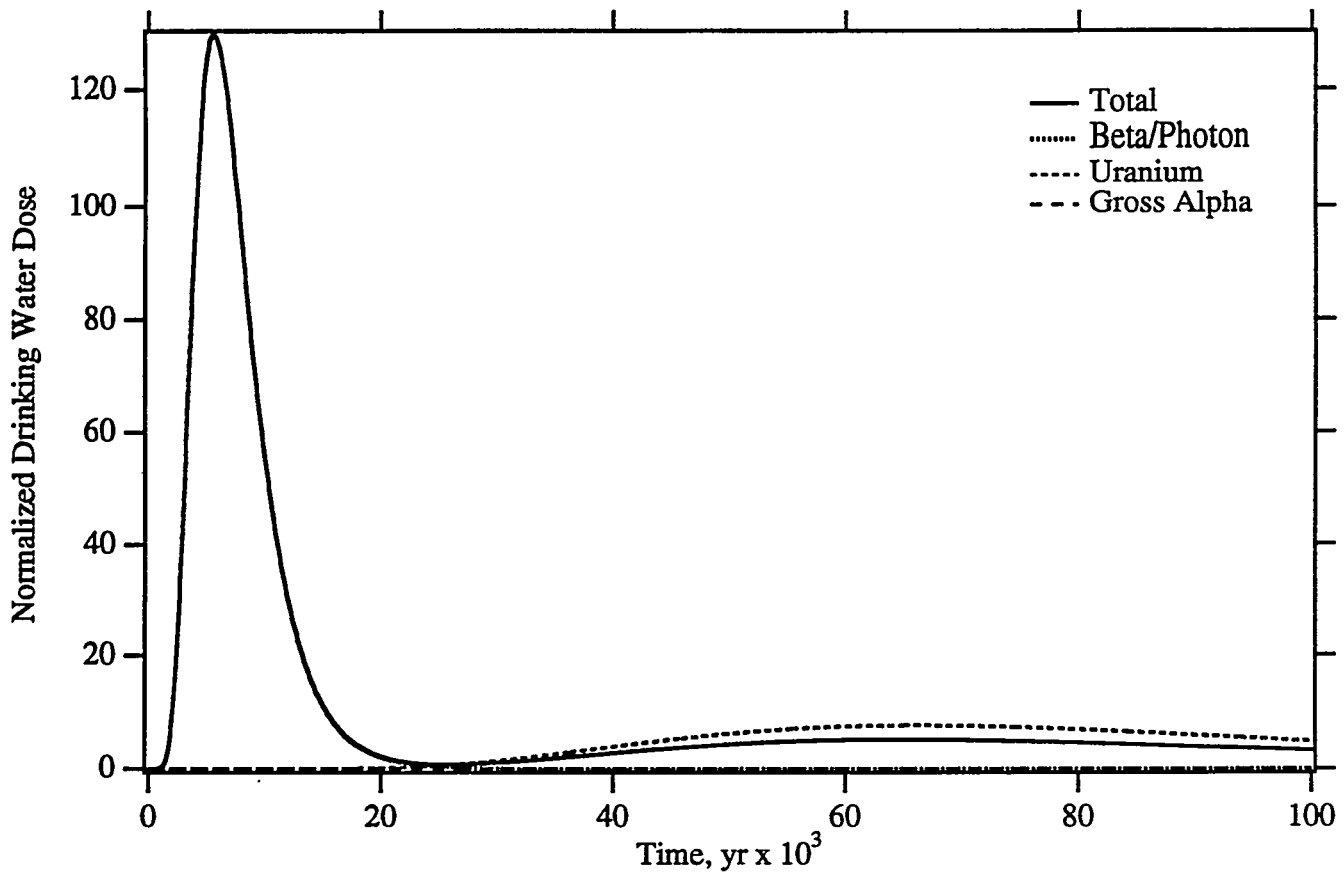


Figure A.12a. Drinking Water Dose

Corrosion: 10^{-4} cm/yr
 Glass Radius: 0.25 cm
 Recharge: 0.1 cm/yr
 Solute Diffusion Coefficient: $D_{ab} = 10^{-8}$ cm²/s, a = 1, b = 0
 Glass Hydraulic Properties: Glass Spheres (SOILPROP)
 Minimum Relative Permeability: 0.
 Retardation Model: Saturation-Dependent
 Hydraulic Dispersion: $\alpha_L = 6.5$ m, $\alpha_T = 0.65$ m
 Well Interception Factor: 0.01
 Grid: Narrow (10 x 162)

Maximum Dose Records 100,000 yr [10,000 yr]

Total	518.2 [518.2] mrem/yr
Beta/Photon	518.2 [518.2] mrem/yr
⁹⁹ Tc	495.9 [495.9] mrem/yr
¹²⁹ I	21.47 [21.47] mrem/yr
Uranium	153.3 [0.001816] µg/L
Gross Alpha	0.1554 [2.876e-21] pCi/L

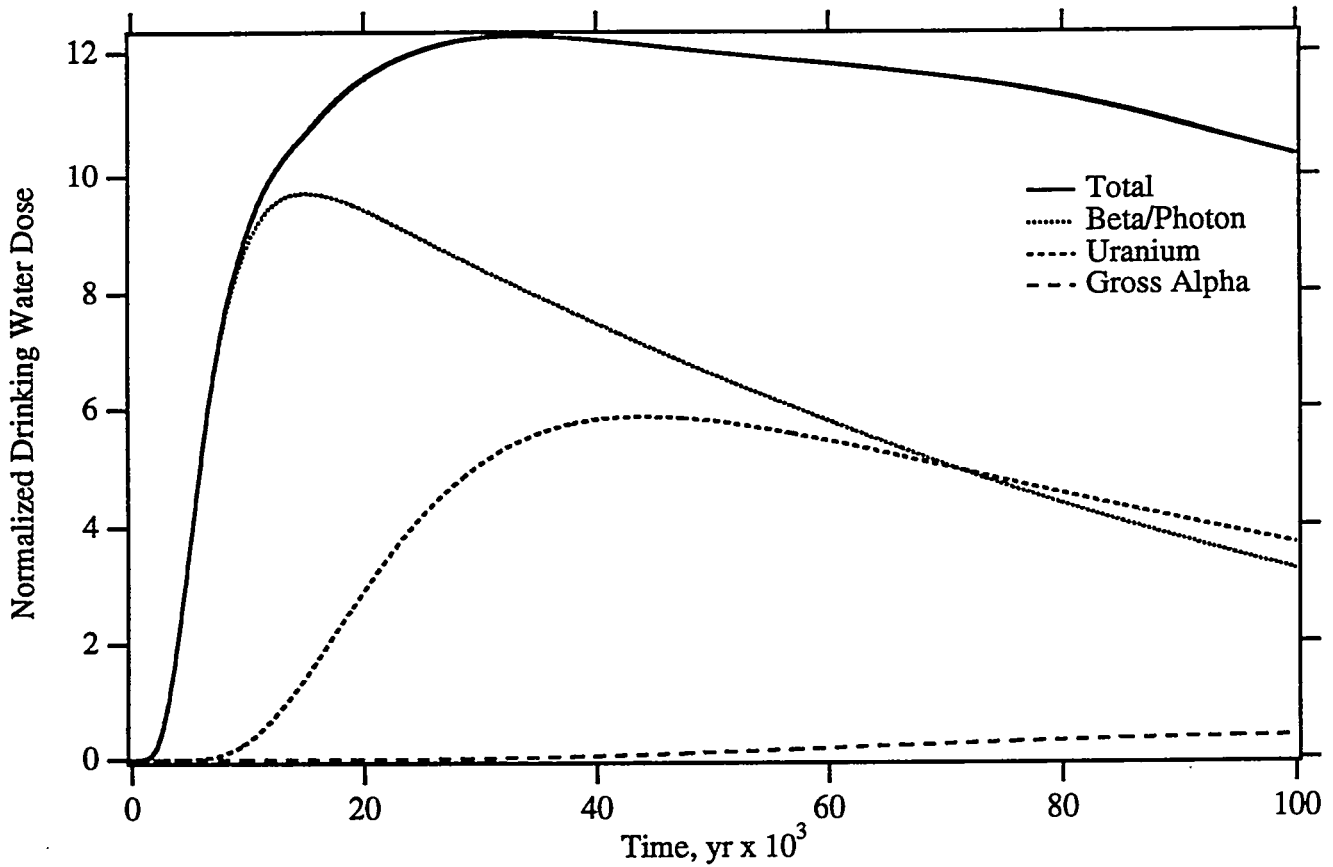


Figure A.13. Drinking Water Dose

Corrosion: 10^{-6} cm/yr
 Glass Radius: 0.25 cm
 Recharge: 0.1 cm/yr
 Solute Diffusion Coefficient: $D_{ab} = 10^{-8}$ cm²/s, $a = 1$, $b = 0$
 Glass Hydraulic Properties: Glass Spheres (SOILPROP)
 Minimum Relative Permeability: 0.
 Retardation Model: Saturation-Independent
 Hydraulic Dispersion: $\alpha_L = 6.5$ m, $\alpha_T = 0.65$ m
 Well Interception Factor: 0.01
 Grid: Narrow (10 x 162)

Maximum Dose Records 100,000 yr [10,000 yr]

Total	49.08 [36.21] mrem/yr
Beta/Photon	38.86 [35.32] mrem/yr
⁹⁹ Tc	37.19 [33.80] mrem/yr
¹²⁹ I	1.661 [1.484] mrem/yr
Uranium	117.3 [5.974] µg/L
Gross Alpha	5.683 [5.477e-06] pCi/L

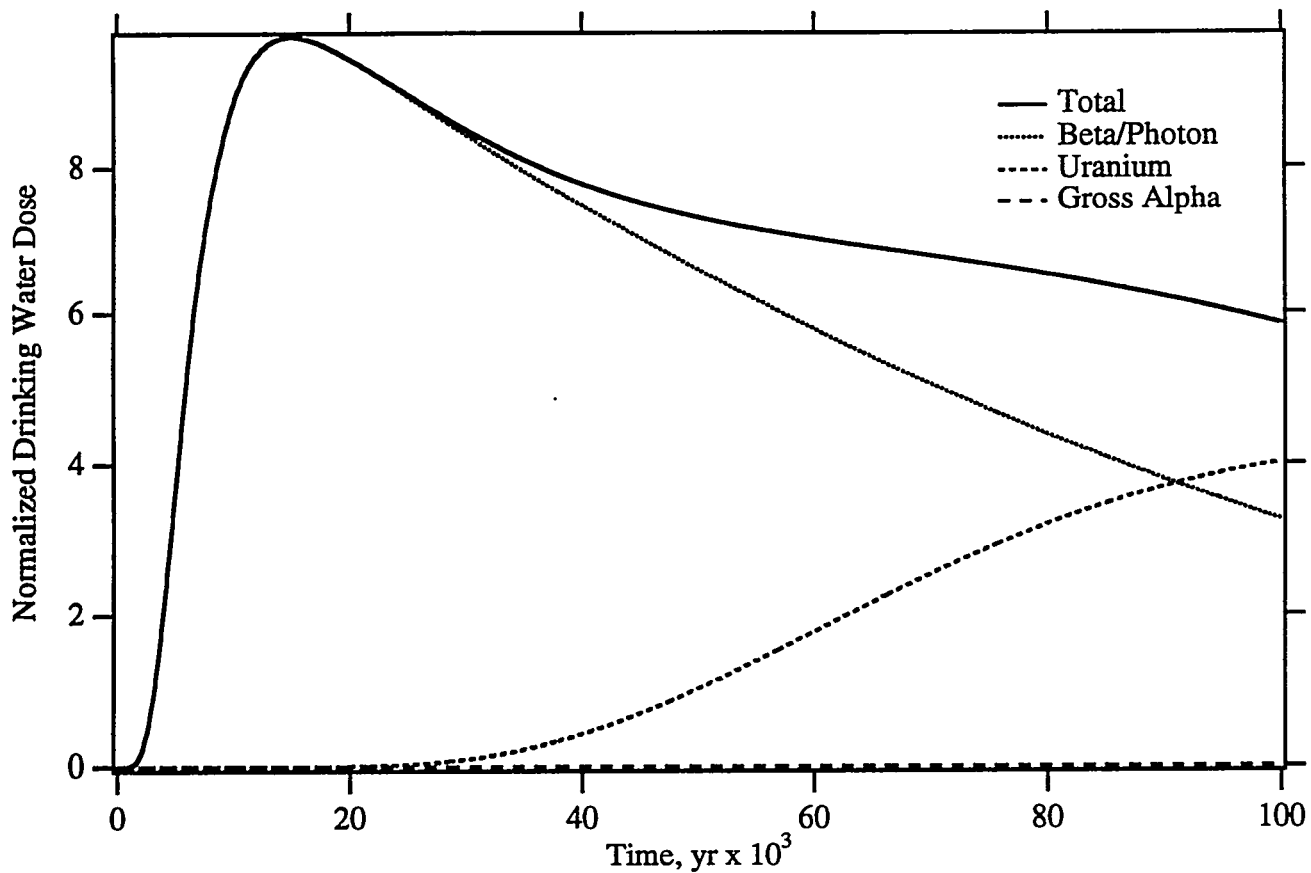


Figure A.13a. Drinking Water Dose

Corrosion: 10^{-6} cm/yr
 Glass Radius: 0.25 cm
 Recharge: 0.1 cm/yr
 Solute Diffusion Coefficient: $D_{ab} = 10^{-8}$ cm²/s, a = 1, b = 0
 Glass Hydraulic Properties: Glass Spheres (SOILPROP)
 Minimum Relative Permeability: 0.
 Retardation Model: Saturation-Dependent
 Hydraulic Dispersion: $\alpha_L = 6.5$ m, $\alpha_T = 0.65$ m
 Well Interception Factor: 0.01
 Grid: Narrow (10 x 162)

Maximum Dose Records 100,000 yr [10,000 yr]

Total	38.86 [35.32] mrem/yr
Beta/Photon	38.86 [35.32] mrem/yr
⁹⁹ Tc	37.19 [33.80] mrem/yr
¹²⁹ I	1.661 [1.484] mrem/yr
Uranium	80.26 [3.047e-05] µg/L
Gross Alpha	0.02336 [3.535e-23] pCi/L

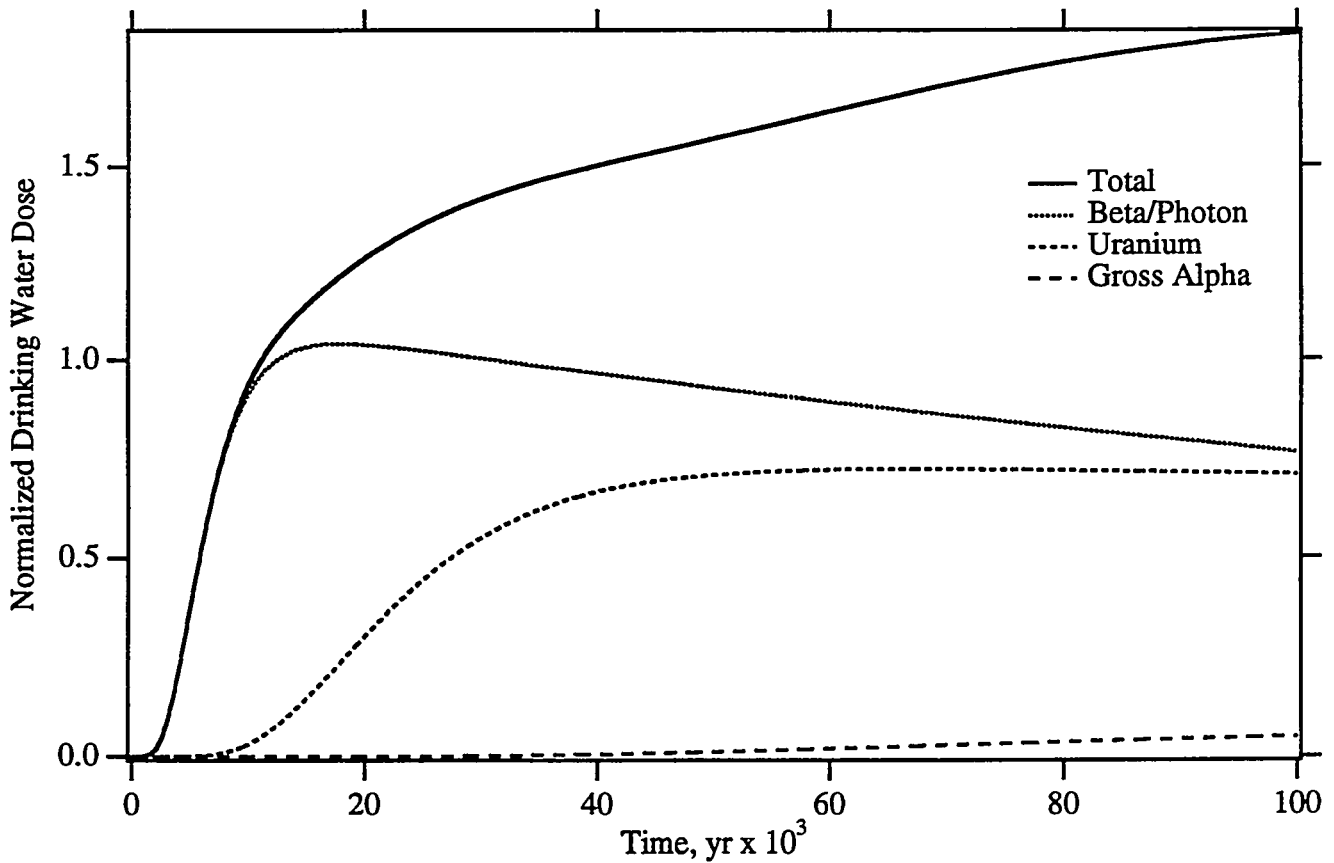


Figure A.14. Drinking Water Dose

Corrosion: 10^{-7} cm/yr
 Glass Radius: 0.25 cm
 Recharge: 0.1 cm/yr
 Solute Diffusion Coefficient: $D_{ab} = 10^{-8}$ cm²/s, $a = 1$, $b = 0$
 Glass Hydraulic Properties: Glass Spheres (SOILPROP)
 Minimum Relative Permeability: 0.
 Retardation Model: Saturation-Independent
 Hydraulic Dispersion: $\alpha_L = 6.5$ m, $\alpha_T = 0.65$ m
 Well Interception Factor: 0.01
 Grid: Narrow (10 x 162)

Maximum Dose Records 100,000 yr [10,000 yr]

Total	7.333 [3.752] mrem/yr
Beta/Photon	4.167 [3.659] mrem/yr
⁹⁹ Tc	3.986 [3.502] mrem/yr
¹²⁹ I	0.1804 [0.1537] mrem/yr
Uranium	14.45 [0.6275] µg/L
Gross Alpha	0.7366 [6.148e-07] pCi/L

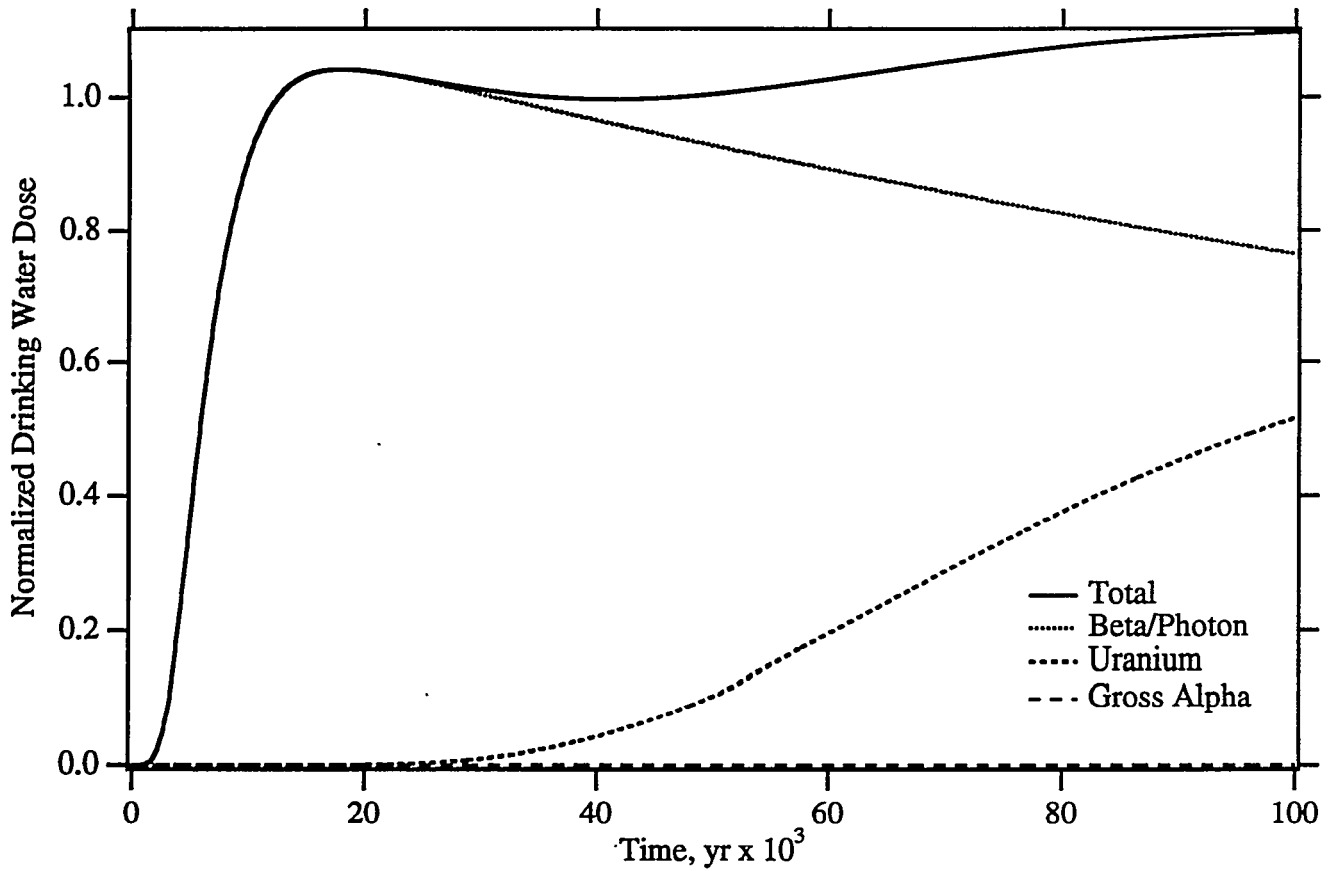


Figure A.14a. Drinking Water Dose

Corrosion: 10^{-7} cm/yr
 Glass Radius: 0.25 cm
 Recharge: 0.1 cm/yr
 Solute Diffusion Coefficient: $D_{ab} = 10^{-8}$ cm²/s, a = 1, b = 0
 Glass Hydraulic Properties: Glass Spheres (SOILPROP)
 Minimum Relative Permeability: 0.
 Retardation Model: Saturation-Dependent
 Hydraulic Dispersion: $\alpha_L = 6.5$ m, $\alpha_T = 0.65$ m
 Well Interception Factor: 0.01
 Grid: Narrow (10 x 162)

Maximum Dose Records 100,000 yr [10,000 yr]

Total	4.392 [3.659] mrem/yr
Beta/Photon	4.167 [3.659] mrem/yr
⁹⁹ Tc	3.986 [3.502] mrem/yr
¹²⁹ I	0.1804 [0.1537] mrem/yr
Uranium	10.31 [3.437e-06] µg/L
Gross Alpha	0.002519 [3.749e-24] pCi/L

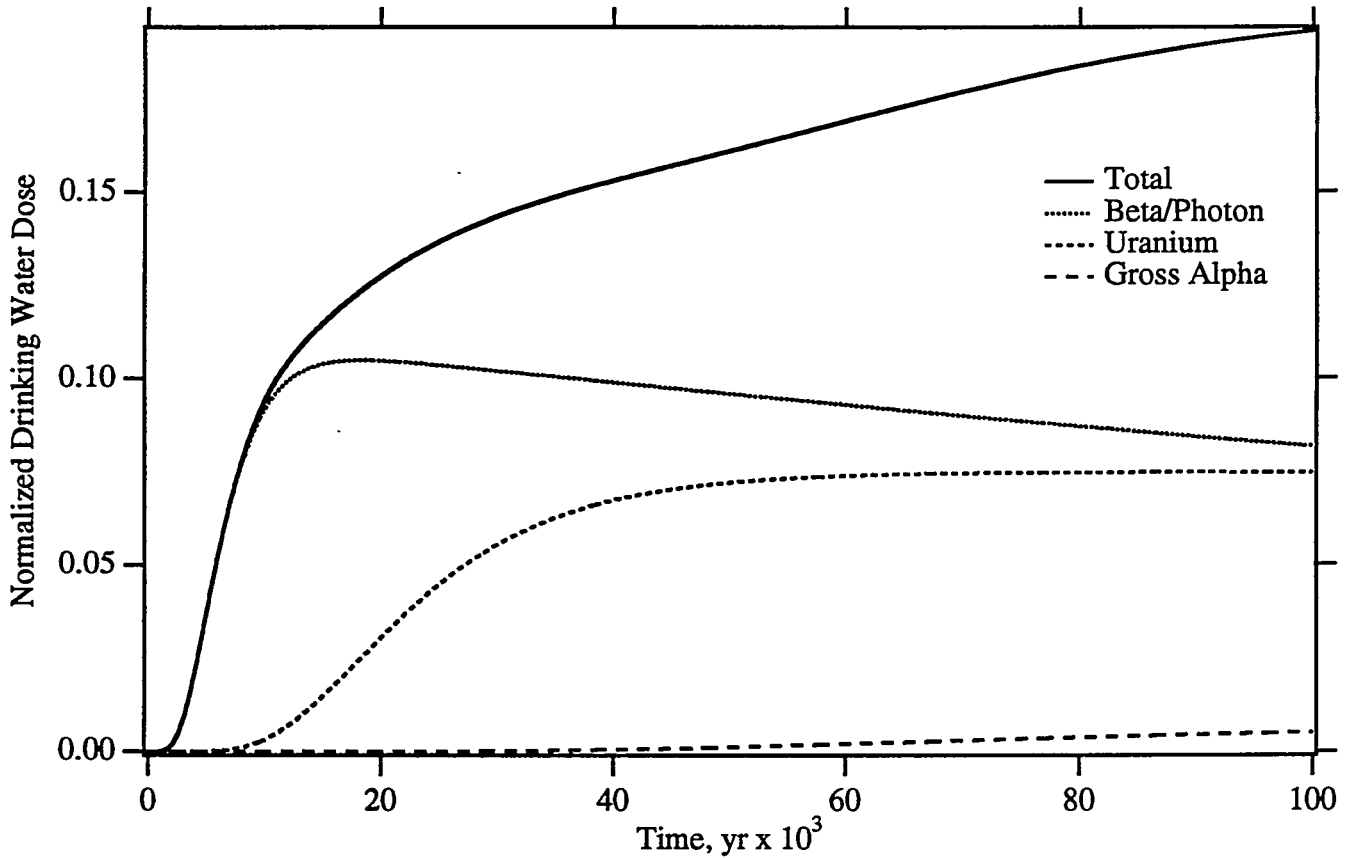


Figure A.15. Drinking Water Dose

Corrosion: 10^{-8} cm/yr
 Glass Radius: 0.25 cm
 Recharge: 0.1 cm/yr
 Solute Diffusion Coefficient: $D_{ab} = 10^{-8}$ cm²/s, a = 1, b = 0
 Glass Hydraulic Properties: Glass Spheres (SOILPROP)
 Minimum Relative Permeability: 0.
 Retardation Model: Saturation-Independent
 Hydraulic Dispersion: $\alpha_L = 6.5$ m, $\alpha_T = 0.65$ m
 Well Interception Factor: 0.01
 Grid: Narrow (10 x 162)

Maximum Dose Records 100,000 yr [10,000 yr]

Total	0.7714 [0.3763] mrem/yr
Beta/Photon	0.4201 [0.3670] mrem/yr
⁹⁹ Tc	0.4019 [0.3512] mrem/yr
¹²⁹ I	0.01827 [0.01542] mrem/yr
Uranium	1.497 [0.06282] µg/L
Gross Alpha	0.07550 [6.151e-08] pCi/L

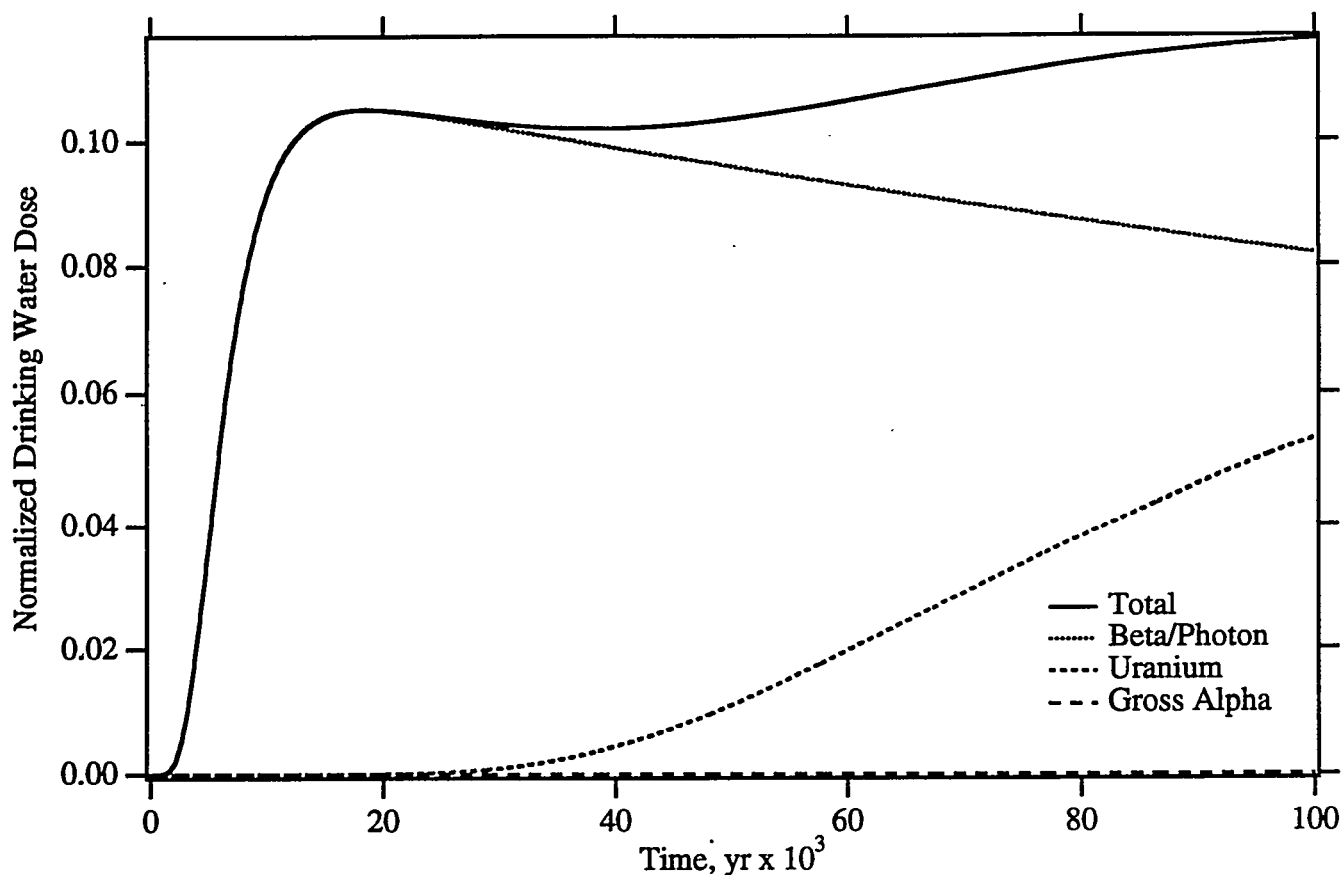


Figure A.15a. Drinking Water Dose

Corrosion: 10^{-8} cm/yr
 Glass Radius: 0.25 cm
 Recharge: 0.1 cm/yr
 Solute Diffusion Coefficient: $D_{ab} = 10^{-8}$ cm²/s, a = 1, b = 0
 Glass Hydraulic Properties: Glass Spheres (SOILPROP)
 Minimum Relative Permeability: 0.
 Retardation Model: Saturation-Dependent
 Hydraulic Dispersion: $\alpha_L = 6.5$ m, $\alpha_T = 0.65$ m
 Well Interception Factor: 0.01
 Grid: Narrow (10 x 162)

Maximum Dose Records 100,000 yr [10,000 yr]

Total	0.4641 [0.3670] mrem/yr
Beta/Photon	0.4201 [0.3670] mrem/yr
⁹⁹ Tc	0.4019 [0.3512] mrem/yr
¹²⁹ I	0.01827 [0.01542] mrem/yr
Uranium	1.056 [3.438e-07] µg/L
Gross Alpha	0.0002537 [2.998e-25] pCi/L

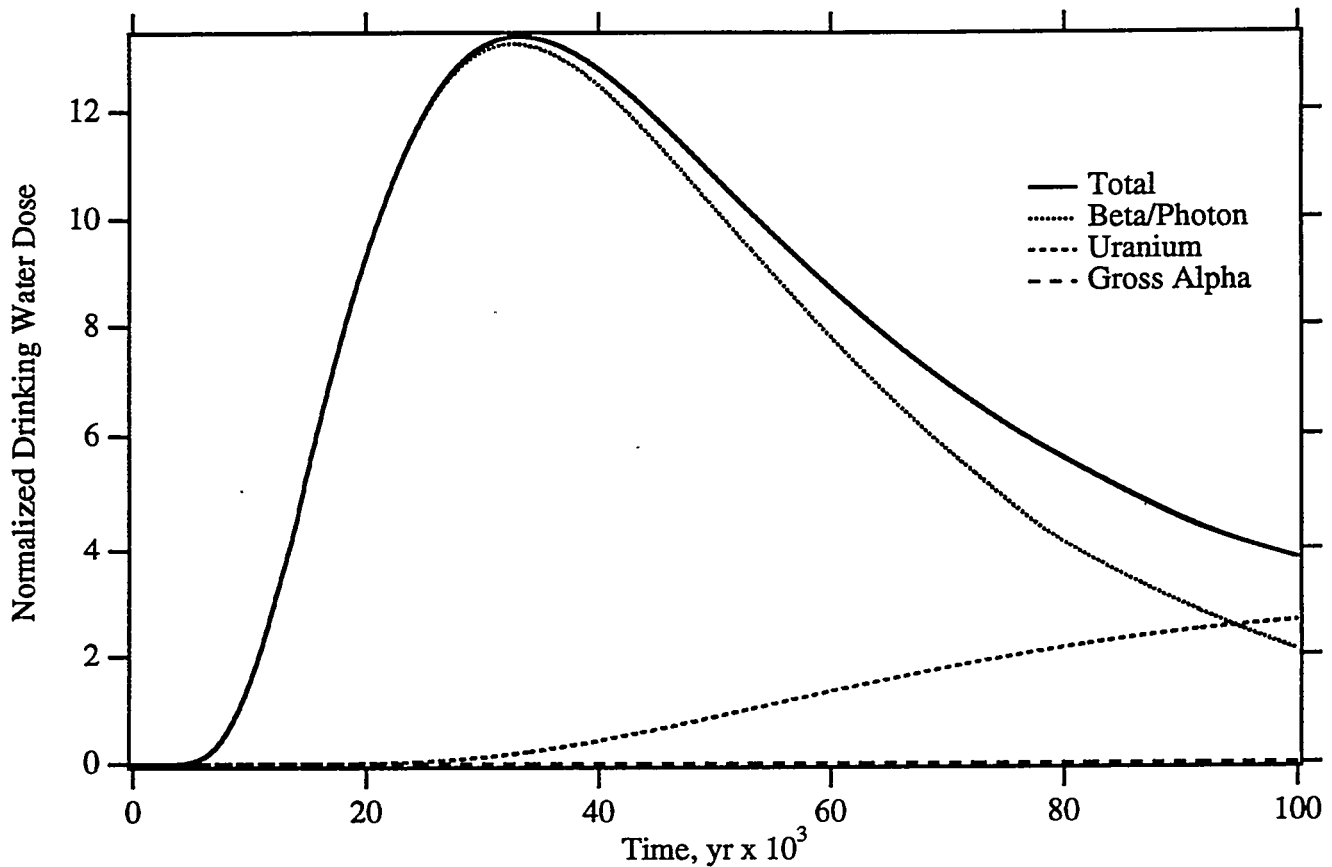


Figure A.16. Drinking Water Dose

Corrosion: 10^{-3} cm/yr
 Glass Radius: 0.25 cm
 Recharge: 0.01 cm/yr
 Solute Diffusion Coefficient: $D_{ab} = 10^{-8}$ cm²/s, a = 1, b = 0
 Glass Hydraulic Properties: Glass Spheres (SOILPROP)
 Minimum Relative Permeability: 0.
 Retardation Model: Saturation-Independent
 Hydraulic Dispersion: $\alpha_L = 6.5$ m, $\alpha_T = 0.65$ m
 Well Interception Factor: 0.001
 Grid: Narrow (10 x 162)

Maximum Dose Records 100,000 yr [10,000 yr]

Total	53.34 [6.053] mrem/yr
Beta/Photon	52.81 [6.053] mrem/yr
⁹⁹ Tc	50.43 [5.793] mrem/yr
¹²⁹ I	2.385 [0.2543] mrem/yr
Uranium	52.42 [0.0001216] µg/L
Gross Alpha	0.03729 [5.417e-20] pCi/L

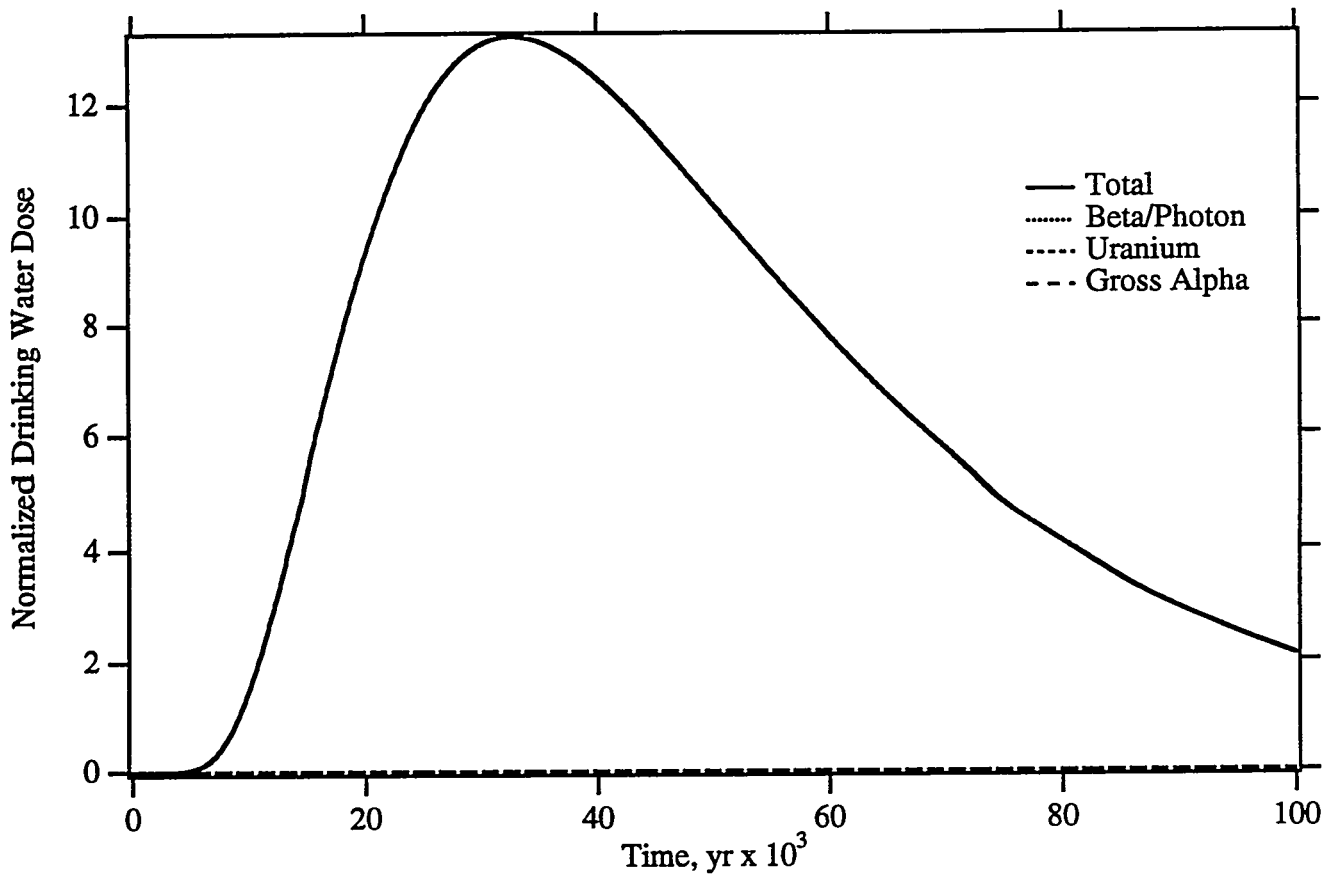


Figure A.16a. Drinking Water Dose

Corrosion: 10^{-3} cm/yr
 Glass Radius: 0.25 cm
 Recharge: 0.01 cm/yr
 Solute Diffusion Coefficient: $D_{ab} = 10^{-8}$ cm²/s, a = 1, b = 0
 Glass Hydraulic Properties: Glass Spheres (SOILPROP)
 Minimum Relative Permeability: 0.
 Retardation Model: Saturation-Dependent
 Hydraulic Dispersion: $\alpha_L = 6.5$ m, $\alpha_T = 0.65$ m
 Well Interception Factor: 0.001
 Grid: Narrow (10 x 162)

Maximum Dose Records 100,000 yr [10,000 yr]

Total	52.81 [6.053] mrem/yr
Beta/Photon	52.81 [6.053] mrem/yr
⁹⁹ Tc	50.43 [5.793] mrem/yr
¹²⁹ I	2.385 [0.2543] mrem/yr
Uranium	0.04929 [3.499e-25] μ g/L
Gross Alpha	1.239e-14 [-0.000] pCi/L

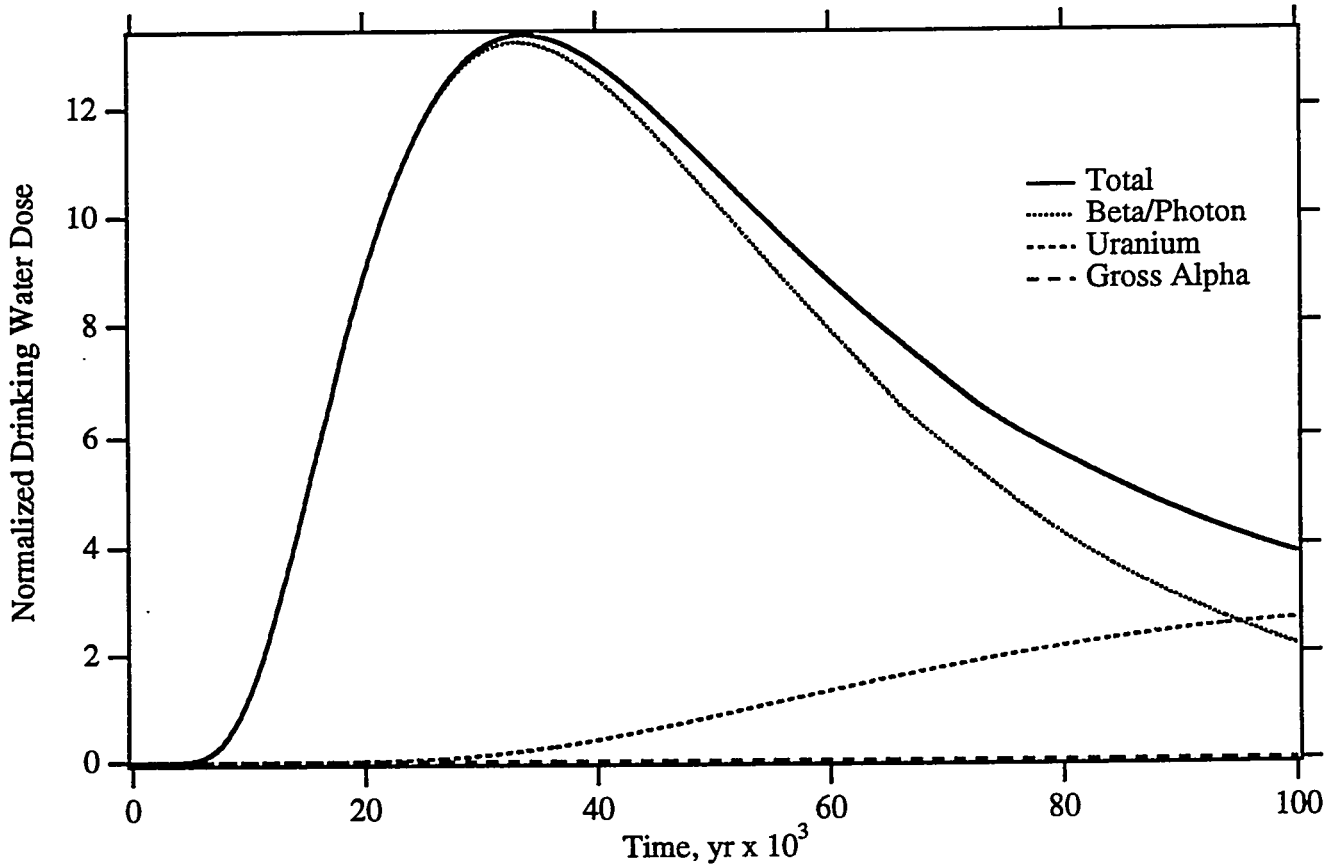


Figure A.17. Drinking Water Dose

Corrosion: 10^{-4} cm/yr
 Glass Radius: 0.25 cm
 Recharge: 0.01 cm/yr
 Solute Diffusion Coefficient: $D_{ab} = 10^{-8}$ cm²/s, a = 1, b = 0
 Glass Hydraulic Properties: Glass Spheres (SOILPROP)
 Minimum Relative Permeability: 0.
 Retardation Model: Saturation-Independent
 Hydraulic Dispersion: $\alpha_L = 6.5$ m, $\alpha_T = 0.65$ m
 Well Interception Factor: 0.001
 Grid: Narrow (10 x 162)

Maximum Dose Records 100,000 yr [10,000 yr]

Total	53.24 [4.982] mrem/yr
Beta/Photon	52.71 [4.982] mrem/yr
⁹⁹ Tc	50.33 [4.768] mrem/yr
¹²⁹ I	2.384 [0.2093] mrem/yr
Uranium	52.25 [6.818e-05] µg/L
Gross Alpha	0.03507 [1.332e-20] pCi/L

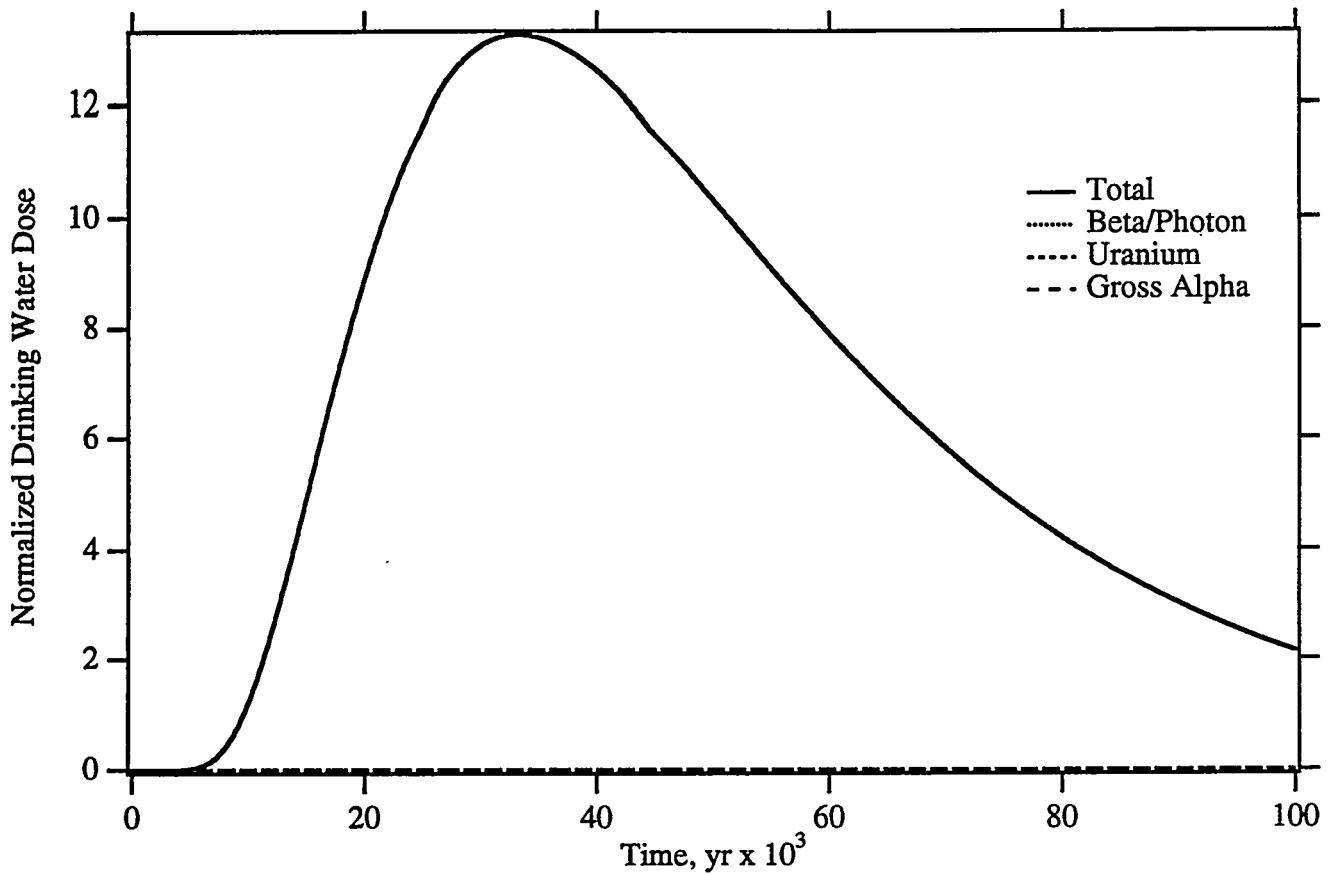


Figure A.17a. Drinking Water Dose

Corrosion: 10^{-4} cm/yr
 Glass Radius: 0.25 cm
 Recharge: 0.01 cm/yr
 Solute Diffusion Coefficient: $D_{ab} = 10^{-8}$ cm²/s, a = 1, b = 0
 Glass Hydraulic Properties: Glass Spheres (SOILPROP)
 Minimum Relative Permeability: 0.
 Retardation Model: Saturation-Dependent
 Hydraulic Dispersion: $\alpha_L = 6.5$ m, $\alpha_T = 0.65$ m
 Well Interception Factor: 0.001
 Grid: Narrow (10 x 162)

Maximum Dose Records 100,000 yr [10,000 yr]

Total	52.71 [4.982] mrem/yr
Beta/Photon	52.71 [4.982] mrem/yr
⁹⁹ Tc	50.33 [4.768] mrem/yr
¹²⁹ I	2.384 [0.2093] mrem/yr
Uranium	0.04724 [8.454e-26] µg/L
Gross Alpha	1.066e-14 [-0.000] pCi/L

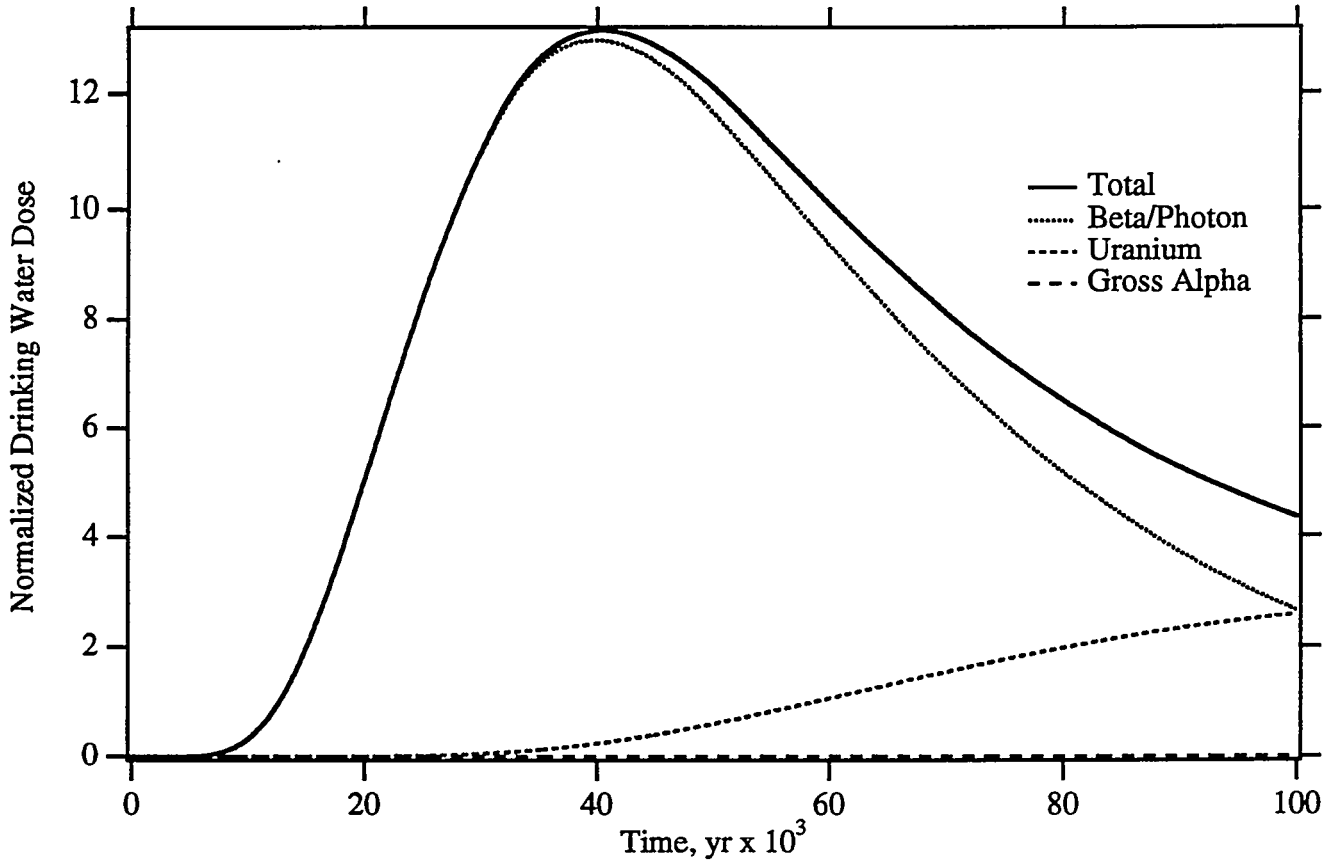


Figure A.18. Drinking Water Dose

Corrosion: 10^{-5} cm/yr
 Glass Radius: 0.25 cm
 Recharge: 0.01 cm/yr
 Solute Diffusion Coefficient: $D_{ab} = 10^{-8}$ cm²/s, $a = 1$, $b = 0$
 Glass Hydraulic Properties: Glass Spheres (SOILPROP)
 Minimum Relative Permeability: 0.
 Retardation Model: Saturation-Independent
 Hydraulic Dispersion: $\alpha_L = 6.5$ m, $\alpha_T = 0.65$ m
 Well Interception Factor: 0.001
 Grid: Narrow (10 x 162)

Maximum Dose Records 100,000 yr [10,000 yr]

Total	52.38 [1.260] mrem/yr
Beta/Photon	51.69 [1.260] mrem/yr
⁹⁹ Tc	49.31 [1.206] mrem/yr
¹²⁹ I	2.386 [0.05296] mrem/yr
Uranium	51.63 [1.129e-05] µg/L
Gross Alpha	0.02680 [1.887e-21] pCi/L

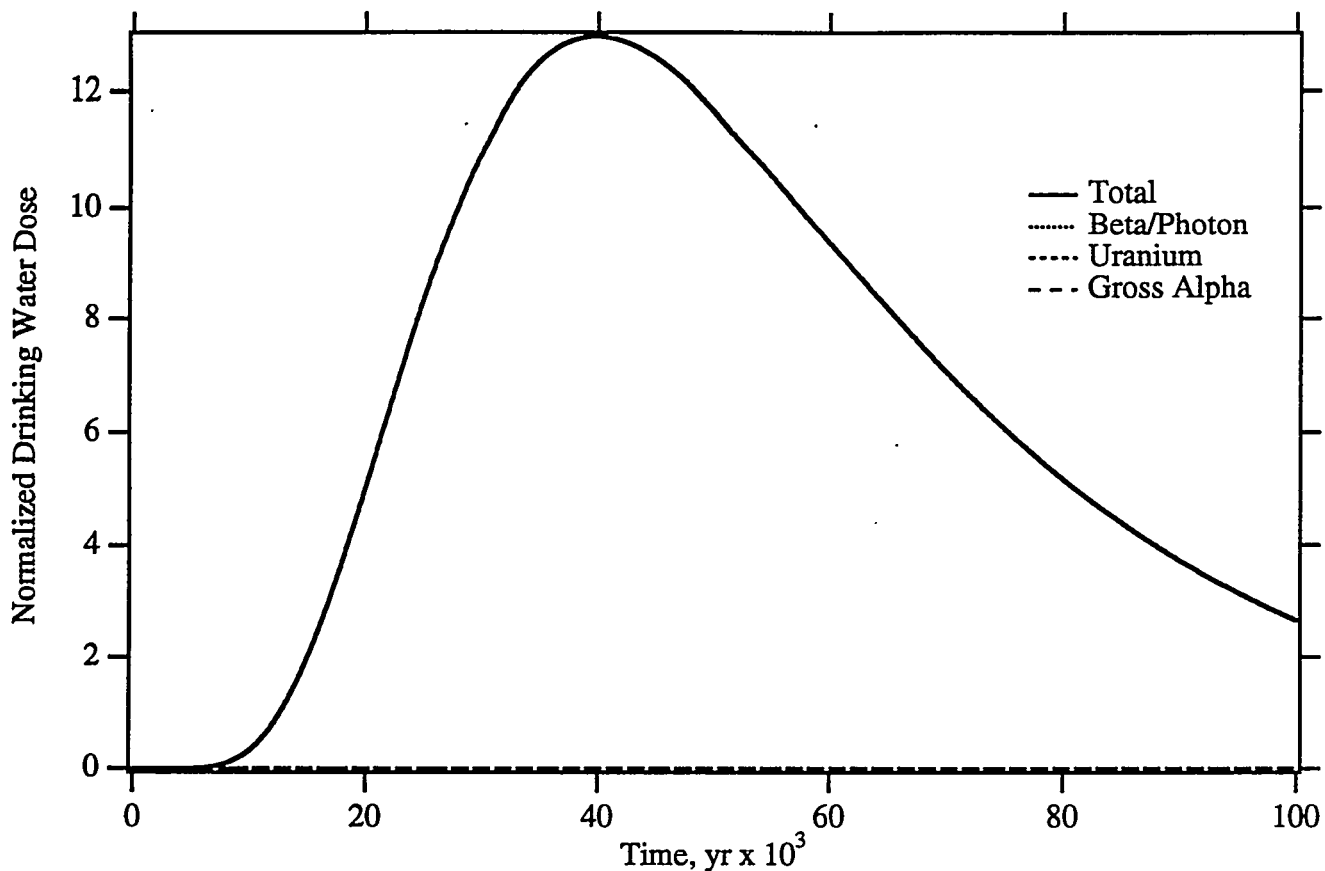


Figure A.18a. Drinking Water Dose

Corrosion: 10^{-5} cm/yr
 Glass Radius: 0.25 cm
 Recharge: 0.01 cm/yr
 Solute Diffusion Coefficient: $D_{ab} = 10^{-8}$ cm²/s, a = 1, b = 0
 Glass Hydraulic Properties: Glass Spheres (SOILPROP)
 Minimum Relative Permeability: 0.
 Retardation Model: SaturationDependent
 Hydraulic Dispersion: $\alpha_L = 6.5$ m, $\alpha_T = 0.65$ m
 Well Interception Factor: 0.001
 Grid: Narrow (10 x 162)

Maximum Dose Records 100,000 yr [10,000 yr]

Total	51.69 [1.260] mrem/yr
Beta/Photon	51.69 [1.260] mrem/yr
⁹⁹ Tc	49.31 [1.206] mrem/yr
¹²⁹ I	2.386 [0.05296] mrem/yr
Uranium	0.03219 [2.854e-27] μ g/L
Gross Alpha	4.002e-15 [-0.000] pCi/L

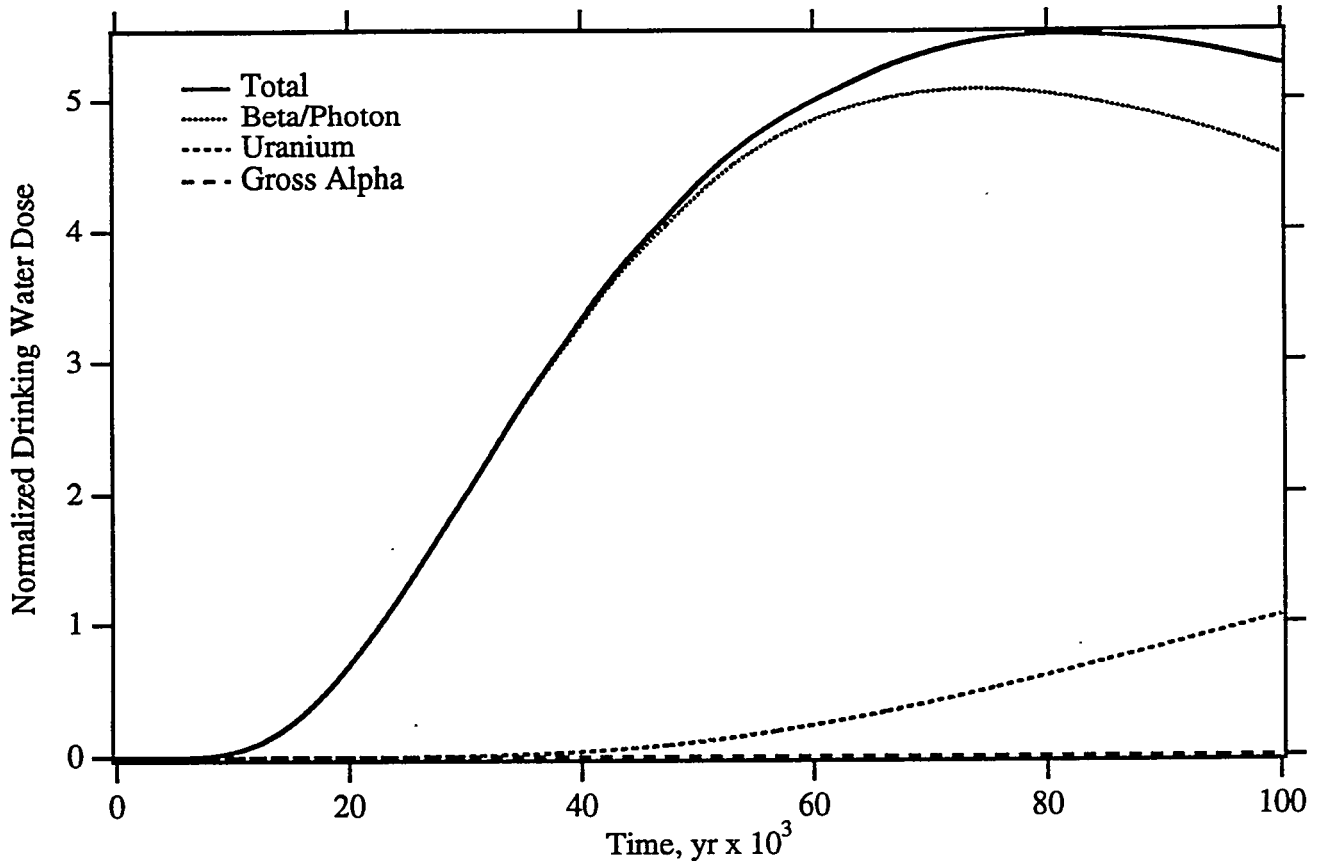


Figure A.19. Drinking Water Dose

Corrosion: 10^{-6} cm/yr
 Glass Radius: 0.25 cm
 Recharge: 0.01 cm/yr
 Solute Diffusion Coefficient: $D_{ab} = 10^{-8}$ cm²/s, a = 1, b = 0
 Glass Hydraulic Properties: Glass Spheres (SOILPROP)
 Minimum Relative Permeability: 0.
 Retardation Model: Saturation-Independent
 Hydraulic Dispersion: $\alpha_L = 6.5$ m, $\alpha_T = 0.65$ m
 Well Interception Factor: 0.001
 Grid: Narrow (10 x 162)

Maximum Dose Records 100,000 yr [10,000 yr]

Total	21.78 [0.1360] mrem/yr
Beta/Photon	20.32 [0.1360] mrem/yr
⁹⁹ Tc	19.28 [0.1301] mrem/yr
¹²⁹ I	1.052 [0.005712] mrem/yr
Uranium	21.06 [1.128e-06] µg/L
Gross Alpha	0.005669 [1.619e-22] pCi/L

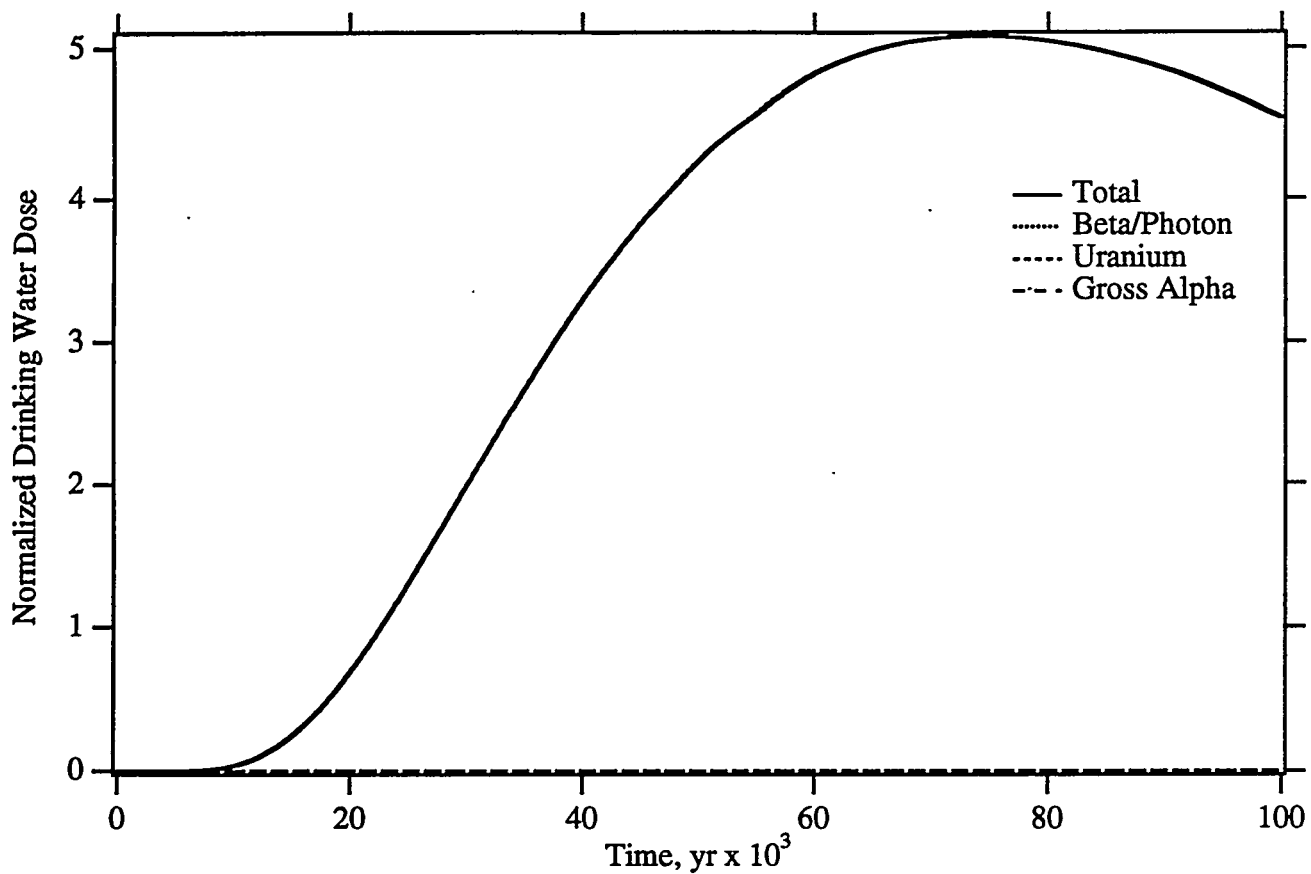


Figure A.19a. Drinking Water Dose

Corrosion: 10^{-6} cm/yr
 Glass Radius: 0.25 cm
 Recharge: 0.01 cm/yr
 Solute Diffusion Coefficient: $D_{ab} = 10^{-8}$ cm²/s, $a = 1$, $b = 0$
 Glass Hydraulic Properties: Glass Spheres (SOILPROP)
 Minimum Relative Permeability: 0.
 Retardation Model: Saturation-Dependent
 Hydraulic Dispersion: $\alpha_L = 6.5$ m, $\alpha_T = 0.65$ m
 Well Interception Factor: 0.001
 Grid: Narrow (10 x 162)

Maximum Dose Records 100,000 yr [10,000 yr]

Total	20.32 [0.1360] mrem/yr
Beta/Photon	20.32 [0.1360] mrem/yr
⁹⁹ Tc	19.28 [0.1301] mrem/yr
¹²⁹ I	1.052 [0.005712] mrem/yr
Uranium	0.005842 [-0.000] µg/L
Gross Alpha	4.985e-16 [-0.000] pCi/L

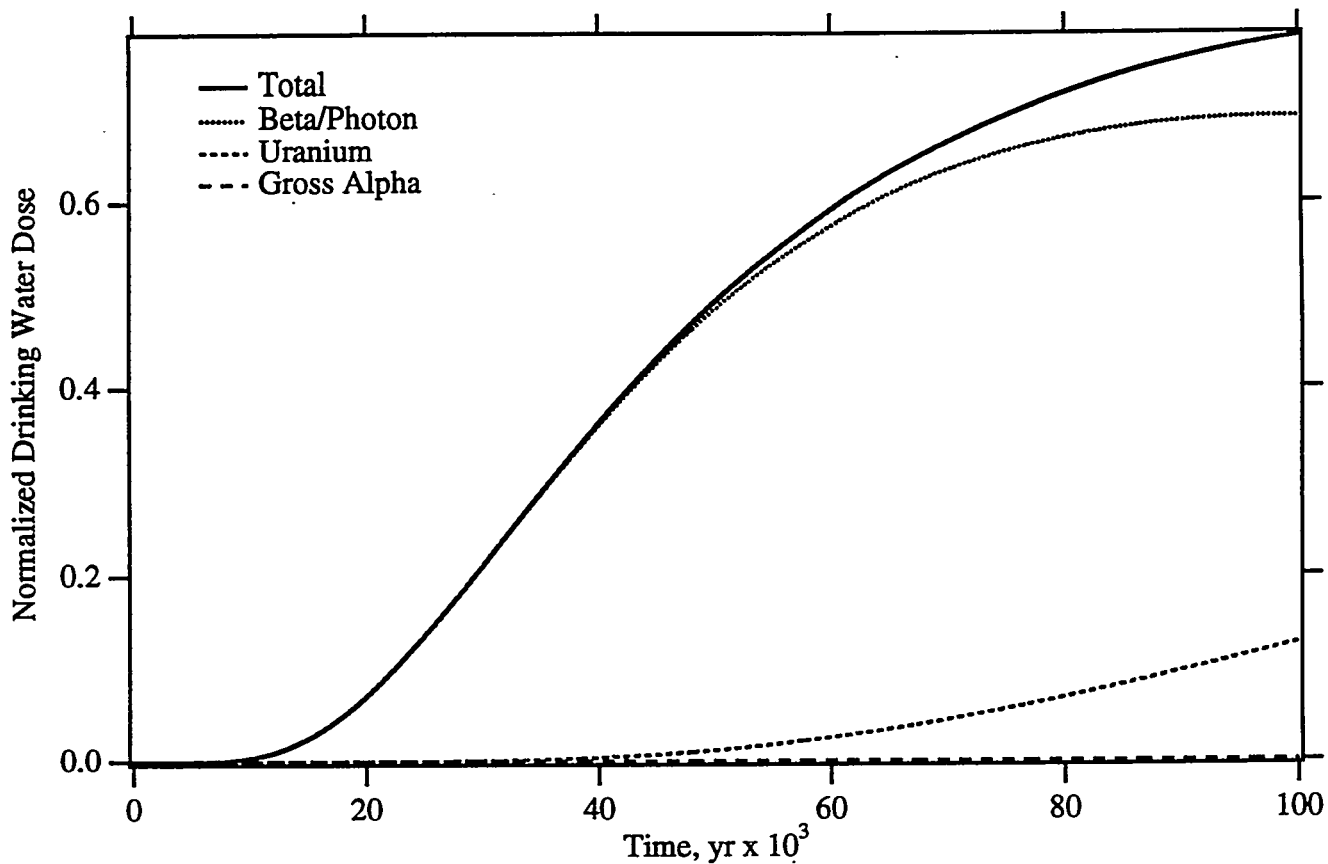


Figure A.20. Drinking Water Dose

Corrosion: 10^{-7} cm/yr
 Glass Radius: 0.25 cm
 Recharge: 0.01 cm/yr
 Solute Diffusion Coefficient: $D_{ab} = 10^{-8}$ cm²/s, a = 1, b = 0
 Glass Hydraulic Properties: Glass Spheres (SOILPROP)
 Minimum Relative Permeability: 0.
 Retardation Model: Saturation-Independent
 Hydraulic Dispersion: $\alpha_L = 6.5$ m, $\alpha_T = 0.65$ m
 Well Interception Factor: 0.001
 Grid: Narrow (10 x 162)

Maximum Dose Records 100,000 yr [10,000 yr]

Total	3.085 [0.01437] mrem/yr
Beta/Photon	2.759 [0.01437] mrem/yr
⁹⁹ Tc	2.607 [0.01375] mrem/yr
¹²⁹ I	0.1527 [0.0006037] mrem/yr
Uranium	2.521 [1.279e-07] μ g/L
Gross Alpha	0.0006148 [1.711e-23] pCi/L

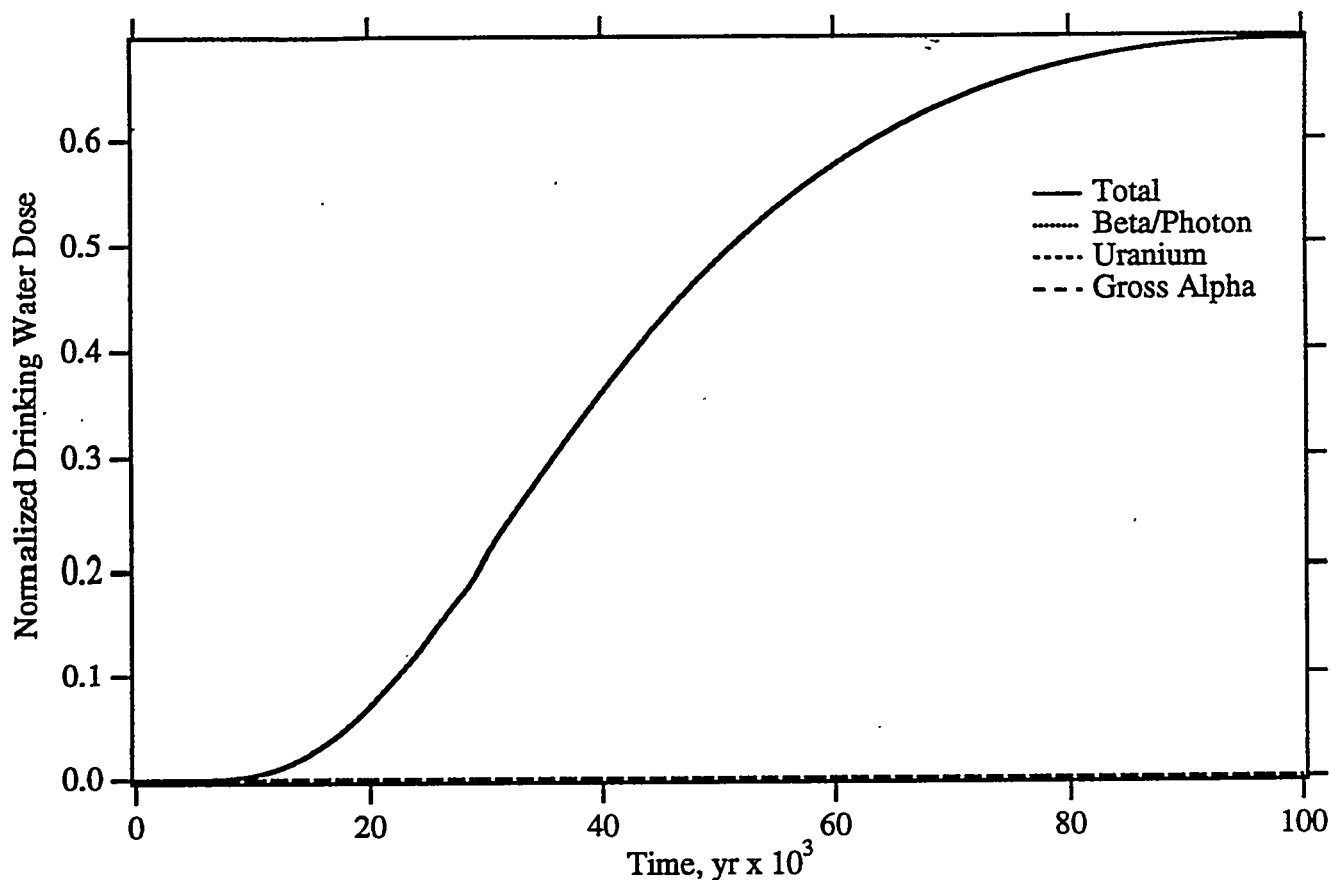


Figure A.20a. Drinking Water Dose

Corrosion: 10^{-7} cm/yr
 Glass Radius: 0.25 cm
 Recharge: 0.01 cm/yr
 Solute Diffusion Coefficient: $D_{ab} = 10^{-8}$ cm²/s, $a = 1$, $b = 0$
 Glass Hydraulic Properties: Glass Spheres (SOILPROP)
 Minimum Relative Permeability: 0.
 Retardation Model: Saturation-Dependent
 Hydraulic Dispersion: $\alpha_L = 6.5$ m, $\alpha_T = 0.65$ m
 Well Interception Factor: 0.001
 Grid: Narrow (10 x 162)

Maximum Dose Records 100,000 yr [10,000 yr]

Total	2.759 [0.01437] mrem/yr
Beta/Photon	2.759 [0.01437] mrem/yr
⁹⁹ Tc	2.607 [0.01375] mrem/yr
¹²⁹ I	0.1527 [0.0006037] mrem/yr
Uranium	0.0006220 [-0.000] µg/L
Gross Alpha	4.772e-17 [-0.000] pCi/L

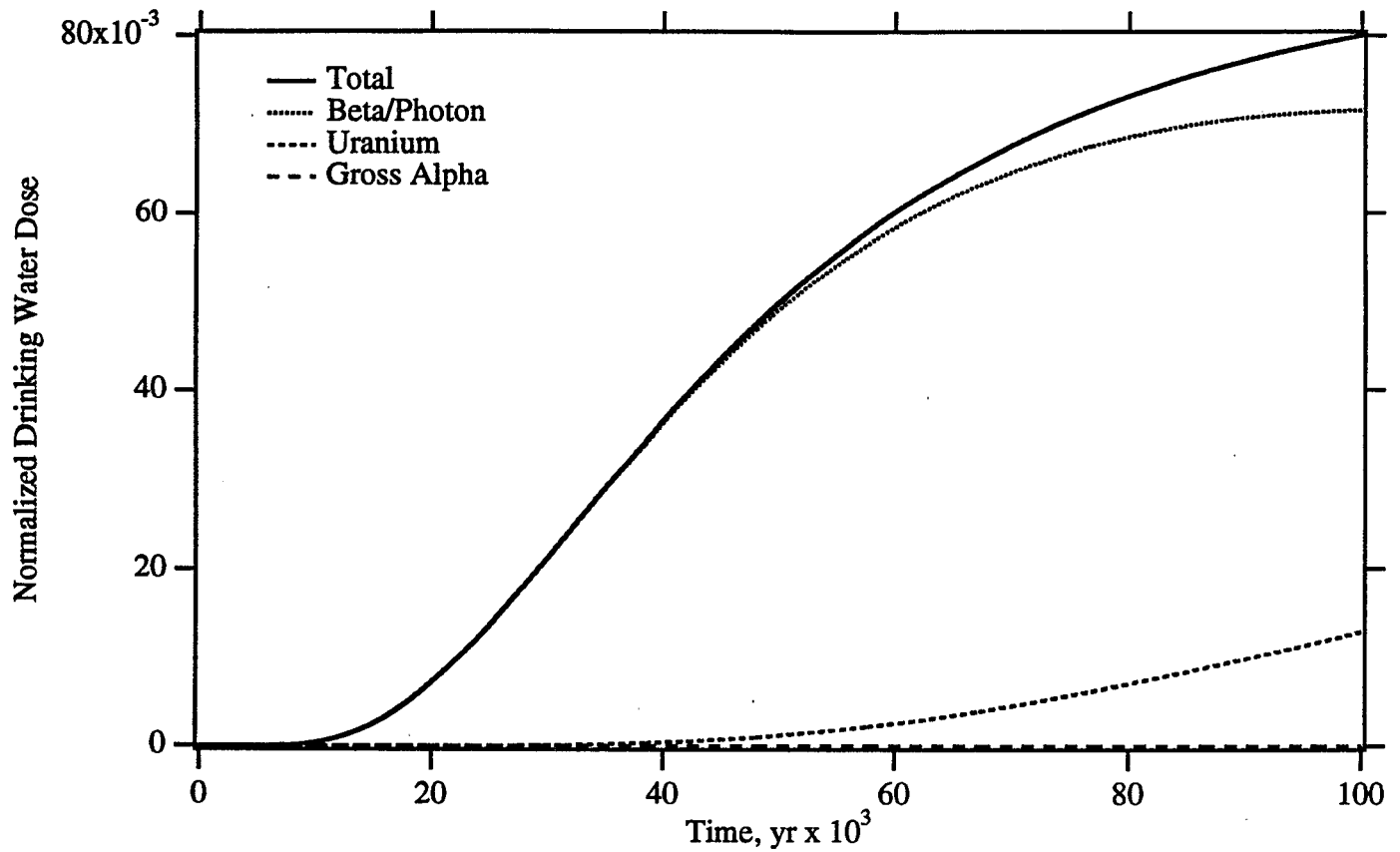


Figure A.21. Drinking Water Dose

Corrosion: 10^{-8} cm/yr
 Glass Radius: 0.25 cm
 Recharge: 0.01 cm/yr
 Solute Diffusion Coefficient: $D_{ab} = 10^{-8}$ cm²/s, $a = 1$, $b = 0$
 Glass Hydraulic Properties: Glass Spheres (SOILPROP)
 Minimum Relative Permeability: 0.
 Retardation Model: Saturation-Independent
 Hydraulic Dispersion: $\alpha_L = 6.5$ m, $\alpha_T = 0.65$ m
 Well Interception Factor: 0.001
 Grid: Narrow (10 x 162)

Maximum Dose Records 100,000 yr [10,000 yr]

Total	0.3198 [0.001438] mrem/yr
Beta/Photon	0.2865 [0.001438] mrem/yr
⁹⁹ Tc	0.2707 [0.001376] mrem/yr
¹²⁹ I	0.01586 [6.043e-05] mrem/yr

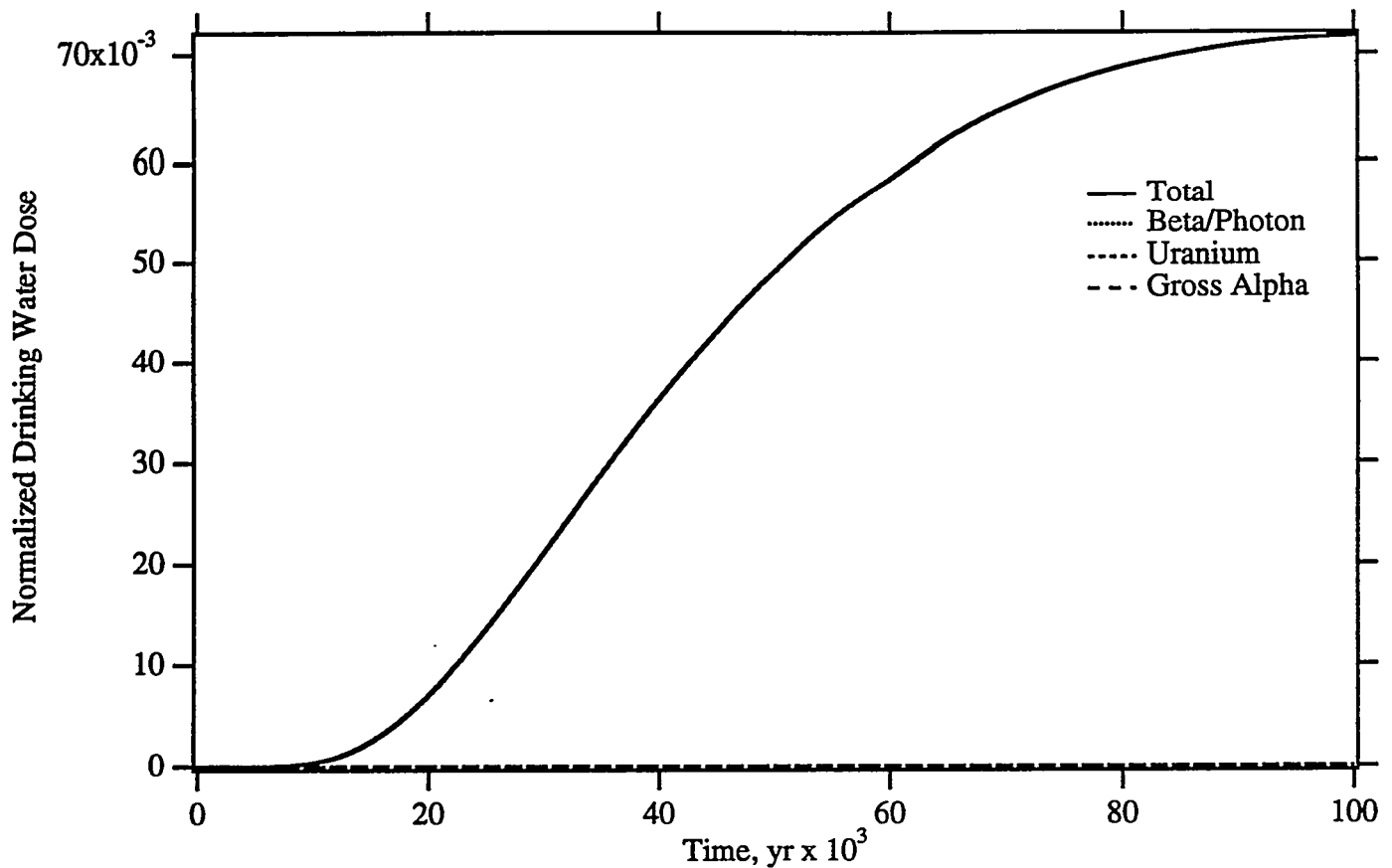


Figure A.21a. Drinking Water Dose

Corrosion: 10^{-8} cm/yr
 Glass Radius: 0.25 cm
 Recharge: 0.01 cm/yr
 Solute Diffusion Coefficient: $D_{ab} = 10^{-8}$ cm²/s, a = 1, b = 0
 Glass Hydraulic Properties: Glass Spheres (SOILPROP)
 Minimum Relative Permeability: 0.
 Retardation Model: Saturation-Dependent
 Hydraulic Dispersion: $\alpha_L = 6.5$ m, $\alpha_T = 0.65$ m
 Well Interception Factor: 0.001
 Grid: Narrow (10 x 162)

Maximum Dose Records 100,000 yr [10,000 yr]

Total	0.2866 [0.001438] mrem/yr
Beta/Photon	0.2865 [0.001438] mrem/yr
⁹⁹ Tc	0.2707 [0.001376] mrem/yr
¹²⁹ I	0.01586 [6.043e-05] mrem/yr
Uranium	6.258e-05 [-0.000] µg/L
Gross Alpha	8.554e-19 [-0.000] pCi/L

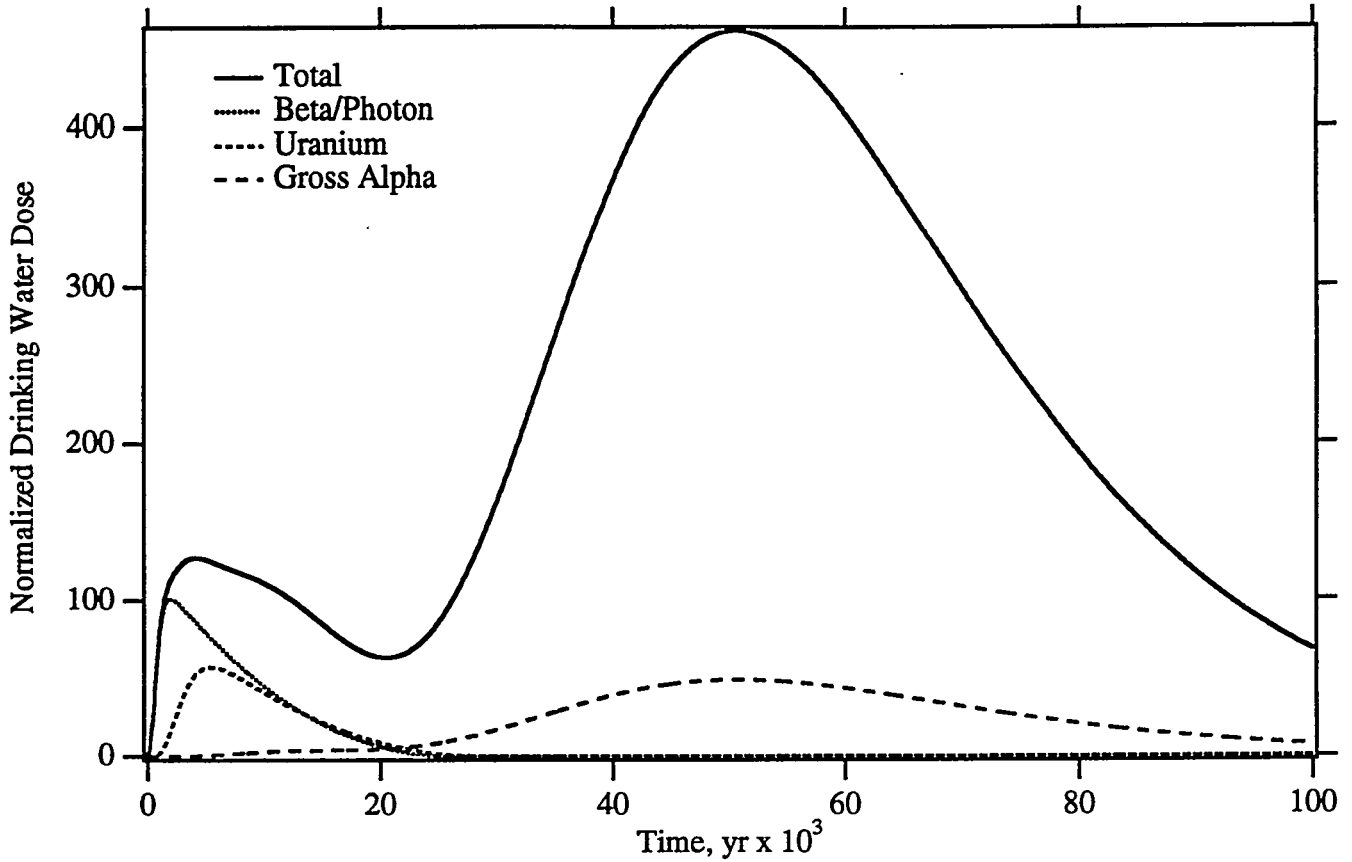


Figure A.22. Drinking Water Dose

Corrosion: 10^{-5} cm/yr
 Glass Radius: 0.25 cm
 Recharge: 1 cm/yr
 Solute Diffusion Coefficient: $D_{ab} = 10^{-8}$ cm²/s, a = 1, b = 0
 Glass Hydraulic Properties: Glass Spheres (SOILPROP)
 Minimum Relative Permeability: 0.
 Retardation Model: Saturation-Independent
 Hydraulic Dispersion: $\alpha_L = 6.5$ m, $\alpha_T = 0.65$ m
 Well Interception Factor: 0.1
 Grid: Narrow (10 x 162)

Maximum Dose Records 100,000 yr [10,000 yr]

Total	1834 [508.6] mrem/yr
Beta/Photon	403.3 [403.3] mrem/yr
⁹⁹ Tc	385.9 [385.9] mrem/yr
¹²⁹ I	16.51 [16.51] mrem/yr
Uranium	1140 [1140] μ g/L
Gross Alpha	733.8 [42.58] pCi/L

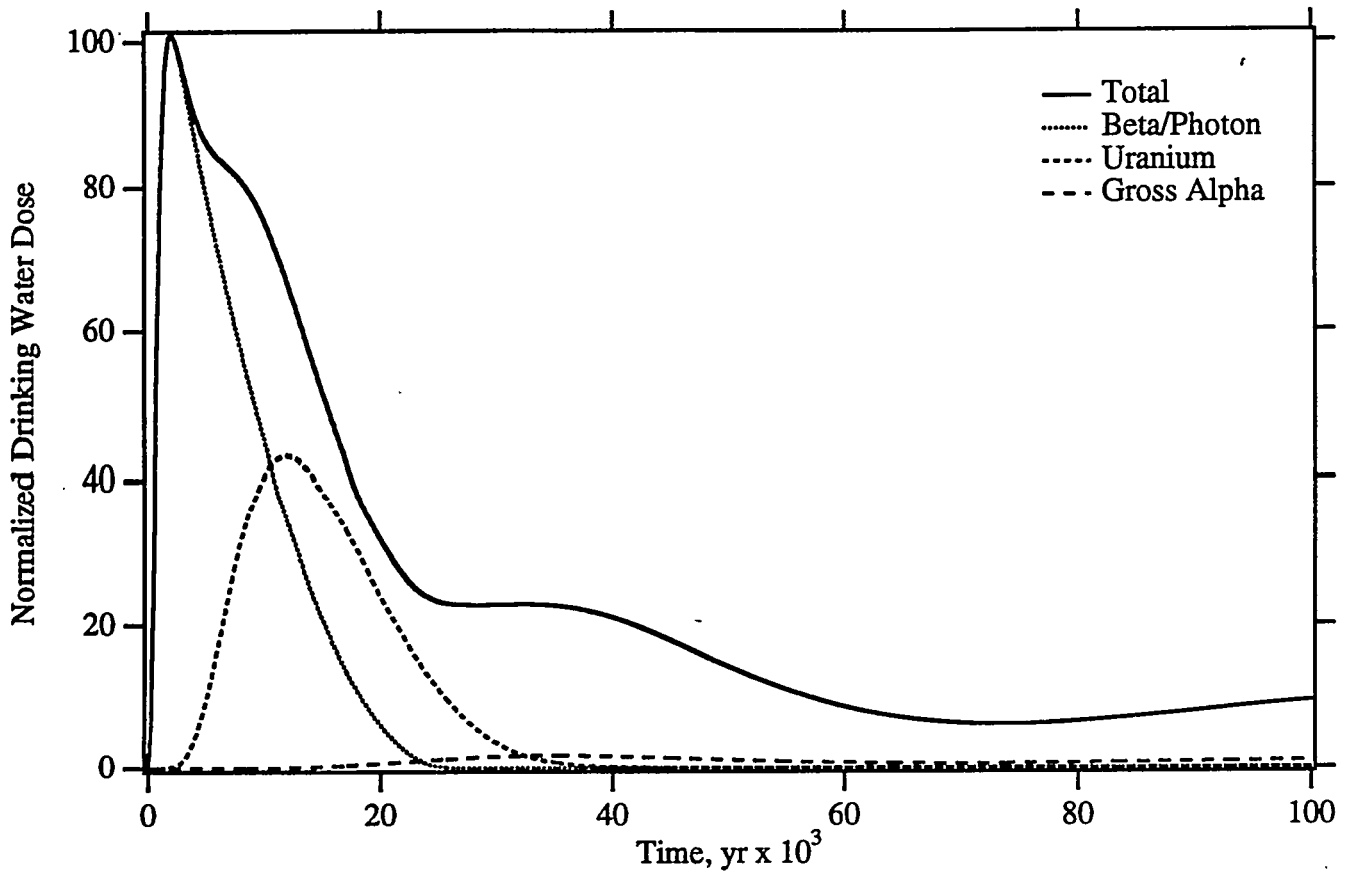


Figure A.22a. Drinking Water Dose

Corrosion: 10^{-5} cm/yr
 Glass Radius: 0.25 cm
 Recharge: 1 cm/yr
 Solute Diffusion Coefficient: $D_{ab} = 10^{-8}$ cm²/s, a = 1, b = 0
 Glass Hydraulic Properties: Glass Spheres (SOILPROP)
 Minimum Relative Permeability: 0.
 Retardation Model: Saturation-Dependent
 Hydraulic Dispersion: $\alpha_L = 6.5$ m, $\alpha_T = 0.65$ m
 Well Interception Factor: 0.1
 Grid: Narrow (10 x 162)

Maximum Dose Records 100,000 yr [10,000 yr]

Total	403.6 [403.6] mrem/yr
Beta/Photon	403.3 [403.3] mrem/yr
⁹⁹ Tc	385.9 [385.9] mrem/yr
¹²⁹ I	16.51 [16.51] mrem/yr
Uranium	859.1 [809.7] µg/L
Gross Alpha	26.62 [0.1928] pCi/L

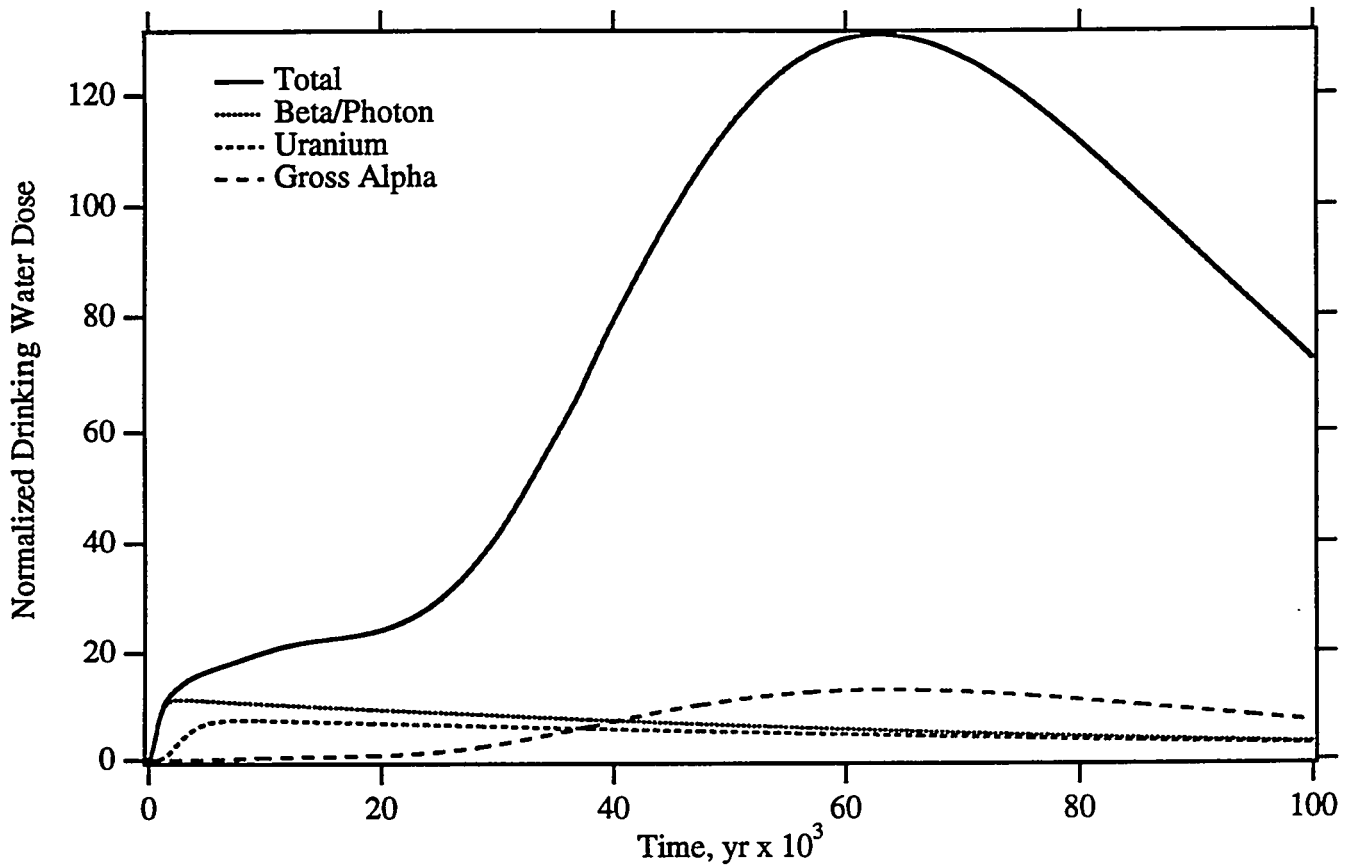


Figure A.23. Drinking Water Dose

Corrosion: 10^{-6} cm/yr
 Glass Radius: 0.25 cm
 Recharge: 1 cm/yr
 Solute Diffusion Coefficient: $D_{ab} = 10^{-8}$ cm²/s, a = 1, b = 0
 Glass Hydraulic Properties: Glass Spheres (SOILPROP)
 Minimum Relative Permeability: 0.
 Retardation Model: Saturation-Independent
 Hydraulic Dispersion: $\alpha_L = 6.5$ m, $\alpha_T = 0.65$ m
 Well Interception Factor: 0.1
 Grid: Narrow (10 x 162)

Maximum Dose Records 100,000 yr [10,000 yr]

Total	522.9 [80.28] mrem/yr
Beta/Photon	44.82 [44.82] mrem/yr
⁹⁹ Tc	42.89 [42.89] mrem/yr
¹²⁹ I	1.840 [1.840] mrem/yr
Uranium	146.6 [146.6] µg/L
Gross Alpha	193.4 [5.137] pCi/L

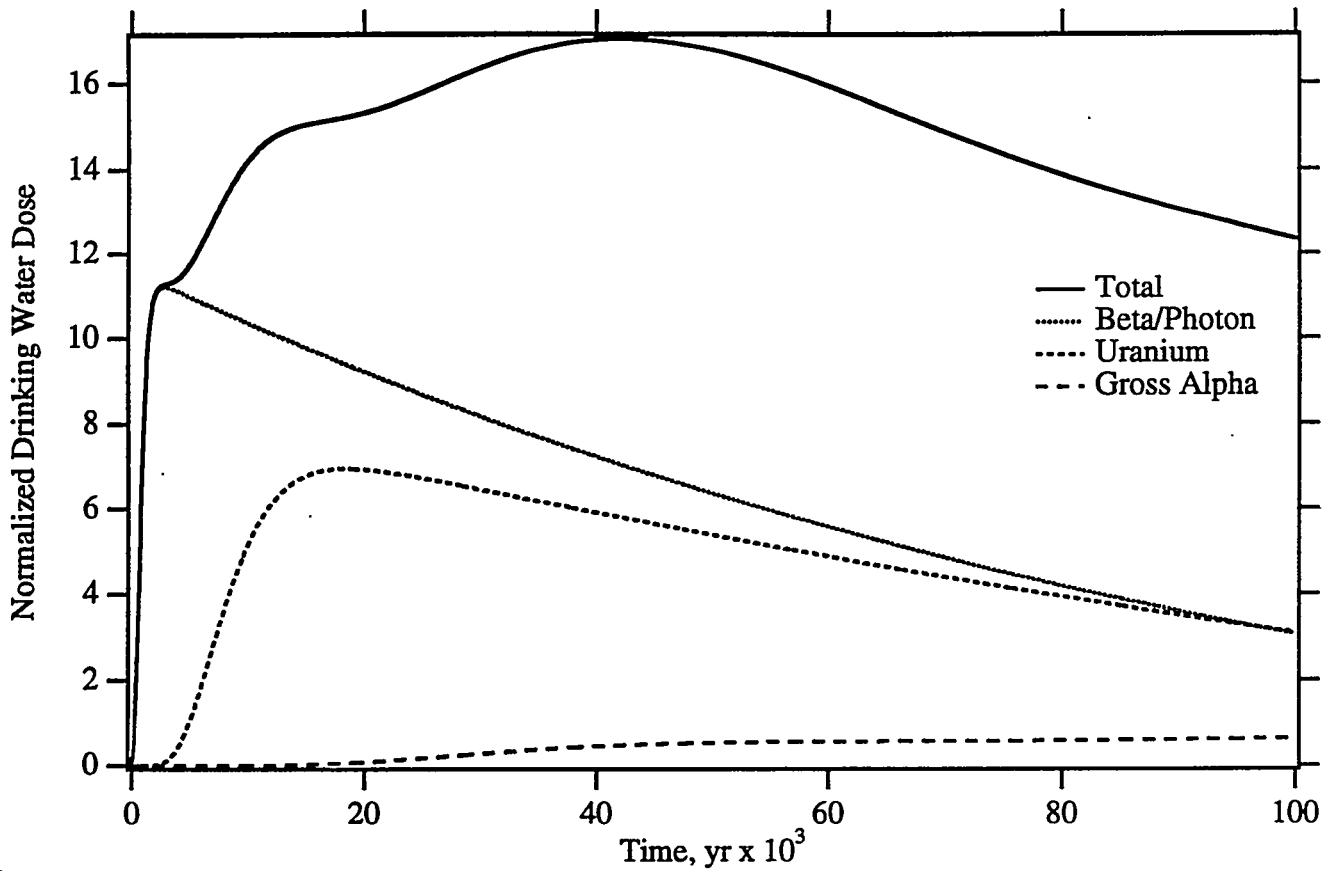


Figure A.23a. Drinking Water Dose

Corrosion: 10^{-6} cm/yr
 Glass Radius: 0.25 cm
 Recharge: 1 cm/yr
 Solute Diffusion Coefficient: $D_{ab} = 10^{-8}$ cm²/s, a = 1, b = 0
 Glass Hydraulic Properties: Glass Spheres (SOILPROP)
 Minimum Relative Permeability: 0.
 Retardation Model: Saturation-Dependent
 Hydraulic Dispersion: $\alpha_L = 6.5$ m, $\alpha_T = 0.65$ m
 Well Interception Factor: 0.1
 Grid: Narrow (10 x 162)

Maximum Dose Records 100,000 yr [10,000 yr]

Total	68.28 [56.85] mrem/yr
Beta/Photon	44.82 [44.82] mrem/yr
⁹⁹ Tc	42.89 [42.89] mrem/yr
¹²⁹ I	1.840 [1.840] mrem/yr
Uranium	138.9 [102.8] µg/L
Gross Alpha	9.573 [0.02009] pCi/L

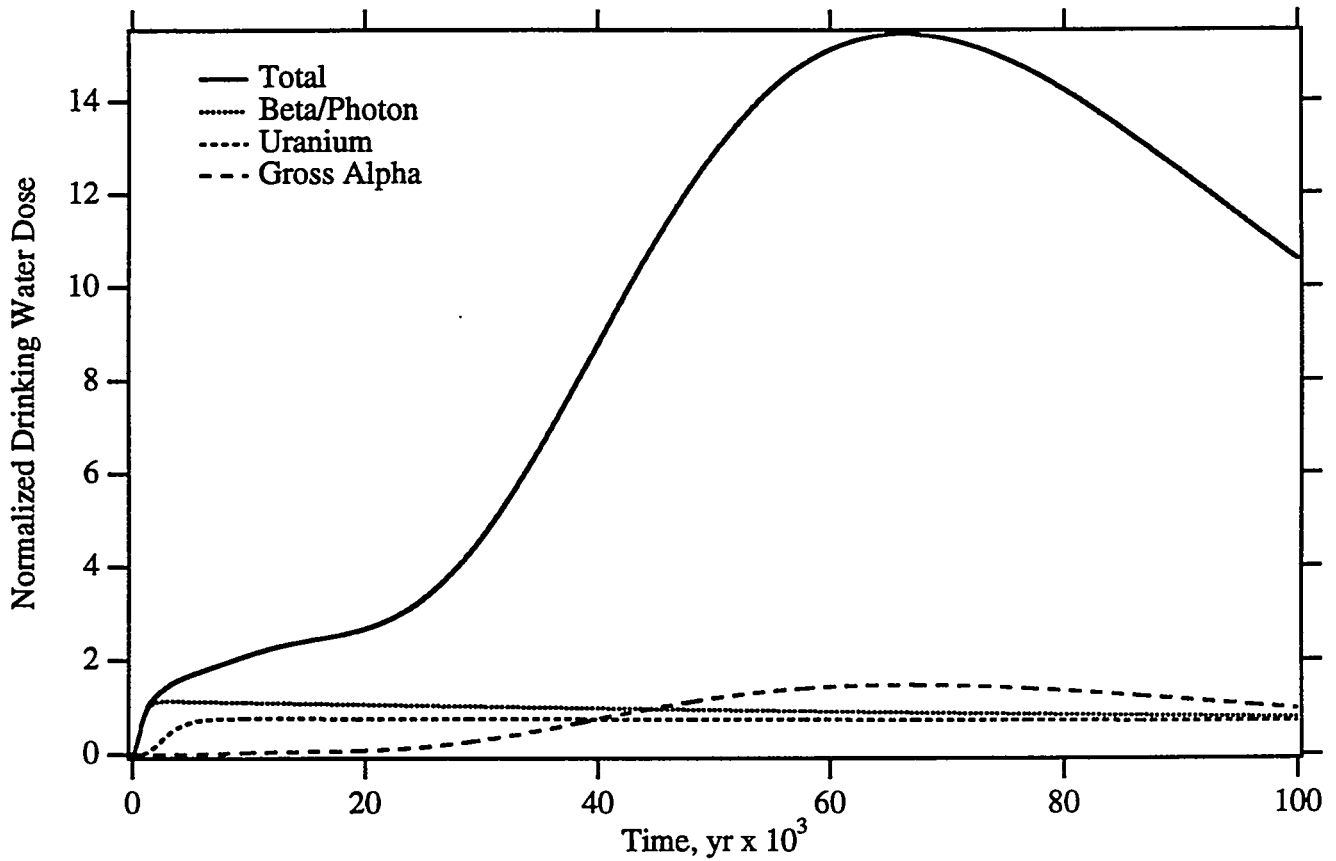


Figure A.24. Drinking Water Dose

Corrosion: 10^{-7} cm/yr
 Glass Radius: 0.25 cm
 Recharge: 1 cm/yr
 Solute Diffusion Coefficient: $D_{ab} = 10^{-8}$ cm²/s, a = 1, b = 0
 Glass Hydraulic Properties: Glass Spheres (SOILPROP)
 Minimum Relative Permeability: 0.
 Retardation Model: Saturation-Independent
 Hydraulic Dispersion: $\alpha_L = 6.5$ m, $\alpha_T = 0.65$ m
 Well Interception Factor: 0.1
 Grid: Narrow (10 x 162)

Maximum Dose Records 100,000 yr [10,000 yr]

Total	61.81 [8.482] mrem/yr
Beta/Photon	4.549 [4.549] mrem/yr
⁹⁹ Tc	4.353 [4.353] mrem/yr
¹²⁹ I	0.1871 [0.1871] mrem/yr
Uranium	15.30 [15.29] µg/L
Gross Alpha	22.15 [0.5318] pCi/L

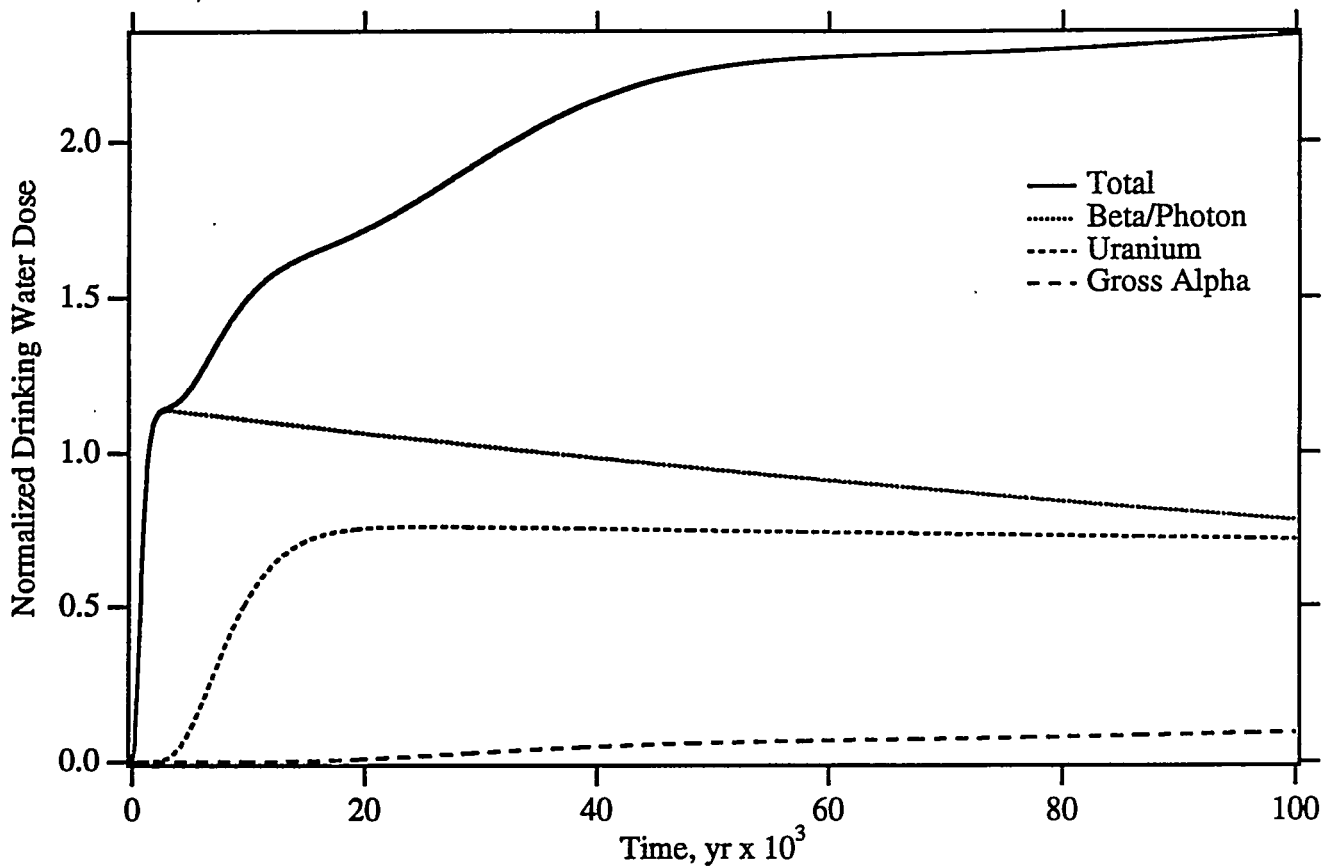


Figure A.24a. Drinking Water Dose

Corrosion: 10^{-7} cm/yr
 Glass Radius: 0.25 cm
 Recharge: 1 cm/yr
 Solute Diffusion Coefficient: $D_{ab} = 10^{-8}$ cm²/s, a = 1, b = 0
 Glass Hydraulic Properties: Glass Spheres (SOILPROP)
 Minimum Relative Permeability: 0.
 Retardation Model: Saturation-Dependent
 Hydraulic Dispersion: $\alpha_L = 6.5$ m, $\alpha_T = 0.65$ m
 Well Interception Factor: 0.1
 Grid: Narrow (10 x 162)

Maximum Dose Records 100,000 yr [10,000 yr]

Total	9.378 [6.021] mrem/yr
Beta/Photon	4.549 [4.549] mrem/yr
⁹⁹ Tc	4.353 [4.353] mrem/yr
¹²⁹ I	0.1871 [0.1871] mrem/yr
Uranium	15.17 [10.63] µg/L
Gross Alpha	1.422 [0.002159] pCi/L

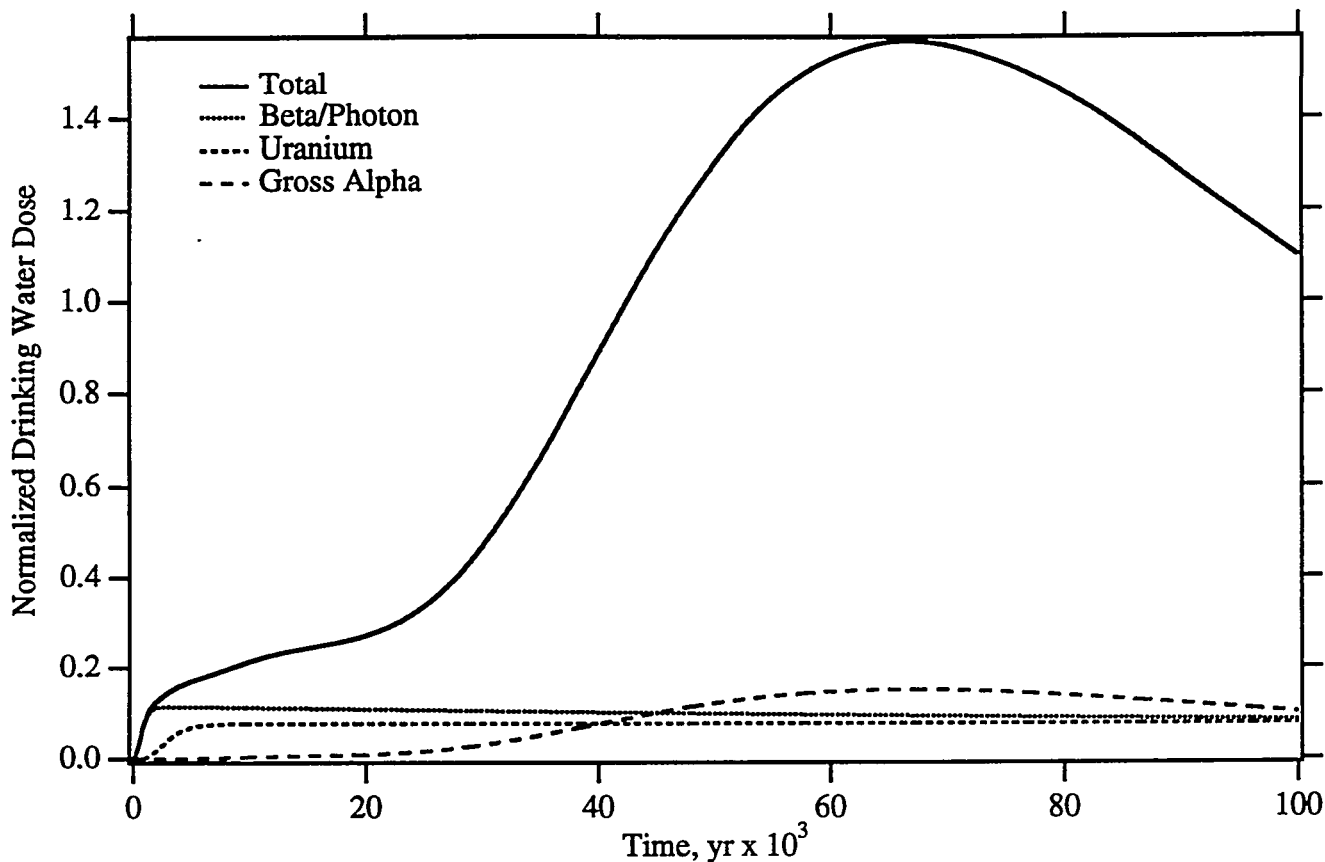


Figure A.25. Drinking Water Dose

Corrosion: 10^{-8} cm/yr
 Glass Radius: 0.25 cm
 Recharge: 1 cm/yr
 Solute Diffusion Coefficient: $D_{ab} = 10^{-8}$ cm²/s, $a = 1$, $b = 0$
 Glass Hydraulic Properties: Glass Spheres (SOILPROP)
 Minimum Relative Permeability: 0.
 Retardation Model: Saturation-Independent
 Hydraulic Dispersion: $\alpha_L = 6.5$ m, $\alpha_T = 0.65$ m
 Well Interception Factor: 0.1
 Grid: Narrow (10 x 162)

Maximum Dose Records 100,000 yr [10,000 yr]

Total	6.288 [0.8525] mrem/yr
Beta/Photon	0.4556 [0.4556] mrem/yr
⁹⁹ Tc	0.4360 [0.4360] mrem/yr
¹²⁹ I	0.01875 [0.01875] mrem/yr
Uranium	1.539 [1.537] µg/L
Gross Alpha	2.246 [0.05328] pCi/L

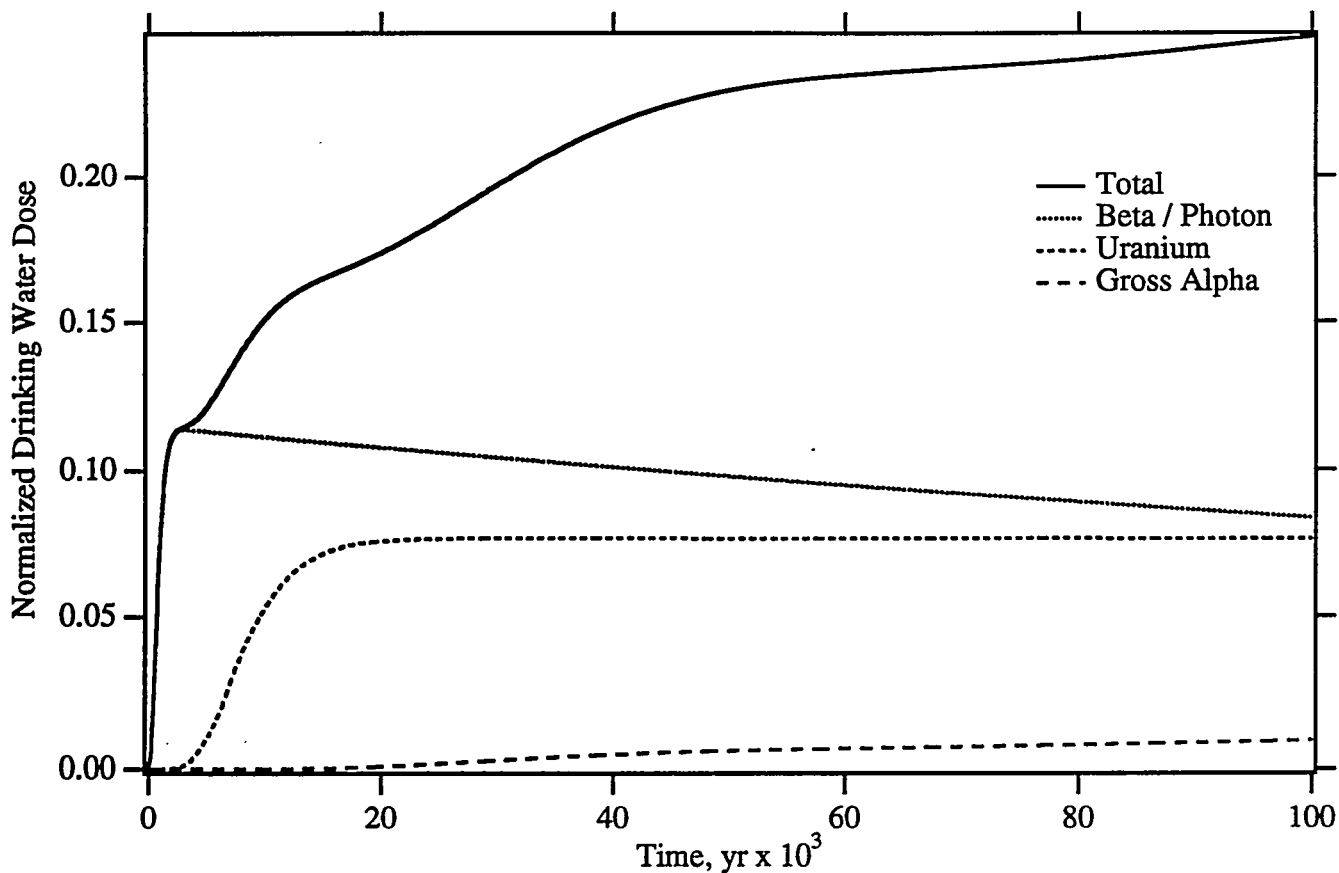


Figure 25a. Drinking Water Dose

Corrosion: 10^{-8} cm/yr
 Glass Radius: 0.25 cm
 Recharge: 1.0 cm/yr
 Solute Diffusion Coefficient: $D_{ab} = 10^{-8}$ cm²/s, a = 1, b = 0
 Glass Hydraulic Properties: Glass Spheres (SOILPROP)
 Minimum Relative Permeability: 0.
 Retardation Model: Saturation Dependent
 Hydraulic Dispersion: $\alpha_L = 6.5$ m, $\alpha_T = 0.65$ m
 Well Interception Factor: 0.1
 Grid: Narrow (10 x 162)

Maximum Dose Records 100,000 yr [10,000 yr]

Total	0.9916 [0.6054] mrem/yr
Beta / Photon	0.4556 [0.4556] mrem/yr
⁹⁹ Tc	0.4360 [0.4360] mrem/yr
¹²⁹ I	0.01875 [0.01875] mrem/yr
Uranium	1.537 [1.065] µg/L
Gross Alpha	0.1475 [0.0002161] pCi/L

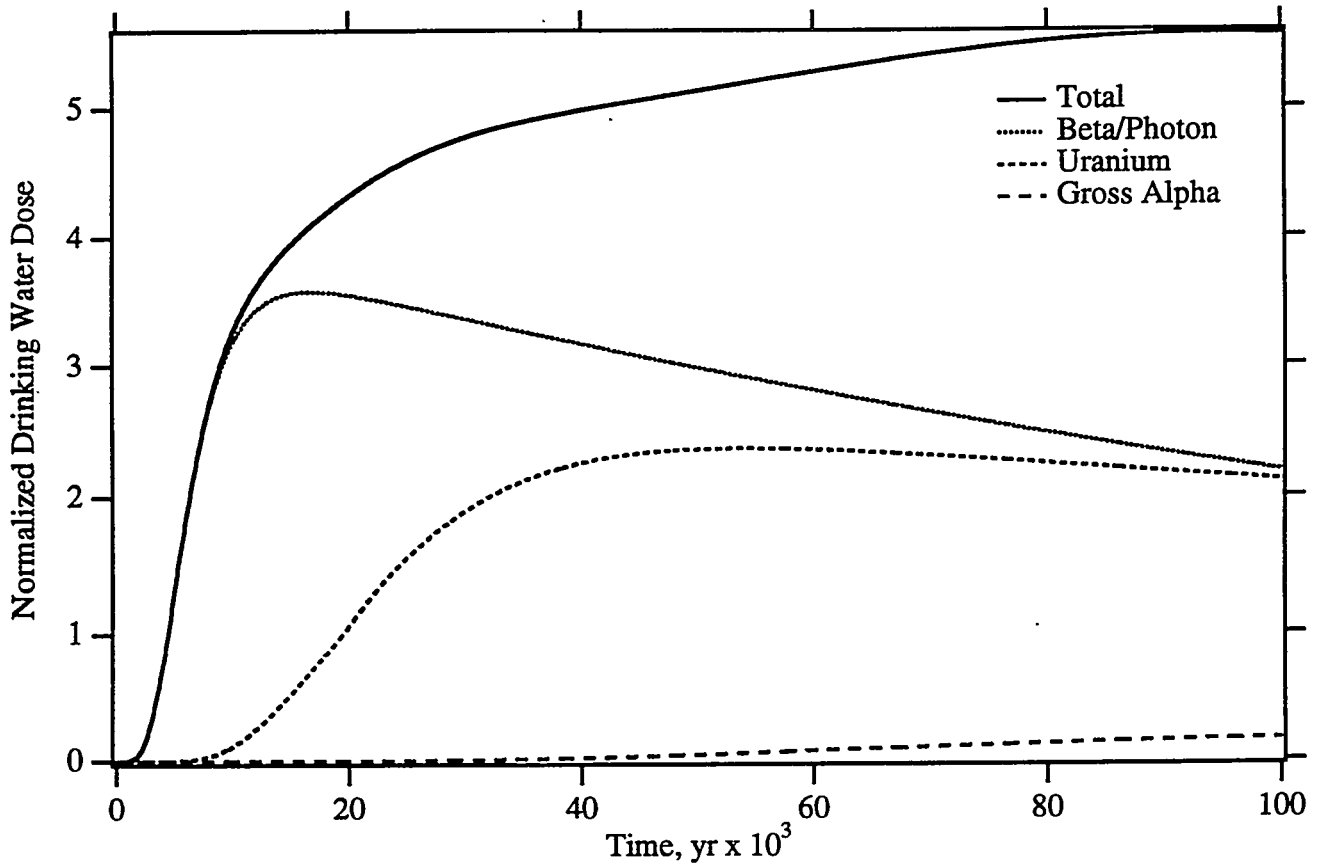


Figure A.26. Drinking Water Dose

Corrosion: 1.405×10^{-5} cm/yr
 Glass Radius: 10. cm
 Recharge: 0.1 cm/yr
 Solute Diffusion Coefficient: $D_{ab} = 10^{-8}$ cm²/s, a = 1, b = 0
 Glass Hydraulic Properties: Glass Spheres (SOILPROP)
 Minimum Relative Permeability: 0.
 Retardation Model: Saturation-Independent
 Hydraulic Dispersion: $\alpha_L = 6.5$ m, $\alpha_T = 0.65$ m
 Well Interception Factor: 0.01
 Grid: Narrow (10 x 162)

Maximum Dose Records 100,000 yr [10,000 yr]

Total	22.26 [13.07] mrem/yr
Beta/Photon	14.33 [12.74] mrem/yr
⁹⁹ Tc	13.71 [12.19] mrem/yr
¹²⁹ I	0.6166 [0.5353] mrem/yr
Uranium	47.24 [2.197] µg/L
Gross Alpha	2.412 [2.157e-06] pCi/L

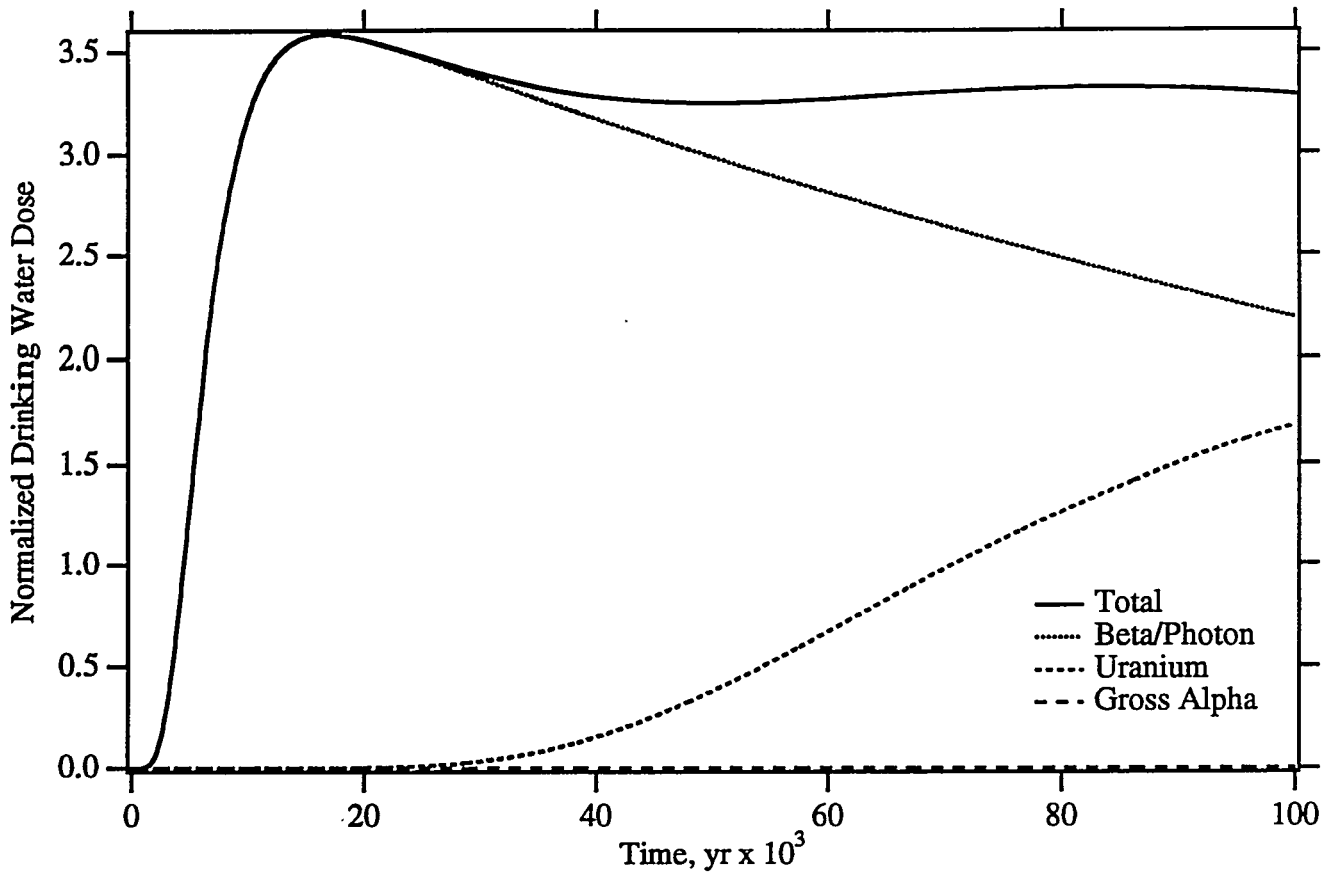


Figure A.26a. Drinking Water Dose

Corrosion: 1.405×10^{-5} cm/yr
 Glass Radius: 10. cm
 Recharge: 0.1 cm/yr
 Solute Diffusion Coefficient: $D_{ab} = 10^{-8}$ cm²/s, a = 1, b = 0
 Glass Hydraulic Properties: Glass Spheres (SOILPROP)
 Minimum Relative Permeability: 0.
 Retardation Model: Saturation-Dependent
 Hydraulic Dispersion: $\alpha_L = 6.5$ m, $\alpha_T = 0.65$ m
 Well Interception Factor: 0.01
 Grid: Narrow (10 x 162)

Maximum Dose Records 100,000 yr [10,000 yr]

Total	14.33 [12.74] mrem/yr
Beta/Photon	14.33 [12.74] mrem/yr
⁹⁹ Tc	13.71 [12.19] mrem/yr
¹²⁹ I	0.6166 [0.5353] mrem/yr
Uranium	33.84 [1.206e-05] µg/L
Gross Alpha	0.008664 [1.480e-23] pCi/L

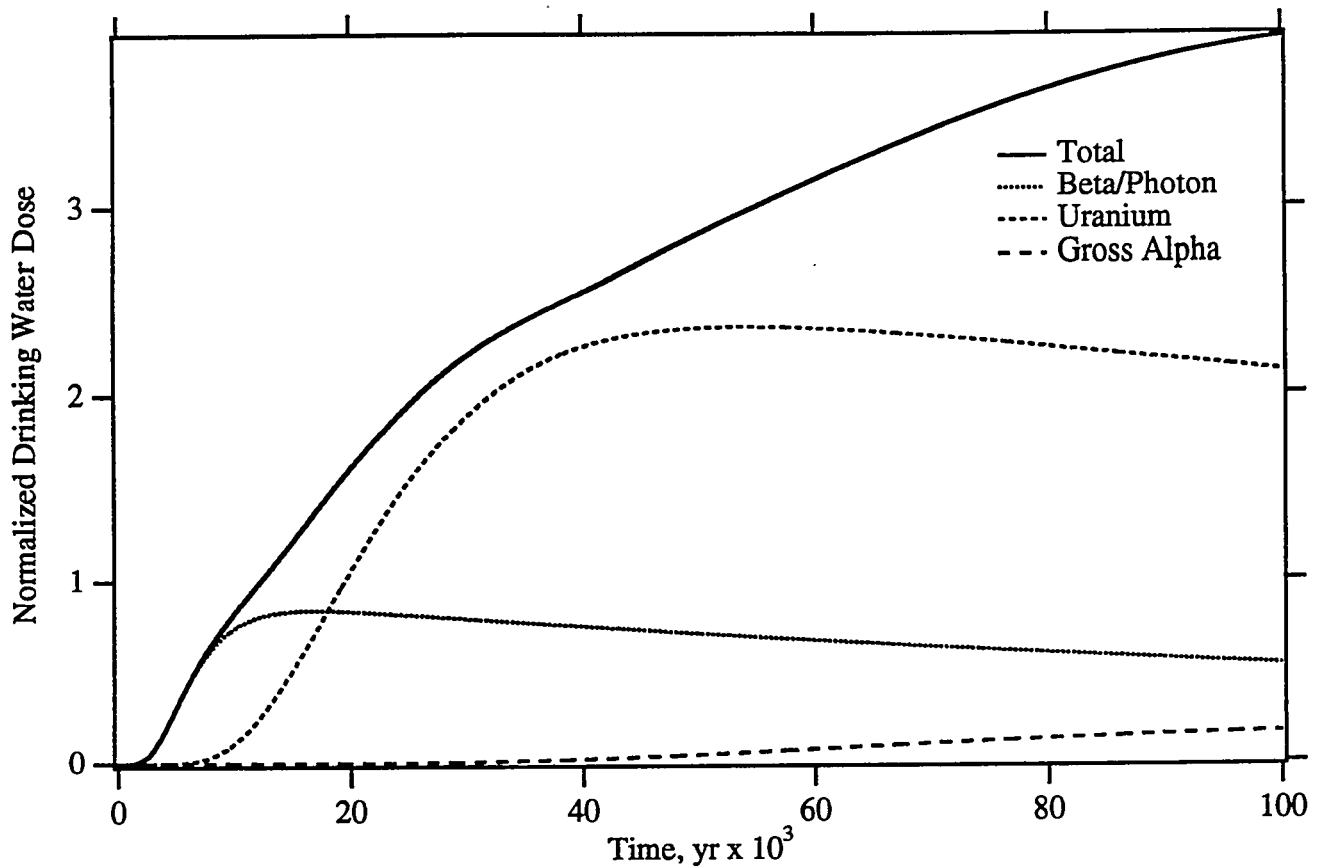


Figure A.26b. Drinking Water Dose (20% ⁹⁹Tc Inventory)

Corrosion: 1.405×10^{-5} cm/yr
 Glass Radius: 10. cm
 Recharge: 0.1 cm/yr
 Solute Diffusion Coefficient: $D_{ab} = 10^{-8}$ cm²/s, a = 1, b = 0
 Glass Hydraulic Properties: Glass Spheres (SOILPROP)
 Minimum Relative Permeability: 0.
 Retardation Model: Saturation-Independent
 Hydraulic Dispersion: $\alpha_L = 6.5$ m, $\alpha_T = 0.65$ m
 Well Interception Factor: 0.01
 Grid: Narrow (10 x 162)

Maximum Dose Records 100,000 yr [10,000 yr]

Total	15.62 [3.313] mrem/yr
Beta/Photon	3.362 [2.985] mrem/yr
⁹⁹ Tc	2.741 [2.439] mrem/yr
¹²⁹ I	0.6166 [0.5353] mrem/yr
Uranium	47.24 [2.197] µg/L
Gross Alpha	2.412 [2.157e-06] pCi/L

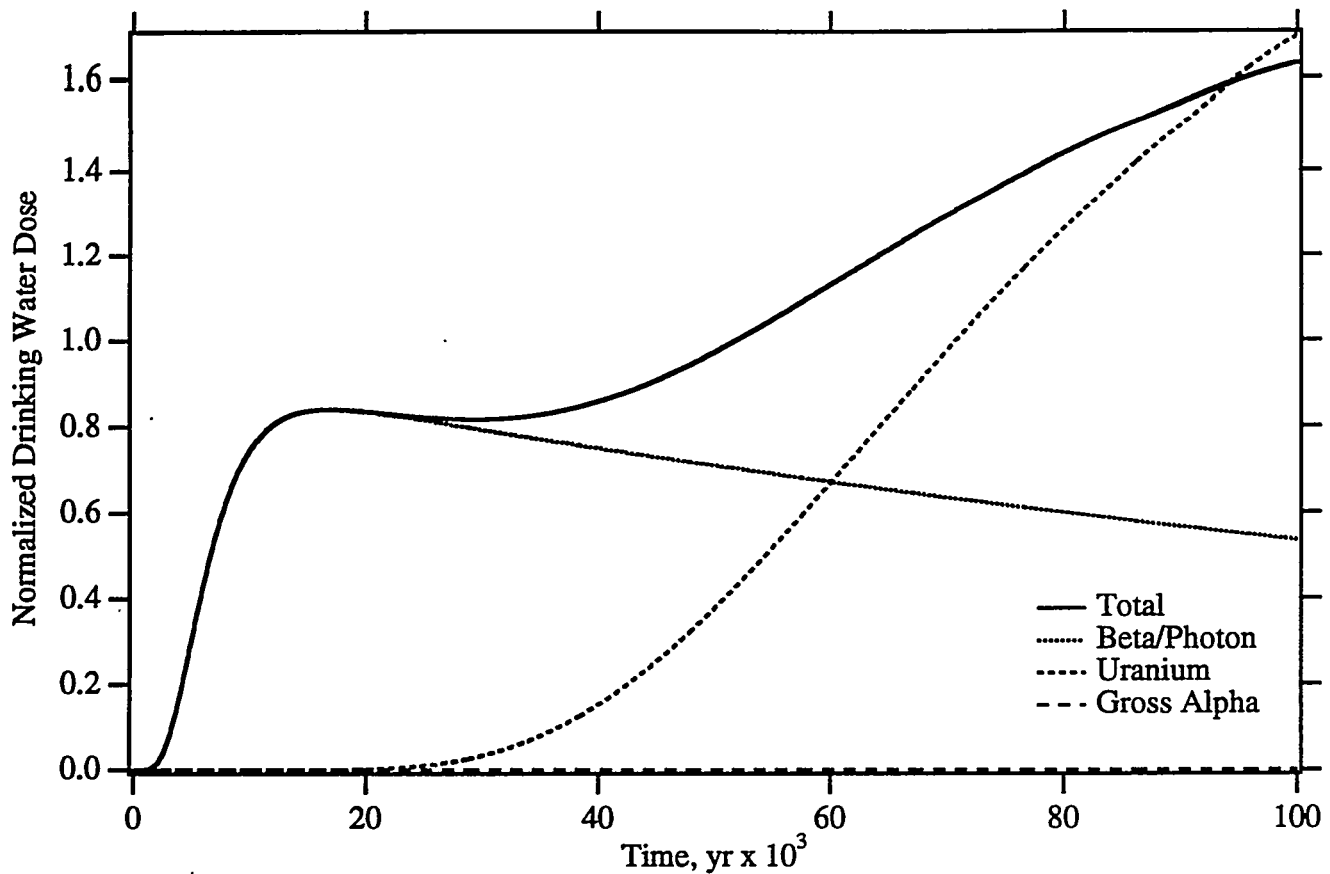


Figure A.26c. Drinking Water Dose (20% ⁹⁹Tc Inventory)

Corrosion: 1.405×10^{-5} cm/yr
 Glass Radius: 10. cm
 Recharge: 0.1 cm/yr
 Solute Diffusion Coefficient: $D_{ab} = 10^{-8}$ cm²/s, a = 1, b = 0
 Glass Hydraulic Properties: Glass Spheres (SOILPROP)
 Minimum Relative Permeability: 0.
 Retardation Model: Saturation-Dependent
 Hydraulic Dispersion: $\alpha_L = 6.5$ m, $\alpha_T = 0.65$ m
 Well Interception Factor: 0.01
 Grid: Narrow (10 x 162)

Maximum Dose Records 100,000 yr [10,000 yr]

Total	6.521 [2.985] mrem/yr
Beta/Photon	3.362 [2.985] mrem/yr
⁹⁹ Tc	2.741 [2.439] mrem/yr
¹²⁹ I	0.6166 [0.5353] mrem/yr
Uranium	33.84 [1.206e-05] µg/L
Gross Alpha	0.008664 [1.480e-23] pCi/L

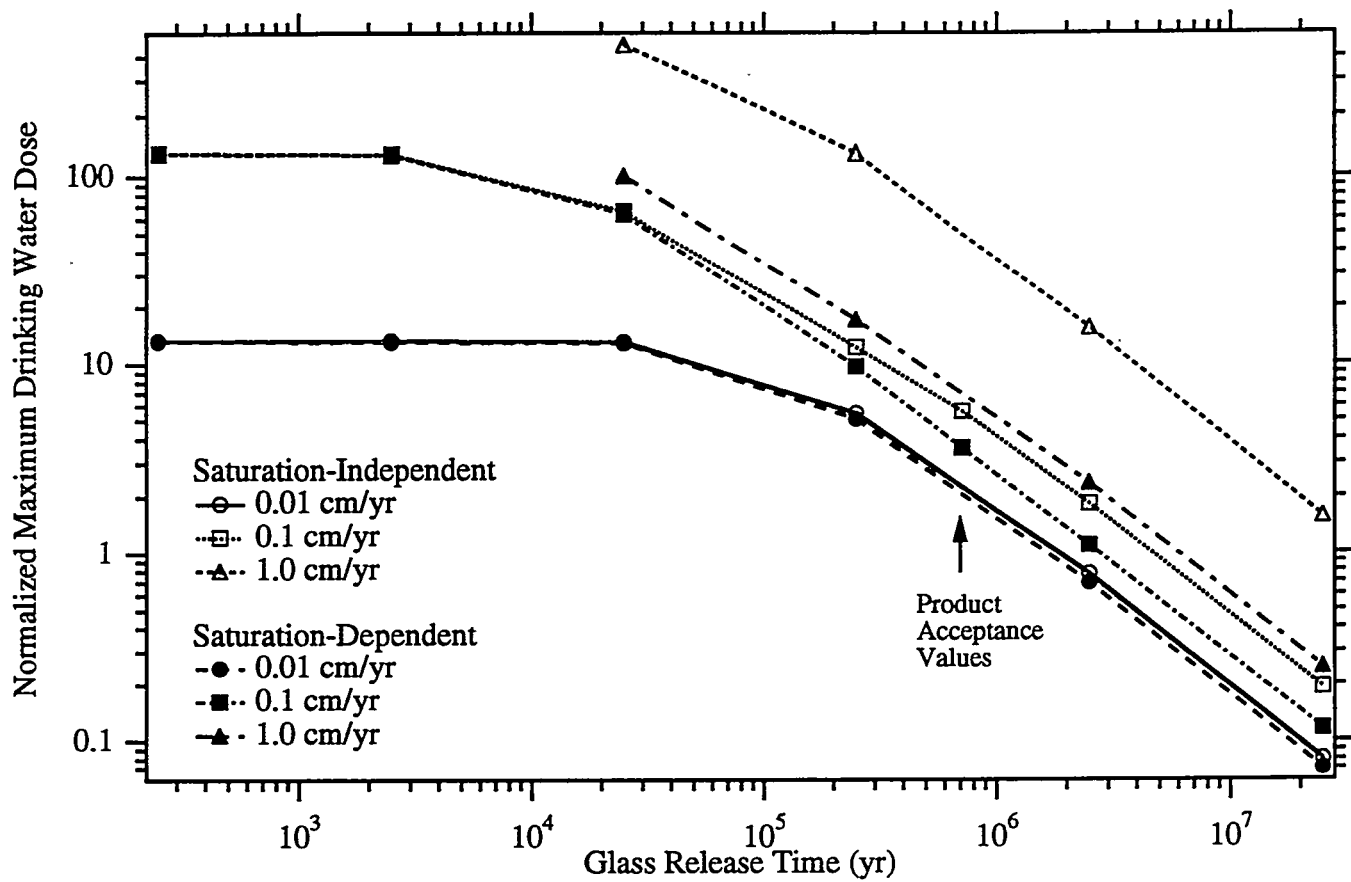


Figure A.27. Normalized Maximum Total Drinking Water Dose

Dose Record Length: 10^5 yr
 Solute Diffusion Coefficient: $D_{ab} = 10^{-8}$ cm²/s, $a = 1$, $b = 0$
 Glass Hydraulic Properties: Glass Spheres (SOILPROP)
 Minimum Relative Permeability: 0.
 Hydraulic Dispersion: $\alpha_L = 6.5$ m, $\alpha_T = 0.65$ m
 Grid: Narrow (10 x 162)

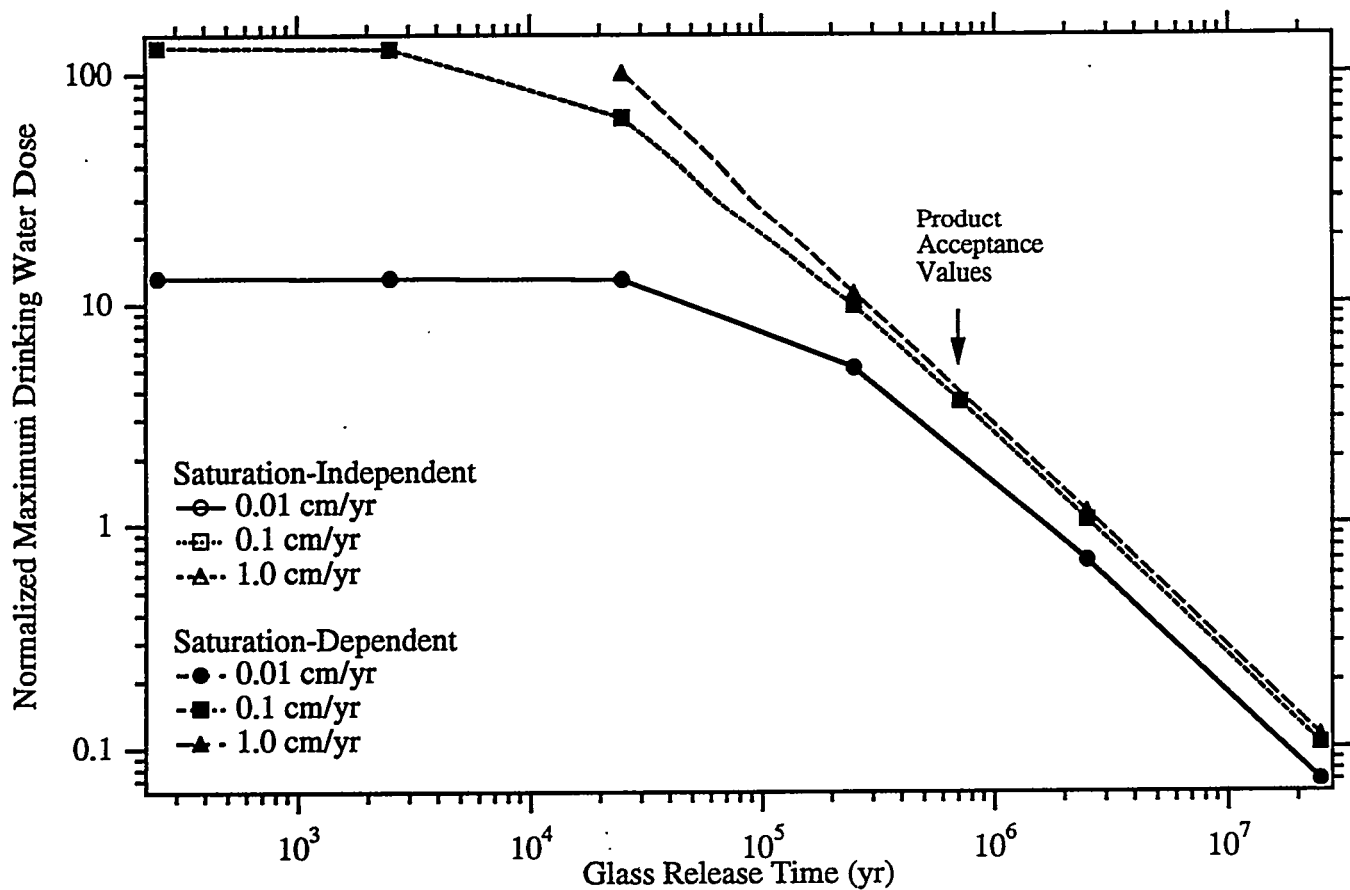


Figure A.28. Normalized Maximum Beta/Photon Drinking Water Dose (curves for a given recharge rate are identical)

Dose Record Length: 10^5 yr

Solute Diffusion Coefficient: $D_{ab} = 10^{-8}$ cm²/s, $a = 1$, $b = 0$

Glass Hydraulic Properties: Glass Spheres (SOILPROP)

Minimum Relative Permeability: 0.

Hydraulic Dispersion: $\alpha_L = 6.5$ m, $\alpha_T = 0.65$ m

Grid: Narrow (10 x 162)

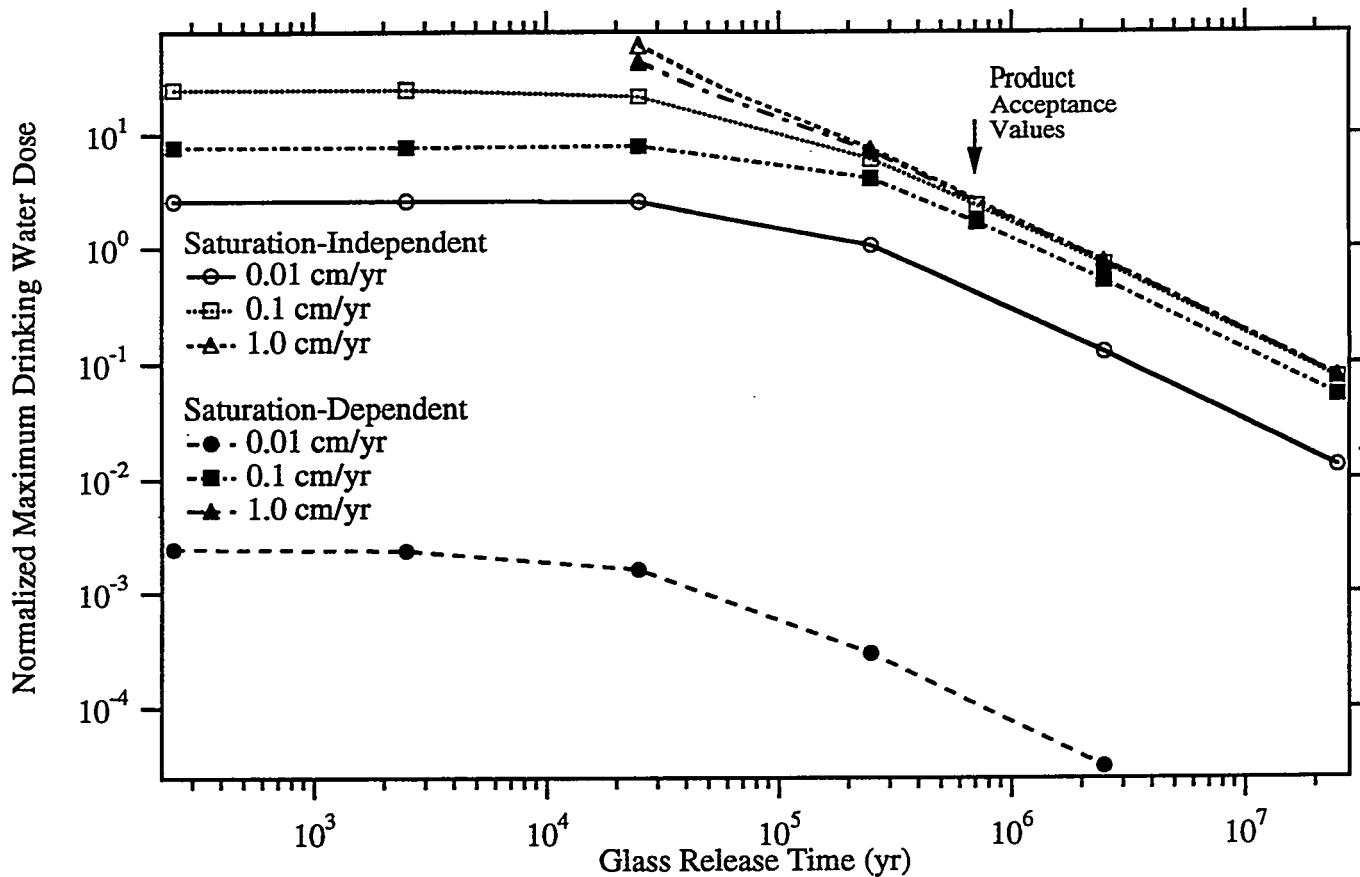


Figure A.29. Normalized Maximum Uranium Drinking Water Dose

Dose Record Length: 10^5 yr
 Solute Diffusion Coefficient: $D_{ab} = 10^{-8}$ cm²/s, $a = 1$, $b = 0$
 Glass Hydraulic Properties: Glass Spheres (SOILPROP)
 Minimum Relative Permeability: 0.
 Hydraulic Dispersion: $\alpha_L = 6.5$ m, $\alpha_T = 0.65$ m
 Grid: Narrow (10 x 162)

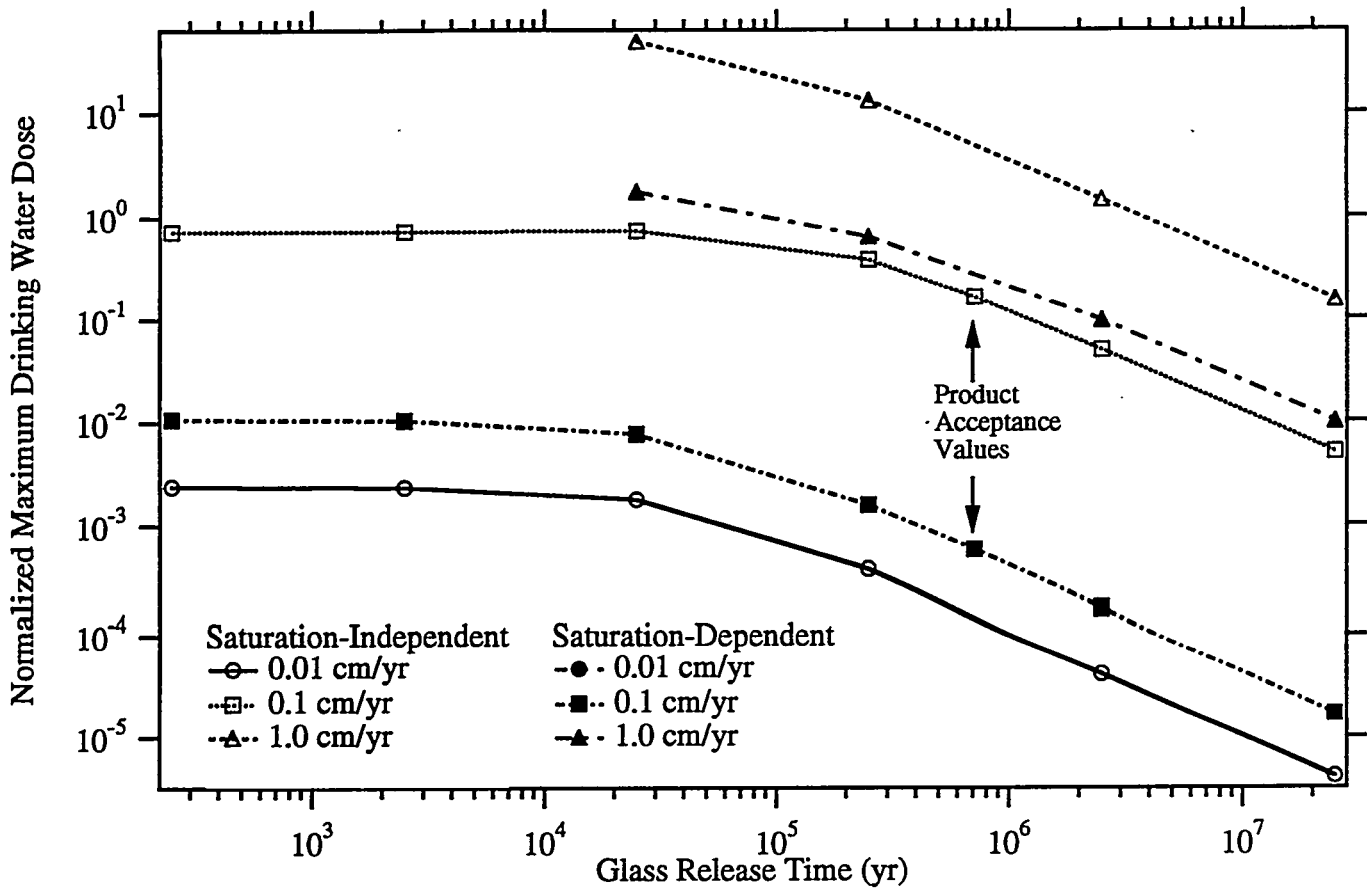


Figure A.30. Normalized Maximum Gross Alpha Drinking Water Dose
(curves for recharge = 0.01 cm/yr are identical)

Dose Record Length: 10^5 yr

Solute Diffusion Coefficient: $D_{ab} = 10^{-8}$ cm²/s, $a = 1$, $b = 0$

Glass Hydraulic Properties: Glass Spheres (SOILPROP)

Minimum Relative Permeability: 0.

Hydraulic Dispersion: $\alpha_L = 6.5$ m, $\alpha_T = 0.65$ m

Grid: Narrow (10 x 162)

Distribution

No. of Copies		No. of Copies	
ONSITE		19	Pacific Northwest National Laboratory
2	U.S. Department of Energy Richland Operations Office		
	N. R. Brown	K6-51	D. H. Bacon K9-36
	P. E. Lamont	S7-53	M. J. Fayer (5) K9-33
			M. D. Freshley K9-36
			D. I. Kaplan K6-81
			C. T. Kincaid K9-33
			B. P. McGrail K6-81
1	LMHC		G. P. Streile K9-33
	J. A. Voogd	H5-03	M. D. White K9-36
			Information Release (7) K1-06
6	FDNW		
	F. M. Mann	H0-31	